Improvement of Propylene Yield via Butene Metathesis

Liesel Harmse

University of Cape Town
2008

TABLE OF CONTENTS: **Page**

Synopsis

There is an increasing interest in finding ways to produce on-purpose propene, due to the significant predicted propene growth in the next few years without the concomitant growth in the ethene demand, One of the technologies available is 1-butene metathesis, which describes a one-step process where isomerisation of 1-butene to 2-butene followed by cross-metathesis taking place. Products of the cross metathesis are propene and 2-pentene. In addition ethene and 3-hexene are expected as products of 1-butene metathesis.

A limited thermodynamic analysis, only considering the primary metathesis and double bond isomerisation of the 1-butene metathesis, showed that at a reaction temperature of ca. 327-427°C a maximum conversion of ca. 70% of the butenes can be expected. Furthermore, it showed that the equilibrium selectivity for propene is ca. 38% indicating a relative low equilibrium yield of this product of ca. 25%.

The 8%WO_3/SiO_2 catalyst was used as a base catalyst for this study. Improved isomerisation was thought to be achieved by changing the support material, i.e. by making it more acidic, which according to literature will increase the isomerisation activity. The catalyst was made more acidic by supporting tungsten on silica-alumina with different Si/Al ratios using the wet impregnation method.

NH_3-TPD showed that the acidity of both the supports and the catalysts increased by the incorporation of alumina in the silica structure (up to a Si/Al ratio of 75%). Data resulting from FTIR of adsorbed pyridine revealed the presence of IR peaks characteristic to Lewis and Brønsted acid sites for the range of commercial Siralox support materials and the corresponding supported tungsten catalysts. The observed IR peaks for Lewis and Brønsted acid sites are in good agreement with those presented in literature. Results from this study revealed that the catalyst composition i.e. silica and alumina content definitely has an effect on the acidity of the Siralox support materials. Differences in the Brønsted and Lewis acidic character was observed with varying amounts of silica and

alumina. It was shown that pure silica does not contain any Lewis or Brønsted acid sites. However, when tungsten is loaded onto the support, the presence of Lewis sites is observed.

Another important factor during the metathesis reaction is the oxidation state of tungsten in the active catalyst. According to literature, the interaction between alumina and tungsten is very strong, thus retarding the reduction of tungsten to the active oxidation state. The interaction between silica and tungsten is much weaker, making the reduction process easier. Hydrogen TPR was used to monitor the reduction temperatures of all the catalysts. The reduction temperature for tungsten on SiO_2 is the lowest. The reduction temperature increased for silica-aluminas and increases with increasing amount of alumina in the silica/alumina support materials. Tungsten on alumina showed the highest reduction temperature. The WO_3/SiO_2 catalyst had the highest activity, whilst activity decreased with added amounts of alumina. This could be explained in the light of the high reduction temperatures of the tungsten supported on the Siralox materials and alumina.

All catalysts were tested for 1-butene metathesis activity at 450°C, $500h^{-1}$ and atmospheric pressure (0.85 bar) and deactivation (TGA analysis), as the main objectives of this project were to improve the metathesis activity and lifetime of the catalyst. The effect that acidity has on the metathesis activity and the effect that reduction temperature has on the metathesis activity were then compared in order to establish which one of these factors has the largest effect on the behaviour of the catalyst. Increasing acidity (increasing silica/alumina ratio), caused increasing amounts of coke formed during 1-butene metathesis, thus decreasing the lifetime of the catalyst. The reduction temperature of catalyst with increasing amounts of alumina, was shown to be very high, thus making it difficult for the tungsten to be reduced to the active oxidation state for metathesis. This resulted in a decrease in metathesis activity, thus a decrease in propene yield.

It can thus be concluded that the effect that reduction to the active oxidation state for metathesis has on the behaviour of the catalyst is much larger than the acidity effect. Increasing acidity causes increasing coke formation and thus shortening the life time of the catalyst.

Acknowledgements

I would like to offer my gratitude to Sasol for granting me the opportunity to finish my degree.

Thank you so much to my whole family for your support during this time and also to my heavenly Father, whom I could not have done this without.

I am also very grateful to Professor Eric van Steen for his help, patience and guidance in writing the thesis during my time at UCT and also at Sasol.

I would like to acknowledge the assistance of Dr. Charl van Schalkwyk and Marietjie du Toit during the practical side of this degree. I extend my appreciation to those at Sasol Library that assisted me in obtaining the necessary literature and all those from materials characterization group involved in the characterization studies of this project.

1. Introduction

1.1 Background

Propene is one of the key petrochemical building blocks used as feedstock in the manufacture of a variety of polymers and intermediates[1]. Predictions are that the demand for propene will grow at a rate of 5.3% per annum during the period 2000-2010 and is expected to grow faster than the demand for ethene. Propene demand is expected to nearly double in the next ten years, reaching about 81 million ton per annum worldwide by 2010[2]. Growth is mainly driven by polypropene demand, which accounts for 58% of propene consumption (see Table 1.1). Other markets include acrylonitrile, oxo chemicals (e.g. butanols, propene oxide and cumene, isopropyl, alcohol)[3]. Approximately 86% of the current propene capacity is situated in North America, Asia and Western Europe. The region of highest growth (20% per annum) is however the Middle East[2].

Table 1.1: World propene consumption (in million ton per annum) by end use for the period 2000-2010[3]

	Million ton per annum		**Growth Rate, 2000-2010 (%/yr)**
	2000	**2010**	
Polypropylene	31.7	59.7	6.5
Acrylonitrile	5.4	7.7	3.6
Propylene Oxide	3.8	5.4	3.6
Oxo Alcohols	3.8	5.8	4.1
Cumene	3.3	4.5	3.2
Acrylic Acid	1.9	2.7	3.4
Isopropyl Alcohol	1.4	2.1	3.8
Polygas Chemicals	1.1	1.2	0.9
Other	1.9	2.1	1.1
Total	**54.4**	**91.1**	**5.3**

Source: SRI Consulting

Note: SRI figures are confirmed by the 2004 CEH Report 436.0000A[3]

Propene is produced almost exclusively as a by-product of either ethene manufacture or petroleum refining. Refineries are one of the major sources of propene with more than 95% of the propene with the majority (globally ca. 65%) originating from either steam crackers or catalytic crackers (see Table 1.2). Propene is obtained mainly from naphtha steam crackers (globally about 65%) as a co-product with ethene, and as a co-product from gasoline-making from fluid catalytic cracking (FCC) units at refineries[6]. The refineries have already maximized readily available production capacity for propene with notable exceptions for refineries in Brazil, China, United States and Venezuela. There are concerns that supplies of propene will be tight in the coming years[1], since ethene consumption and the demand for petroleum-based fuels are not expected to grow as fast.

Relatively small amounts of propene are produced via alternative routes, viz. propane dehydrogenation, metathesis of ethene and butylenes or the Fischer-Tropsch process.

Additional capacity may be introduced by expansion of existing ethene plants or grass roots facilities (see Table 1.2). Further capacity may become available through the construction of splitters in refineries and from on-purpose production like metathesis. Of the additional 36.7 million tonnes required, 63% of the new capacity is expected to come from "speculative additions". This provides a good opportunity for metathesis.

As propene demand continues to outpace ethene demand, there is an increasing interest in finding ways to produce on-purpose propene to meet the expected shortfall. Due to the significant predicted propene growth in the next few years, alternative routes to propene will be come more important to maintain or expand market share. Some on-purpose propene technologies are commercially available, such as propane dehydrogenation (OLEFLEX, CATOFIN), olefin metathesis (META-4, OCT) and deep catalytic cracking. Other possible technologies are catalytic pyrolysis, Methanol to Olefins (MTO)/Methanol to Propene (MTP), although these technologies are not yet economically viable[4], or olefin inter-conversion processes (SUPERFLEX, Propylur).

Table 1.2: World propene supply and demand for the period 2000-2010 (in million ton per annum)[3]

	2000	2005	2010
Demand	54.4	70.7	91.1
Ethene co product	40.0	47.4	48.8
Refinery by-product	21.2	23.8	23.8
Propane dehydrogenation	1.2	3.2	3.4
Metathesis of ethene and butylenes	0.4	0.8	0.9
Deep catalytic cracking	0.7	0.7	0.7
Other	0.3	0.3	0.3
Speculative additions	0.1	6.6	23.9
Total capacity	63.9	82.9	101.8

Source: SRI Consulting

Note: SRI figures are confirmed by the 2004 CEH Report 436.0000A[3]

The increase in the demand of propene provides a good opportunity for metathesis technology[5]. Hence, Mitsiu Chemicals is starting up a 140k ton per annum C4 metathesis plant for captive use of the propene. Korea Petrochemical Industry Co (KPIC) has announced plans to produce 110k ton per annum propene via ABB Lummus metathesis technology. These current commercial metathesis technologies utilize ethene and butene for the production of propene[5].

Alternatively, propene may be produced by metathesis of solely butylene[6]. This would allow the production of propene without consumption of the relatively expensive raw material ethene.

1-butene + cis-2-butene → propene + cis 2-pentene (1)

1.2 Olefin Metathesis

Catalytic metathesis is a technique to achieve selective organic synthesis. 'Metathesis' means 'change places' (Meta: change, thesis: place) and in the metathesis of olefins the double bonding atom groups exchange places with one another[7]. For example, in the metathesis reaction involving two propene molecules shown in Scheme 1.1 (known as the Phillips Triolefin process[3]), 2-butene and ethene will form in the presence of catalyst. This reaction is also called disproportionation of propene[7].

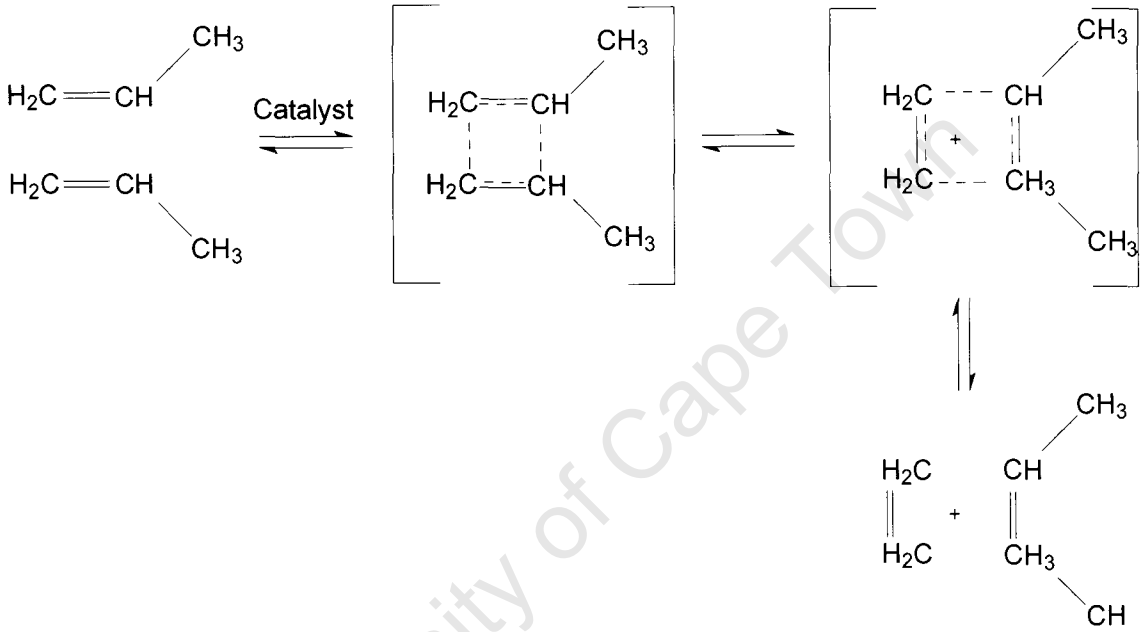

Scheme1.1: Metathesis of propene yielding ethene and 2-butene

The olefin metathesis reaction was discovered in the mid 1950's[8]. It appears that the olefin reaction has been discovered independently by research groups of DuPont[9, 10, 11]. Standard Oil from Indiana[12], and Phillips Petroleum[13]. The earliest discoveries made by these research groups were basic exchange olefin metathesis reactions of propene converted into butene and ethene, known as the Phillips Triolefin Process[14], and the ring-opening metathesis polymerisation of norborene and cyclopentene. The connection between these two discoveries was made much later[15].

The process of direct metathesis describes a one-step process where isomerisation of 1-butene to 2-butene followed by cross-metathesis takes place (Scheme 1.2). Products resulting from this process are propene and 2-pentene. This method offers

the production of propene without the addition of expensive ethene[6]. This method however requires optimum double bond isomerisation in order for the metathesis reaction to take place.

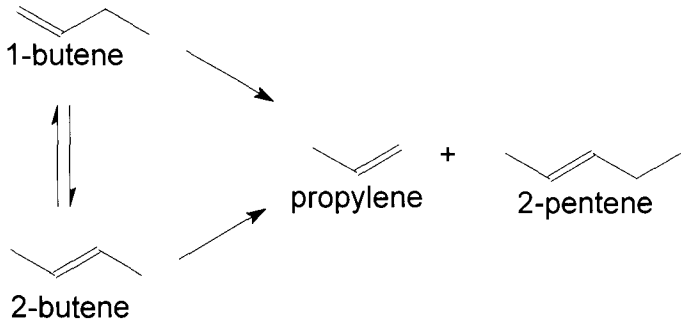

Scheme1.2: Isomerisation of 1-butene followed by cross metathesis of the two isomers

1.3 Processes for olefin metathesis

Metathesis is a key integrating technology which allows the facile inter-conversion or disproportionation of olefins. Metathesis technologies can provide flexibility in leveraging the considerable wealth of α-olefins produced via e.g. the Fischer Tropsch process, especially for the formation of propene through conversion of less desired olefins. Two technologies are currently available, which involve conversion of butenes and ethene to propene. These technologies are marketed by ABB Lummus (utilizing a WO_3/SiO_2 catalyst) and Axens (formerly IFP utilizing a Re_2O_7/Al_2O_3 catalyst) (see Table 1.3).

Table 1.3: Process characteristics of the two metathesis technologies available for licensing[6]

	ABB Lummus	**IFP-CPC (Axens)**
Catalyst	WO_3/SiO_2	Re_2O_7/Al_2O_3
$T_{reaction}$, °C	300-375	20-50
$p_{reaction}$, bar	30-35	ensuring liquid phase operation
Reactor system	Fixed bed , vapour phase	Fixed bed , liquid phase
Catalyst regeneration	In-situ/spare reactor	continuous or cyclic
Feed Pre-treatment	Selective hydrogenation of butadiene; isobutene removal if present above certain levels	Selective hydrogenation of butadiene; isobutene removal

Phillips commercialized the Triolefin process, which operated between 1966 and 1972 converting propene to a mixture of butenes and ethene[3]. The plant was closed when the economics of this conversion became unfavourable. Lyondell in the mid-1980's operated a process, which was essentially the reverse of the Phillips process, converting ethene and butenes to propene. This process became economically favourable because of the feedstock position.

The Institut Francais du Petrole (IFP) and the Chinese Petroleum Corporation (Kaoshiang, Taiwan) have jointly developed a process for the production of propene, called Meta-4. In their process, ethene and 2-butene react with each other in the liquid phase in the presence of a Re_2O_7/Al_2O_3 catalyst at 35°C and 60 bar[3]. The process is not yet commercialized, mainly because of the cost of the catalyst and the requirement of a high purity of the feed stream. This metathesis technology is presently offered by France's Axen, a subsidiary of IFP, formed in 2001 through the merger of IFP's licensing division with Procatalyse Catalysis & Adsorbents.

A large-scale industrial process incorporating olefin metathesis is the Shell higher olefins process (SHOP) for producing linear higher olefins from ethene[3]. The process takes place in three steps. In the first step, ethene is oligomerized in the presence of a nickel-phosphine catalyst to yield a mixture of linear even-numbered α-olefins ranging from C_4 to C_{40}. In the second step, the lighter alkenes ($<C_6$) and heavier alkenes ($>C_{18}$) undergo double bond isomerisation over a solid potassium metal catalyst to give an equilibrium mixture of internal olefins. In the third step, this mixture is passed over an alumina-supported molybdate metathesis catalyst, resulting in a statistical distribution of linear internal alkenes with both odd and even numbers of carbon atoms via cross-metathesis reactions such as reaction (2)[3].

$$CH_3CH{=}CHCH_3 + CH_3(CH_2)_7CH{=}CH(CH_2)_9CH_3 \rightleftharpoons CH_3CH{=}CH(CH_2)_7CH_3 + CH_3CH{=}CH(CH_2)_9CH_3 \quad (2)$$

Shell Chemicals operates a SHOP unit at Stanlow (UK) with a capacity of 270 000 ton per annum and three large-scale SHOP units at Geismar, Louisiana (USA) with a total capacity of 920 000 ton per annum of higher olefins. The third SHOP unit at

their Geismar location was brought on stream in 2002 for the production of 320 000 ton per annum of higher olefins. This expansion brought Shell Chemicals' total worldwide production capacity to 1 190 000 t of linear alpha and internal olefins per year[3].

1.4 Mechanism of olefin metathesis

Early mechanistic proposals for olefin metathesis were put forward by Herrison and Chauvin[16] involving a non-pairwise metal carbene olefin exchange (see Scheme 1.3). They proposed that the active catalyst was a metal carbene compound, in which the metal is bound to the carbon with a double bond with a vacant coordination site at the transition metal. The olefin coordinates at this site and the metallocyclobutane intermediate is formed, which is unstable and cleaves to form a new metal carbene complex and a new olefin. The mechanism proposed by Chauvin, received strong support from experimental investigations by Grubbs, Katz and Schrock which stated that the mechanism involved metallocarbene and metallocycle intermediates[17].

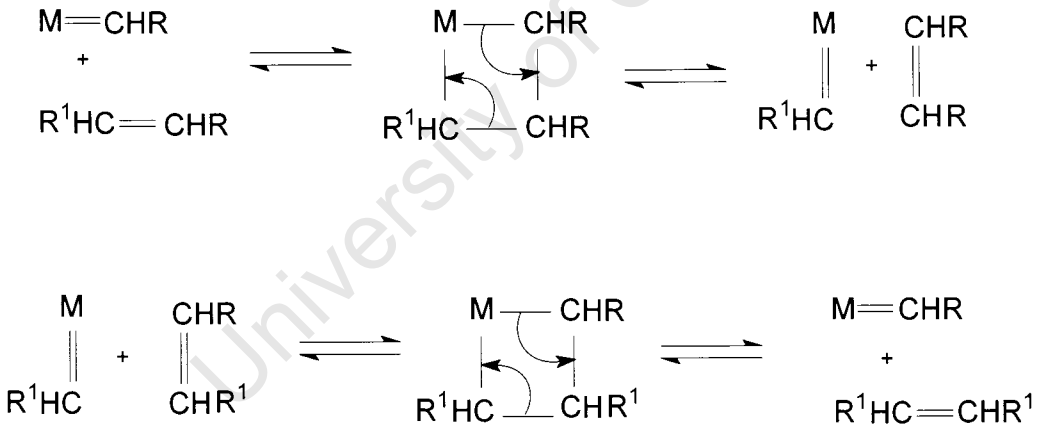

Scheme 1.3: Mechanism for olefin metathesis[16, 17]

This mechanism requires the presence of metal carbene species. They can be formed via a metal hydride[18, 19] (see Scheme 1.4) or via a π-allyl species[18, 19] (see Scheme 1.5). According to the transition metal hydride mechanism, a metal alkyl species is formed upon addition of an olefin to the metal hydride followed by β-hydrogen addition. The subsequent α-hydrogen elimination of the metal alkyl results in the metal carbene complex[20]. Hence, the presence of a metal hydride is essential

for the formation of a metal carbene. In heterogeneous catalyst systems, the support may serve as the source for the hydrogen atom and the metal hydride can be created via hydrogen migration from the support.

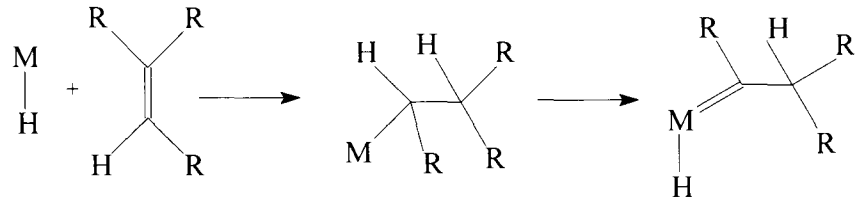

Scheme 1.4: Metal carbene formation via a metal hydride[18, 19]

A second more acceptable mechanism proceeds via a π-allyl species, formed upon coordination of an olefin to the metal centre. This species is subsequently converted to a metallacyclobutane species via nucleophilic hydride attack on the central carbon of the π-allylic group[20]. Thus, the reactant olefin must contain an allylic hydrogen. For simple olefins it is suggested that a co-catalyst activates the catalyst by generating the first carbene ligand.

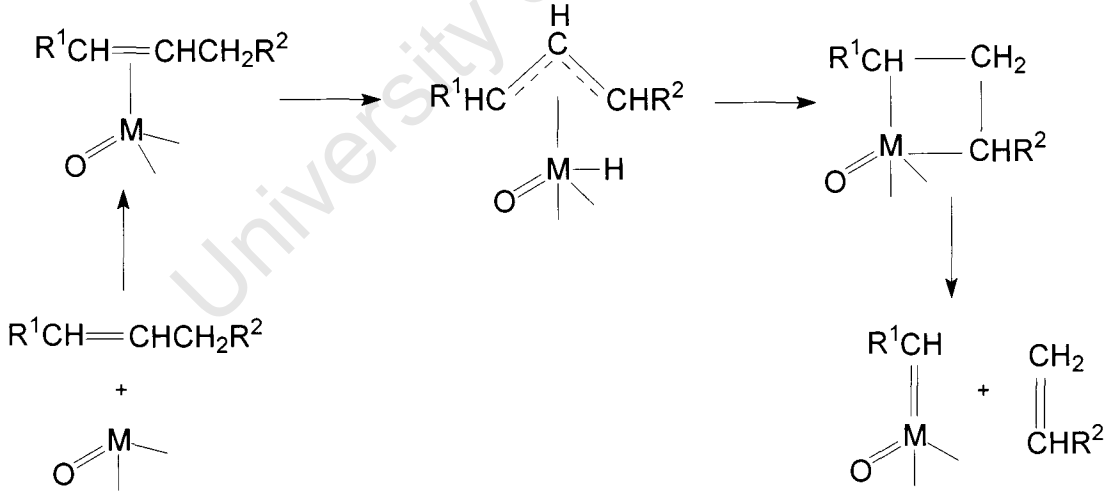

Scheme 1.5: Metal carbene formation via a π-allyl species[18, 19]

The reaction mechanism is directly related to the role of the catalyst[21]. The activity of a given catalyst system will be determined by both the nature and the concentration of the active species. As previously mentioned, the accepted mechanism for the metathesis reaction is the metal carbene or metallacyclobutane mechanism, and thus

the active species will be a metal carbene complex, formed in some way from the transition metal compound.

1.5 Thermodynamic analysis of olefin metathesis

Equilibrium calculations were performed for the metathesis of Butenes. The following set of equilibrium metathesis reactions were considered:

2 1-butene → cis 3-hexene + ethene (3)

1-butene + cis 2-butene → cis 2-pentene + propene (1)

In addition to the metathesis reaction, the following double bond isomerisation was considered to be at equilibrium:

1-butene → cis 2-butene → trans 2-butene

cis 2-pentene → trans 2-pentene → 1-pentene

cis 3-hexene → trans 3-hexene → cis 2-hexene → trans 2-hexene → 1-hexene

Cracking reactions, which may happen at high reaction temperatures, were not considered.

All considered reactions are equimolar and therefore the pressure will not influence the position of the equilibrium. The inclusion of the double bond isomerisation allows the consideration of a feed consisting solely of 1-butene. Double bond isomerisation is generally seen as a relatively fast reaction, and thus the composition of the incoming feed is immaterial. The equilibrium composition as a function of the reaction temperature was calculated with all compounds as an ideal gas using the data given by Stull et al[22]. The equilibrium conversion increases with increasing reaction temperature (see Figure 1.1). The increase is small and at 27°C the conversion of the Butenes is ca. 53 mol-%, whereas increasing the temperature to ca. 423°C results in an increase of the equilibrium conversion to ca. 70 mol-% (see Figure 1.1).

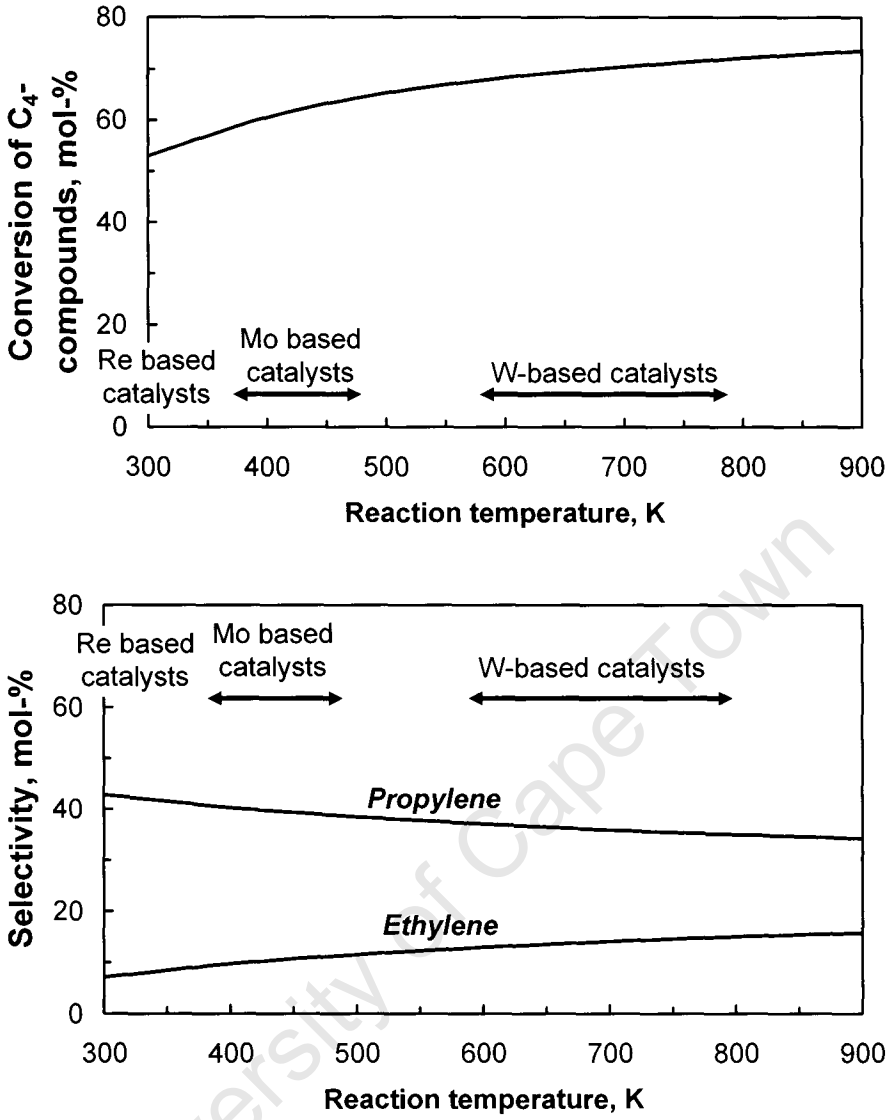

Figure 1.1: Equilibrium conversion (top) and selectivity (bottom) in the metathesis of Butenes as calculated with data from Stull et al.. Furthermore indicated, is the working temperature range of various metathesis catalysts (see Table 1.5)

With increasing temperature the selectivity for propene decreases (see Figure 1.1). High reaction temperature favours the formation of ethene (and as a co-product Hexenes). Thus, the yield of propene in the conversion of Butenes passes through a maximum, since the conversion increases and the selectivity decreases with increasing temperature. The yield in the investigated temperature range (27-627°C) is

however not a strong function of temperature. Between 127 and 627°C, the thermodynamically predicted propene yield varies between 24.3 and 25.3 mol-%

1.6 Catalysts for olefin metathesis

A large number of catalyst systems, homogeneous or heterogeneous, are effective for olefin metathesis[23]. The well-defined catalysts are essentially identical to or resemble the active species in term of metal oxidation state and ligand coordination sphere. Compounds of the nine transition elements shown in Table 1.4 are the most important catalytic systems, because it forms a transition metal carbene with a vacant coordination site at, which is the active species in the metathesis reaction. Molybdenum, tungsten, rhenium and ruthenium are the most effective metathesis catalysts[23].

Table 1.4: Transition metals effective for olefin metathesis[23]

IV_A	V_A	VI_A	VII_A	VIII	
Ti	V	Cr	Mn	Fe	Co
Zr	Nb	**Mo**	Tc	**Ru**	Rh
	Ta	**W**	**Re**	Os	Ir

1.6.1 Heterogeneous metathesis catalysts

Heterogeneous metathesis catalysts have two major advantages over homogeneous metathesis catalysts, i.e. greater thermal stability and ease of separation of products from the catalyst[24]. Previous and current industrial applications of olefin metathesis employed an array of different heterogeneous catalysts[25]. Among the more effective heterogeneous metathesis catalysts are the oxides of molybdenum, rhenium and tungsten, supported on high-surface alumina or silica[26]. The above-mentioned catalysts can be categorized according to their operating temperatures[27] (see Table 1.5).

Table 1.5: Operating temperatures of heterogeneous metathesis catalysts

Metathesis Catalyst	*Operating Temperature*
Re_2O_7/Al_2O_3	Room Temperature
MoO_3/Al_2O_3	100-200°C
WO_3/SiO_2	300-500°C

1.6.1.1 Supported rhenium catalysts

Supported rhenium catalysts have attracted much attention due to their ability to tolerate a variety of heteroatom-containing functional groups[23], and their operation at relatively low temperatures (ranging from 0-100°C[20]). It can be used for the metathesis of all types of olefins, when supported on Al_2O_3. The oxide catalyst is typically prepared by impregnating γ-alumina with ammonium perrhenate solution, drying at 110°C, and heating first in dry air at 550°C and then in nitrogen[23]. The activity of the catalyst could be correlated with the Brønsted acidity of the support and the corresponding catalysts (as measured using pyridine adsorption) for various supported Re_2O_7 catalysts[51,52] The catalytic activity of the original heterogeneous Re_2O_7/Al_2O_3 catalyst has been improved[53] by phosphating the support, the addition of metal oxides such as MoO_3, V_2O_5 or WO_3 and by addition of a tetra-alkyl tin promoter. Furthermore, supports such as silica-alumina have shown improved activity.

1.6.1.2 Supported molybdenum (MoO_3) catalysts

Supported molybdenum oxide catalysts have received much attention because they are widely used in industrial petrochemical processes, including metathesis (SHOP process) [23]. The surface properties as well as catalytic activity are influenced by the type of support used, surface Mo-oxide content, pre-treatment temperature, etc. These catalysts can be prepared[23] by impregnation of the support with a molybdate solution, treatment of the support with $Mo(CO)_6$ or treatment of the support with organomolybdenum compounds. The supported molybdenum compound is brought into its active state by heat treatment coupled with oxidation or reduction.

For the MoO_3/Al_2O_3 catalyst, the best selectivity is obtained if the MoO_3 is only slightly reduced during activation[31]. If MoO_3/Al_2O_3 is activated at 550°C, the propene

metathesis activity at 200°C is dependent on the Mo content, which increases sharply between 0.5 and 2 Mo atoms/nm[32]. The activity increases with increasing activation temperature, especially at low Mo content. The low activity at low Mo loadings and lower temperatures is due to the fact that at low Mo loadings, the highly stable tetrahedrally coordinated Mo(VI) species are the dominant species, which are difficult to reduce. At higher molybdenum loadings, Mo is mainly present in the octahedrally coordinated state which is a lot easier to reduce to the active state.

1.6.2.3 Supported tungsten catalysts

The two best known tungsten oxide catalysts are WO_3/SiO_2 and WO_3/Al_2O_3[20]. The most common method of preparing supported catalysts is by impregnation of the support with the metal cation precursor solution[20].

Bulk WO_3 was reported to be an active catalyst for several reactions, besides metathesis, such as isomerisation, dehydration and cracking[21]. However, high temperatures are required because of its low surface area and weak acid sites[33].

The density and strength of acid sites, and the rate of catalytic reactions on tungsten oxide catalysts increase with slight reduction of the W^{6+} centres. This may even happen during a catalytic reaction in a reducing, hydrocarbon-containing environment. It was first reported by Sabatier that yellow WO_3 crystallites were readily reduced by alcohol reactions above 250°C to a stoichiometry corresponding to $WO_{2.95}$[34]. This slightly reduced blue oxide was more active than WO_3 towards metathesis.

The interaction of the metal (oxide) with the support can lead to the formation of Lewis acid sites. It was suggested that this acidity is needed for the formation of the initial metal carbene[35]. This generation of active centres for metathesis activity was explained by van Roosmalen and co-workers as proton donation by a hydroxyl group adjacent to a Lewis acid site-alkene complexes to tetravalent tungsten[35] The Si-O bridges to the silica lattice are electrophilic, due to the p_π-d_π back bonding between oxygen and silicon resulting in the Lewis acidity. In the presence of an olefin, the

olefin can chemisorb onto tungsten surface compounds (see Scheme 1.6) to form a Lewis acid-alkene complex (see Scheme 1.7).

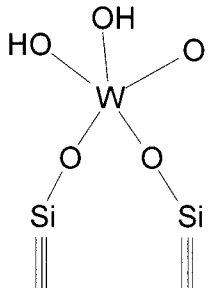

Scheme 1.6: Tungsten surface compound on dehydrated WO_3/SiO_2[35]

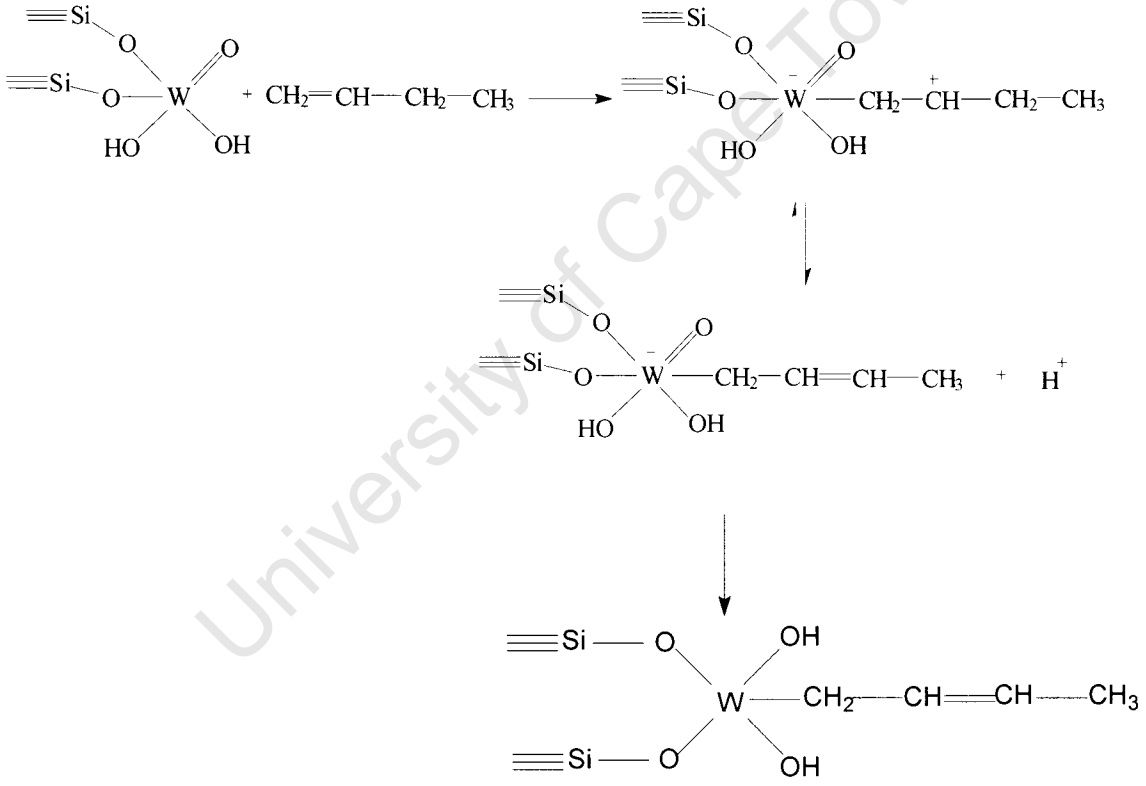

Scheme 1.7: The interaction of 1-butene with the Lewis acid sites on WO_3/SiO_2[35]

Support materials themselves may posses Brønsted and Lewis acid sites. Brønsted acidity is attributed to acidic protons of surface hydroxyl groups, while Lewis acidity is attributed to surface cations which can accept electronic charge from an electron donor[36, 37]. The Brønsted acid sites in e.g. silica-alumina are the hydroxyl groups

shared by silica and alumina tetrahedra (as in zeolites). Brønsted acid sites can be converted to Lewis acid sites by dehydration (see Scheme 1.8).

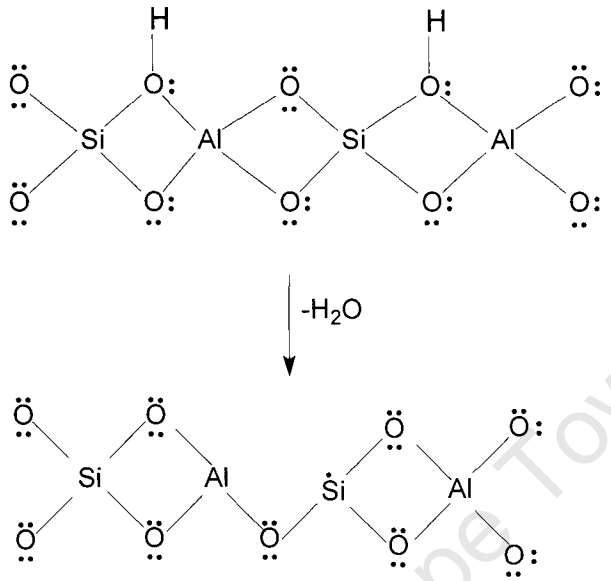

Scheme 1.8: Brønsted and Lewis acidity in silica-alumina

Andreini et al.[38] reported that the Brønsted acidity of the support does not play a role in the metathesis reaction. They evaluated several acidic supports for metathesis activity at different activation temperatures and observed that for Al_2O_3 and Al_2O_3/SiO_2, the Brønsted acidity decreased with increased activation temperature, while the metathesis activity increased. This concurs with a study using WO_3/SiO_2[39] and WO_3 supported on silica treated with hexamethyldisilazane. Brønsted acid groups are responsible for double bond isomerisation, but not precursors for active sites for metathesis[40].

The influence of metal loading on the tungsten catalyst's selectivity and activity was investigated by testing a series of WO_3/SiO_2 catalysts with different loadings of WO_3 in the range of 3%-30% WO_3[41]. A decrease in surface area and pore volume was observed with increasing loading, indicating the formation of a multilayer of crystalline material. XRD analysis revealed an increase in crystalline material from 3% to 20% metal loading where an extremely crystalline WO_3 material was observed. An increase in conversion of 1-octene during the metathesis reaction (at 460°C, 5.6

LHSV and atmospheric pressure) was observed upon increasing the metal loadings up to 6%. The conversion stabilizes with further addition of WO_3 and it seems as if a further increase in tungsten loading does not have any effect on the conversion (see Figure 1.2). Lower conversion at lower metal loadings probably occurs due to a small amount of active surface species present. It was speculated that this was due to a constant level of a surface tungsten complex.

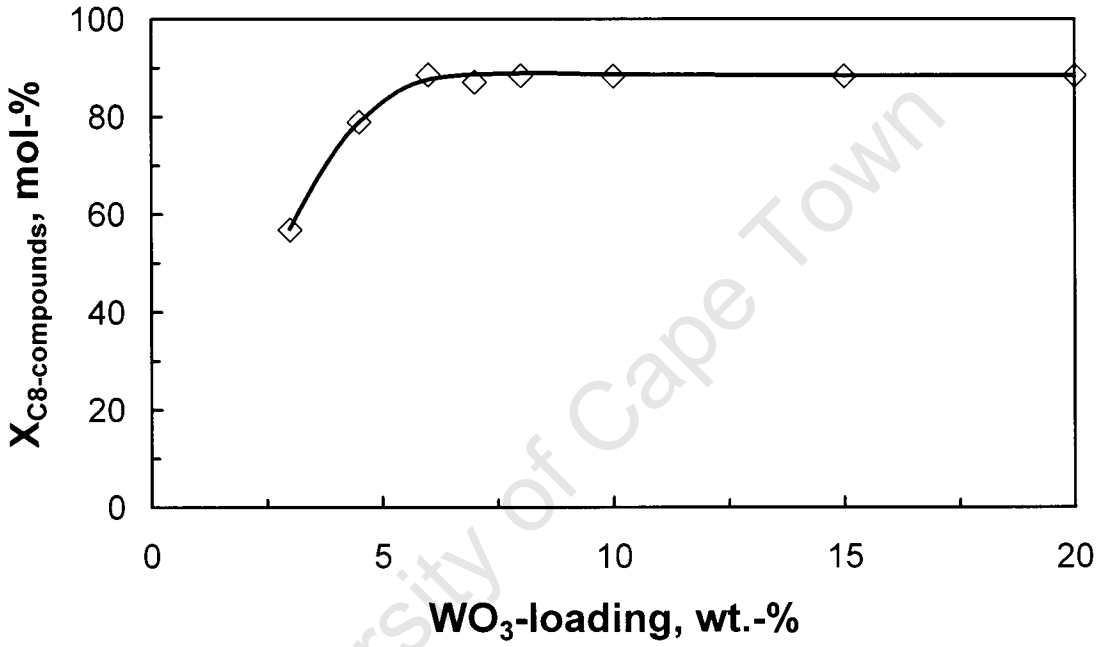

Figure 1.2: Relation between WO_3 loading on a WO_3/SiO_2 catalyst and activity (conversion) in 1-octene metathesis at 460°C, 5.6 LHSV and atmospheric pressure after 8 hours on line[41]

The active sites of tungsten based heterogeneous metathesis catalysts are widely considered to contain the metal in an oxidation state lower than +6[42]. It has been concluded a higher activity is obtained with more reducible tungsten-based catalysts[32]. Santiesteban *et al.*[43] reported a relation between reducibility and catalytic properties in WO_x-ZrO_2. During the metathesis reaction, the active species is reduced by the olefinic feed to the desired oxidation state. Over-reduction of the active species however can result in deactivation of the catalyst.

1.7 Catalyst deactivation in olefin metathesis

Catalyst deactivation is defined as the loss over time of catalytic activity and/or selectivity[44]. This is a great problem and of major concern in the practice of industrial catalytic processes. The causes of deactivation are basically three-fold: chemical, thermal and mechanical[44] and can be grouped into six intrinsic mechanisms of catalyst decay:

- Poisoning(chemical)
- Fouling(chemical)
- Thermal degradation/sintering(thermal)
- Vapour compound formation accompanied by transport(thermal)
- Vapour-solid and/or solid-solid reactions(chemical)
- Attrition/crushing(mechanical)

Poisoning is the strong chemisorption of reactants, products or impurities on catalytic sites[44, 45], thereby blocking sites for catalytic reaction. A species will act as a poison if its adsorption strength is stronger relative to the other species when competing for the same catalytically active sites[44]. The toxicity of the poison can be decreased if it can react with other reagents present in the feed resulting in the removal of the poison from the surface.

Fouling can be explained in terms of deposition of species from the fluid phase onto the catalyst surface. This will result in activity loss due to blockage of active sites and/or pores. Disintegration of catalyst particles and plugging of reactor voids may occur in advanced stages of fouling. Important examples include deposits of carbon and coke in porous catalysts[44]. Carbon is typically a product of CO disproportionation while coke is produced by decomposition or condensation of hydrocarbons on catalyst surfaces and typically consists of polymerized heavy hydrocarbons. The chemical structures of coke or carbons formed in catalytic processes vary with reaction type, catalyst type, and reaction conditions. The rate of coke formation is also a function of acidity and pore structure of the catalyst[44]. The rate and extent of coke formation will generally increase with increasing acid strength and concentration. The yield of coke formation will decrease with decreasing pore size for a fixed acid strength and concentration[44]. It was also observed that the mechanism of coke formation also varies with catalyst type, e.g. whether it is a metal or metal oxide.

Deactivation of supported metals or metal oxides by carbon or coke may occur chemically due to chemisorption or carbide formation or physically due to blocking of surface sites, metal crystallite encapsulation, plugging of pores, and destruction of catalyst pellets by carbon filaments[44]. Blocking of catalytic sites by chemisorbed hydrocarbons, surface carbides or relatively reactive films is generally reversible in hydrogen, steam, CO_2 or oxygen[46].

The formation of coke on oxide catalysts is mainly due to cracking reactions involving coke precursors like olefins or aromatics which are catalyzed by acidic sites on the catalyst surface[47]. Dehydration and cyclization reactions of carbocation intermediates formed on acid sites lead to aromatics which react further to higher molecular weight poly-nuclear aromatics and condense as coke[44].

The formation of coke as a result of the polymerization of olefins can be explained as follows (see Scheme 1.9). The reaction of an olefin with Brønsted acid will yield a secondary carbocation ion. The condensation reaction of a carbocation with an additional olefin yields a condensed, branched longer chain carbocation ion. Desorption from the acid site yield the long chain olefin. The formation of this type of coke is expected to be a low temperature process.

Coke formation due to cyclization from olefins can be described as follows (see Scheme 1.10). The first step involves the formation of an allylic carbocation by reaction of a diene with a primary carbocation. The reaction of an allylic carbocation ion with a Brønsted base yields a triene. Cyclization of the triene yields a substituted cyclohexadiene, which can react with a carbocation to yield a tertiary carbocation ion. The reaction of a tertiary carbocation with Brønsted base yields substituted aromatics.

$$H_2C{=}CHCH_3 + HX \rightleftharpoons CH_3{-}\overset{+}{C}HCH_3 + X^-$$

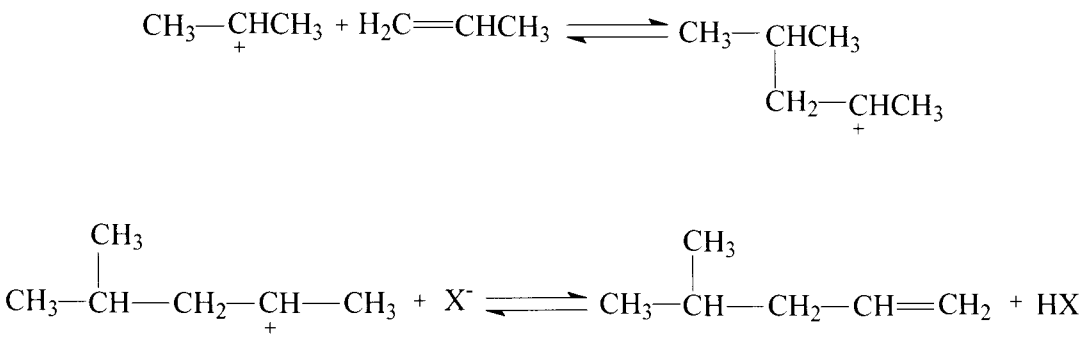

Scheme 1.9: Coke formation due to polymerization of olefins as shown for propene[44]

Coke formation resulting in the formation of polynuclear aromatics is illustrated in Scheme 1.11. The highly stable polynuclear carbocations grow on the surface for a relatively long time before a termination reaction occurs through the back donation of a proton.

1.7.1 Catalyst deactivation on WO_3-based olefin metathesis catalysts

The WO_3/SiO_2 metathesis catalyst requires high reaction temperatures for maximum metathesis activity and operates at temperatures ranging from 450°C-550°C. This high reaction temperature favours coke formation on the catalyst. The amount of coke formation seems to be critical in controlling the lifetime of the catalyst. It was observed that the coke formation increased almost linearly over time and 46% coke is probably the maximum amount of coke formation that the catalyst can handle before it starts to interfere with its performance[48].

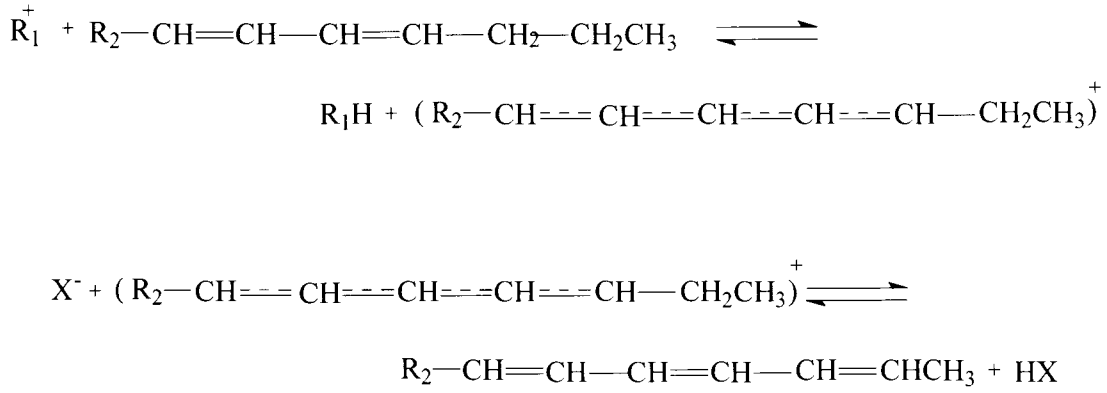

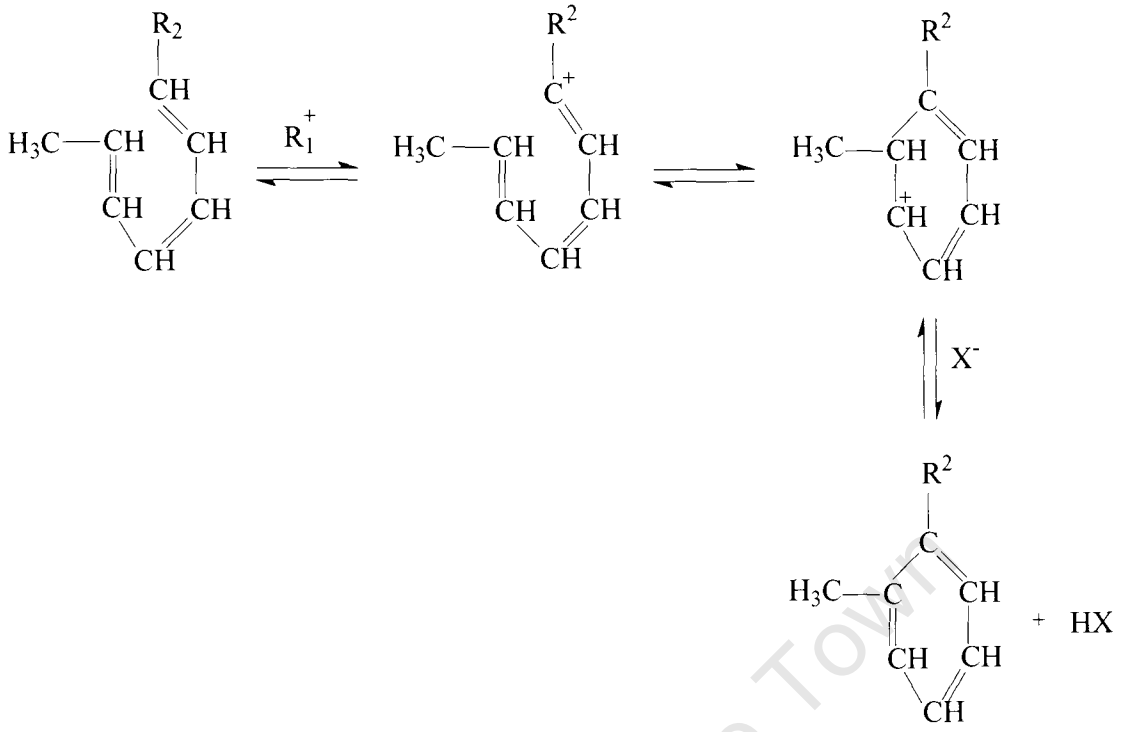

Scheme 1.10: Coke formation due to cyclization of olefins[44]

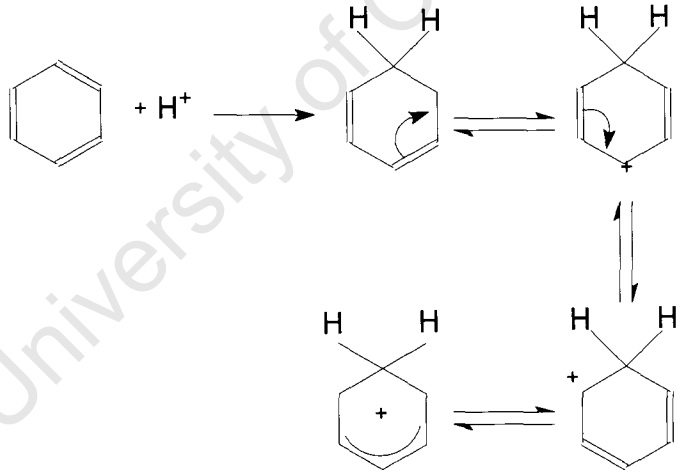

Scheme 1.11: Coke formation due to formation of polynuclear aromatics form benzene

A large amount of coke forms inside the pores of the WO_3/SiO_2 catalyst during the continuous process[49]. All indications are that this coke is predominantly formed inside the pores of the catalyst and not on the surface where the active species are present. This excessive build-up of coke inside the pores of the catalyst does not seem to

cause any cracking of break-up of the catalyst and is easily removed by regeneration treatment.

It has been established that coking increases with increasing acidity of the surface[44]. It is believed that both Lewis and Brønsted acid sites may take part during coking, the former by strongly interacting with basic species in the feed, and the latter by supplying protons to form carbocations, which are also responsible for the formation of coke[50]. This formation of coke is mainly due to cracking reactions involving coke precursors like olefins which are catalyzed by acidic sites on the catalyst surface[44].

The coke build up requires that the catalyst must be periodically regenerated. Repeating the activation procedure with a controlled amount of oxygen to burn off accumulated coke and oxidize the metal to a higher oxidation state can regenerate catalysts that were deactivated during use. The catalyst is regenerated according to a calcination procedure, i.e. 550°C in air for 8 hours.

Gas phase coke formation, as in the case of high temperature metathesis, can be limited by using free radical traps, by introducing gasifying agents like hydrogen or steam. These gasifying agents reduce coke formation by "washing out" heavier hydrocarbon precursors[51].

$$C + 2H_2O \rightarrow CO_2 + H_2 \quad (4)$$

Co-feeding hydrogen facilitates in removing carbonaceous deposits from the surface in the form of methane[51].

$$C + 2H_2 \rightarrow CH_4 \quad (5)$$

1.7.2 Regeneration of the WO_3/SiO_2 catalyst

The tungsten on silica olefin metathesis catalyst can be regenerated, e.g. by calcining in air[49]. This regeneration step had a positive effect on the lifetime and selectivity of the catalyst in 1-octene metathesis performed at 460°C, 5.6 LHSV and atmospheric pressure in a fixed bed reactor. The deactivated catalyst had significant amounts of the coke in the pores of the catalyst, but not on the surface where the active species are present. This coke is easily removed by regeneration. After regeneration of the catalyst, tungsten was found to be present in two oxidation states, viz. WO_3 (W in +6 oxidation state) and $W_{24}O_{68}$, whereas it was only present as WO_3

in the fresh catalysts. TEM analysis of a fresh and regenerated catalyst indicated a decrease in the average crystallite size after regeneration which indicated that the active tungsten species on the support might become mobile during regeneration, covering a larger area of the support and thus exposing more active tungsten sites.

1.8 Aim of study

This study involves the investigation of an 8wt.% WO_3/SiO_2 catalyst in a metathesis reaction. 1-Butene will be used as feedstock for the process. The main focus will be to improve the propene yield and minimize the formation of carbonaceous deposits due to side-reactions during the metathesis reaction. In order to get maximum propene production and minimum coke formation, improvement of the double bond isomerisation activity, lifetime of the catalyst and metathesis activity are of major importance and will be investigated.

The first step to improve the double bond isomerisation will be the investigation of alternative support material for the WO_3/SiO_2 catalyst. The aim will be to use a support material that will increase the isomerisation as well as the metathesis activity. The resulting catalyst will be a bi-functional catalyst of tungsten oxide supported on either an acidic or basic support and will be tested to see the influence of the different support materials on the metathesis activity and coke formation.
The acidic and basic sites on the supports are believed to be mainly responsible for the isomerisation reaction, while WO_3 is responsible for the actual metathesis process as well as part of the isomerisation. In order to increase the metathesis activity, thus propene yield, the double bond isomerisation needs to be improved.

Another possible way of achieving maximum propene production and minimum carbon formation will be to optimize the reaction conditions at which the metathesis reaction takes place. Previous studies involved optimisation of the reaction conditions for butene metathesis using the 8% WO_3/SiO_2 catalyst, incorporating pressure as a variable. The criteria for determining the optimum reaction conditions were set as maximum propene yield, maximum pressure, chemical grade purity of propene (higher than 95%), and minimum coke formation.

2. Experimental

Metathesis of 1-butene was carried out over a series of supported 8wt.-% WO_3-catalysts with the aim to investigate the effect of the acidic properties of the support material on the metathesis reaction. The acidity of the support was changed by varying the amount of alumina in silica-alumina support materials.

2.1 Catalyst synthesis

2.1.1 Catalyst support materials

The silica-alumina materials used in this study belong to the Siralox-series (Sasol Germany GmbH), which are prepared according to the co-hydrolysis method (see Figure 2.1). In this procedure an alumina alkoxide is mixed with silicic acid. Silicic acid catalyses the hydrolysis reaction resulting in the formation of a precipitate containing both aluminium and silicon. The resulting slurry is spray-dried and calcined.

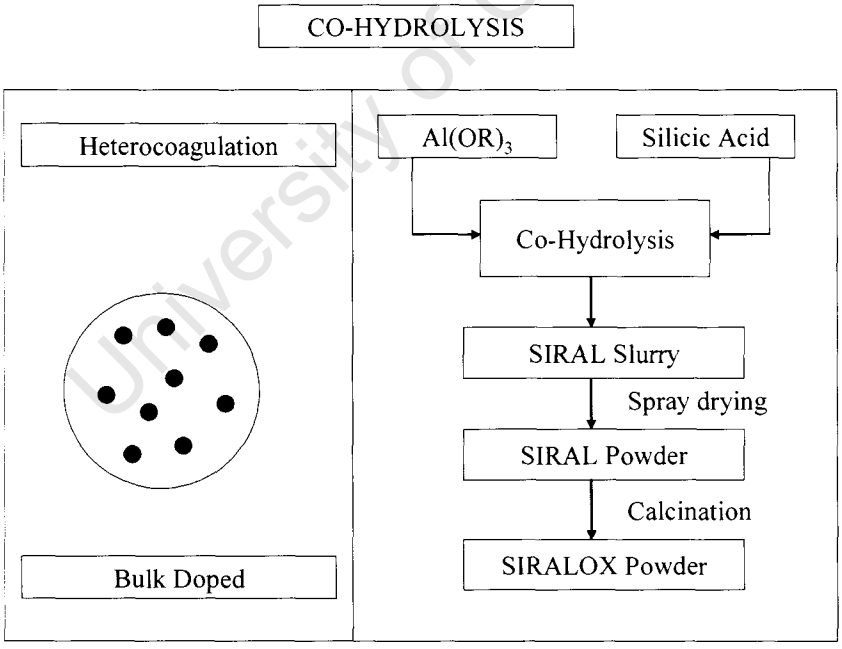

Figure 2.1: Co-hydrolysis preparation method for Siralox support materials

The properties of the silica-alumina materials used in this study are listed in Table 2.1. Pure alumina prepared in a similar process was used as the material without any

silica. The BET-surface area of the support materials varies between 240 and 410 m^2/g. The addition of silicic acid to the hydrolysis process seems to result in an initial increase in the obtained BET-surface area, but high silica loading leads to a decrease of the BET surface area. It can be further noted, that the average pore diameter significantly decreases as a function of the amount of silicic acid added to the hydrolysis process.

For comparison silica from Aldrich was taken as well. The BET-surface area of the chosen material is comparable to that of the silica-aluminas. However, the pore volume, and the average pore diameter are significantly larger than that of the silica-aluminas (but comparable to that of the pure alumina).

Table 2.1: Characteristics of support materials

Support Material	**Supplier**	**SiO_2 (wt.-%)**	**Al_2O_3 (wt.-%)**	**S_{BET} (m^2/g)**	**V_{Pore} (cm^3/g)**	**d_{Pore} (Å)**
Al_2O_3	Sasol[1]	0	100	242	0.80	133
Siralox 20	Sasol[1]	20	80	351	0.70	80
Siralox 40	Sasol[1]	40	60	409	0.84	82
Siralox 75	Sasol[1]	75	25	339	0.31	37
SiO_2	Aldrich	100	0	300	1.15	149

[1]Sasol Germany GmbH

The support materials were crushed to a particle size of 300-500 µm prior to the reaction studies and further used as received from the supplier.

2.1.2 Impregnation

The catalysts (20 g) were prepared by wet-impregnation of the different supports with an aqueous solution of ammonium metatungstate hydrate ($(NH_4)_6(H_2W_{12}O_{40}$ (0.00556 moles) from Aldrich and used as obtained) to yield an 8 wt.-% WO_3-loading on the support. The concentration of the tungsten salt was 0.2778 $mol.dm^{-3}$ before impregnation with the silica and silica/alumina mixtures (18.4 g). Only enough water (300ml) was added to the silica and other support materials to cover it. The dissolved metal solution was mixed with the silica-water mixture and stirred on the rotavap for

2hours, after which the excess water was removed with a Büchi Vacuum controller V-800 at ca. 100 °C and 100 mbar by evaporation.

The catalysts were subsequently calcined according to the following calcinations procedure (see Figure 2.2): The catalysts were dried in an oven using a porcelain dish with diameter of 15 mm at 110 °C for 2 hours. The temperature was then increased to 250 °C at a rate of 1 °C/minute and kept at this temperature for 2 hours. In the final step, the temperature was raised to 600 °C at a rate of 3 °C/minute and maintained at this temperature for 8 hours.

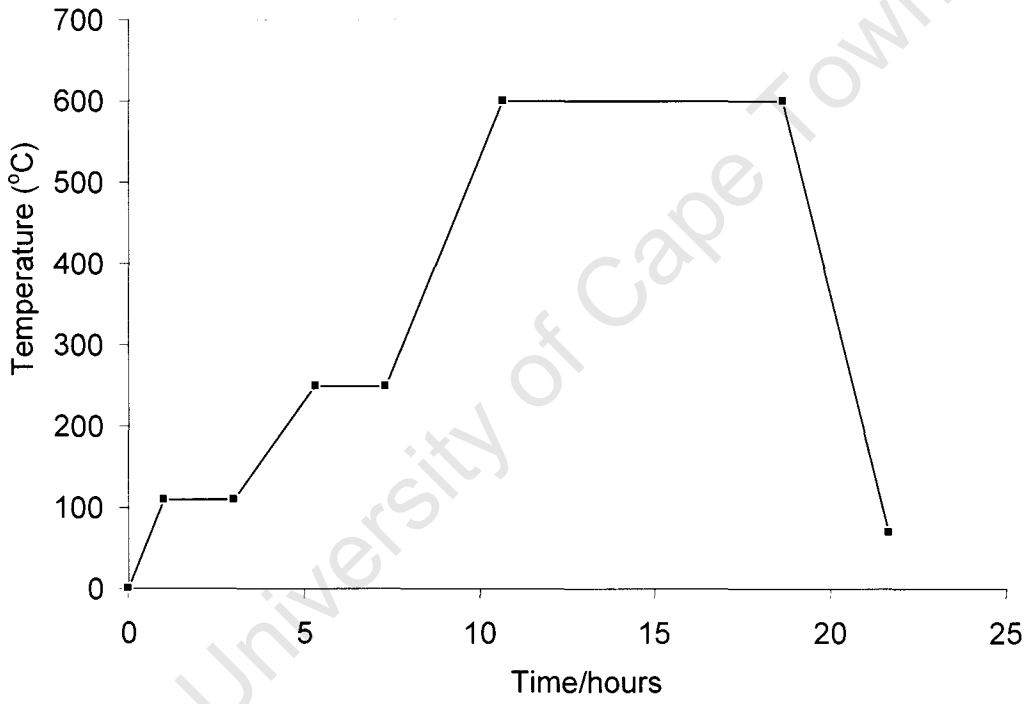

Figure 2.2: Temperature profile during the calcination of the various support materials and catalysts

2.2 Catalyst and support material characterisation

2.2.1 Surface Area Analysis

The specific surface area, pore volume and pore diameter were determined for all the fresh and spent samples using BET analyses on a TRISTAR-Micromeritics apparatus. Approximately 0.25 g of the sample was degassed under N_2 flow at 200 ^{o}C overnight in order to remove any contaminates from the pores. The sample was subsequently cooled to ambient temperature and re-weighed to determine the exact mass of the sample. The method is a measure of the quantity of gas taken up by the solid at a constant temperature (77K) as a function of gas pressure (N_2). The results are expressed as volume of gas at STP while the pressure is expressed as relative pressure (actual pressure divided by vapour pressure of adsorbing gas). The relative pressure range for BET surface area calculation, range between 0.08 to 0.25 in this method and to complete the adsorption over the whole pore size distribution, the relative pressures range between 0.1 to 0.998. The total pore volume is calculated from the volume of gas adsorbed at a relative pressure of 0.998.

The BET surface area is calculated from the following equation:

$V_a = V_m CP / [(P_0-P)(1+(C-1)(P/P_0)]$

C is a constant calculated from the heat of adsorption of the first layer, the heat of liquefaction of the adsorptive, the gas constant and absolute temperature (Analytical methods in fine particle technology by Webb and Orr).

P_0 is the saturation pressure of the gas

Va is the quantity of gas adsorbed at pressure P

Vm the volume of gas adsorbed at monolayer coverage of surface

Using the mass of the sample the BET is expressed as cm3/g

2.2.2 X-Ray Diffraction (XRD)

The crystallinity of the samples was measured on an X'Pert Pro Multi Purpose Diffractometer (MPD), Unit 2. The catalyst samples were packed in individual sample holders with a flat surface that was initially tangent to the focussing circle of the goniometer. The sample holder was mounted in a theta-theta configuration inside the Philips X'Pert Plus powder diffractometer. The diffractometer is equipped with a fast,

solid state X'Celerator detector. It did not require a receiving slit or monochromator. The X-ray generator was operated at 40 kV and 40 mA, using a 1.8 kW long fine-focus cobalt tube. A programmable divergent slit of 1° was used, together with an anti-scatter slit of 2°, both in fixed mode. Scans were done in the continuous mode using a step size of 0.0167 °2theta, and counting time of 75 seconds per step. The scanning range was between 5° 2θ and 105° 2θ and the scan speed was 0.028 °/second. The complete analysis took 1 hour per scan.

2.2.3 Scanning Electron Microscopy (SEM)

Cross sectional samples were prepared and polished to finest grid of 3μm. The catalyst samples were analysed and viewed on a LEO 1450 scanning electron microscope fitted with a Link ISIS energy dispersive X-ray analytical system (EDX). For EDX, the samples were mounted on a graphite stub using double-sided graphite tape. For SEM imaging, the samples were subsequently gold splutter coated using a Polaron E5100 SEM coating unit.

2.2.4 Hydrogen Temperature Programmed Reduction (TPR)

TPR method can be used for characterizing the interaction between active metal and support. TPR is a method by which a reducing gas mixture such as hydrogen diluted in argon (or other inert gas) flows over a sample of an oxide[52]. The initial temperature is usually below the reduction temperature after which the sample temperature is raised at a constant rate and, as reduction begins, hydrogen is consumed from the carrier mixture. Several reduction peaks may be detected over the course of the temperature ramp because reduction likely will be initiated over various thermal energy levels. The general reduction reaction is

$$MO(s) + H_2(g) \longrightarrow M(s) + H_2O$$

Where MO (s) is the solid metal oxide and H_2 the reduction gas.

TPR analysis was performed on all the catalysts to investigate the reducibility of the tungsten on the supports as well as the interaction that the tungsten metal has with the different support materials. An Autochem 2910 (Micromeritics) instrument was used for the measurements. Approximately 0.15 g of sample was dried under argon flow at 120 °C for 10 minutes. The sample was then cooled to room temperature. The

sample was then heated in a flow of 10%H_2/90%Ar with a flow rate of 50 ml (0.85 bar, RT)/minute to 900 °C at a heating rate of 10 °C/minute.

2.2.5 Ammonia Temperature Programmed Desorption (NH_3-TPD)

The number of acid sites on solid catalysts can be determined by the adsorption of suitable and volatile base molecules such a NH_3, pyridine, n-butylamine, quinoline. An excess of the base is adsorbed, and what is considered physically adsorbed is removed by prolonged evacuation or flushing. Whatever is left on the surface is accounted for as chemically adsorbed, and is a measurement for the total number of acid sites. The strength of the acid sites can be found by direct calorimetric measurements giving the heat of adsorption at different base coverages, or by thermal desorption (TPD) of the pre-adsorbed base and calculation of the proportion of adsorbed base evacuated at various temperatures.

NH_3-TPD has been extensively used to measure the acidity of solid catalysts in this sense[53]. This method can however be misleading if ammonia dissociates to give NH_2^- and H^+ species which are adsorbed on both acid and basic sites and this depends on the kind of solid and on the adsorption conditions. Acidity measurements by adsorption of NH_3 and desorption onto a series of silica-alumina catalysts (0-100% alumina) was done by Corma[36]. It was shown that the heat of adsorption drops rapidly with surface coverage. This could be interpreted by assuming that the strongest acid sites, i.e., those with a larger heat of adsorption are the first to adsorb NH_3.

The use of ammonia in the measurement of acid site strengths by TPD is limited. Ammonia is a very small molecule capable of penetrating into small pores in the solid. In addition, ammonia is a rather strong base which is capable of reacting with weak acid sites which do not contribute to the overall activity of the catalysts. Larger molecules such as pyridine are preferable because they penetrate only the range of pores active in catalytic reactions such as cracking and isomerisation. NH_3-TPD measurements were performed on the series of catalysts and supports to investigate the total acidity. An Autochem 2910 (Micromeritics) instrument was used to carry out the acidity studies. Prior to the NH_3 adsorption measurements, approximately 0.150 g

of catalyst was activated at 550 °C for 60 minutes under continuous helium flow at 10 ml (0.85 bar, RT)/minute at local conditions. The catalyst was cooled to 100 °C and then saturated with a 5% NH_3/He gas mixture at a flow rate of 10ml (0.85 bar, RT)/minute for a period of 60 minutes. Physisorbed and gaseous NH_3 were removed by purging with helium for 30 minutes. Thereafter, the sample was heated to 550 °C at 10 °C/minute under a helium atmosphere. During the last step at 550 °C, all the NH_3 which was chemically adsorbed on the acidic sites were desorbed. A calibration was performed prior to the analysis and before peak integration the calibration file was used to subtract the background and water peaks. The peaks were then integrated using build-in software (Peak Editor). The volume of NH_3 desorbed is given as ml (STP) of NH_3 per gram of support/catalyst Using the ideal gas law, the volume of one mole of gas at standard temperature and pressure is equal to 22,4 L[54]. The amount of moles of ammonia desorbed per gram of catalyst was calculated according to:

Number of moles of NH_3 in mmol/g of catalyst = Volume NH_3 (ml/g) / 22.4 ml/mmole

2.2.6 Pyridine adsorption using Fourier Transform Infra Red (FTIR) Spectroscopy

The TPD method cannot differentiate between Brønsted and Lewis acid sites. The infrared technique can be used for this identification and to determine acidity of solid catalysts[55, 56, 57, 58]. IR spectroscopy allows one to look directly at the hydroxyl groups present on a solid acid catalyst and to see which of them can interact with basic molecules, thus which presents Brønsted acidity. The concentration of hydroxyl groups, and therefore the concentration of Brønsted and Lewis acid sites could be obtained form the intensity of the corresponding IR bands. Moreover, when IR is combined with thermal desorption, it can provide estimation of acid strength distribution.

Commonly used probe molecules for measuring concentration of acid sites are[36, 55]:

1. NH_3, Pyridine, piperidine, quinolines, etc., these probe molecules can be used to distinguish between Lewis and Brønsted acid sites
2. CO, CO_2 – CO is good for strong Lewis acid sites. It is less strongly bonded than NH_3 and pyridine and thus more selectively probing strong Lewis acid sites. The

ν_{CO} depends on the cation to which it bonds. CO_2 adsorption occurs selectively on certain sites containing exposed cations and anions.

3. NO – It is similar to CO with the added factor that ν_{NO} shows greater variation in complexes than ν_{CO}. A disadvantage is the high reactivity of NO which can lead to oxidation or reduction of metal (oxides) and salts.
4. Hydrocarbons – Good probes for acidity, since monitoring occurs with reactant. Olefins are more basic than saturated hydrocarbons and thus more selectively adsorbed. They are less basic than NH_3 and pyridine. However, olefins are reactive on acidic sites.

Pyridine adsorption for monitoring acidity

Consider a catalyst which contains both Brønsted and Lewis acid sites. Pyridine will interact as follows:

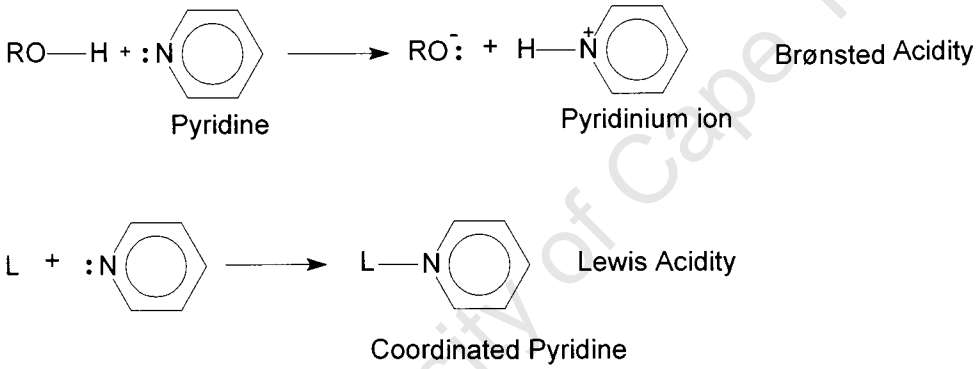

The adsorption bands associated with pyridine are affected by the type of interaction of the acid with the nitrogen atom. From IR frequencies of the bands from pyridine adsorbed on solid acids, it can be seen that the characteristic bands of pyridine protonated by Brønsted acid sites (pyridinium ions) appear at ~1540 and 1640 cm^{-1}, while the bands for pyridine coordinated by Lewis acid sites appear at ~1450 and 1620 cm^{-1}. By measuring the intensity of those bands and from the values of the extinction coefficients given by several authors[59, 60, 61], it is possible to calculate the number of Lewis and Brønsted acid sites capable of retaining pyridine at certain desorption temperatures. The pyridine molecule is thus able to simultaneously determine the concentration of Brønsted and Lewis acid sites.

FTIR of adsorbed pyridine was used to study the acidity of the support materials and tungsten oxide supported on the support materials. This technique can differentiate

between different types of acid sites, i.e. Brønsted and Lewis acid sites. A Bruker Vector 22 FTIR spectrometer fitted with an AABSPEC #-2000 high temperature/pressure cell was used. The samples were ground to a fine powder from which a self-supporting 13 mm diameter wafer was prepared using a pressure of 3 tons. The sample was dried at 500 °C in vacuum for 12 hours. Pyridine was adsorbed at 100 °C and room temperature and allowed to equilibrate for 12 minutes. Excess pyridine was evacuated for 1 hour prior to cooling the sample to room temperature. Sample spectrum was collected using 128 scans. Air was used as the background. The area under the peak at around 1450 cm^{-1} and 1540 cm^{-1} representing the Lewis and the Brønsted acid sites respectively, were integrated using a baseline, a straight line that connects the frequency limits and the peak envelope[36].

2.2.7 Thermogravimetry Analysis (TGA)

Thermogravimetric analysis (TGA) of the spent catalysts and supports was done on a TA Instrument (SDT 2960 Simultaneous DSC-TGA) to determine the amount of coke (wt %) formed. The step prior to the TGA experiments were performed in nitrogen at 100°C, standard pressure and a flow rate of 140 ml (0.85 bar, RT)/minute at ambient conditions. This step was included to remove any traces of moisture or feed condensed on the catalysts. In the next step, the gas was changed to air to determine the mass loss due to carbon deposits. The temperature was increased to 100 °C, kept constant for 30 minutes before it was increased to 350 °C and kept constant at this temperature for 30 minutes. The temperature was then ramped to 550 °C and held at this temperature for 30 minutes to burn the coke from the catalyst. The heating rate was 10 °C/minute for all of the temperature ramping steps.

2.3 Reaction studies

2.3.1 Experimental Set-up

Figure 2.3 shows schematically the reactor set-up used for the reaction studies of both metathesis and isomerisation reactions. The dried feed was fed to a fixed bed reactor equipped with a sliding thermocouple. The liquid products were collected in the product pot at atmospheric pressure. Samples of the off-gas could be taken at the gas sample point.

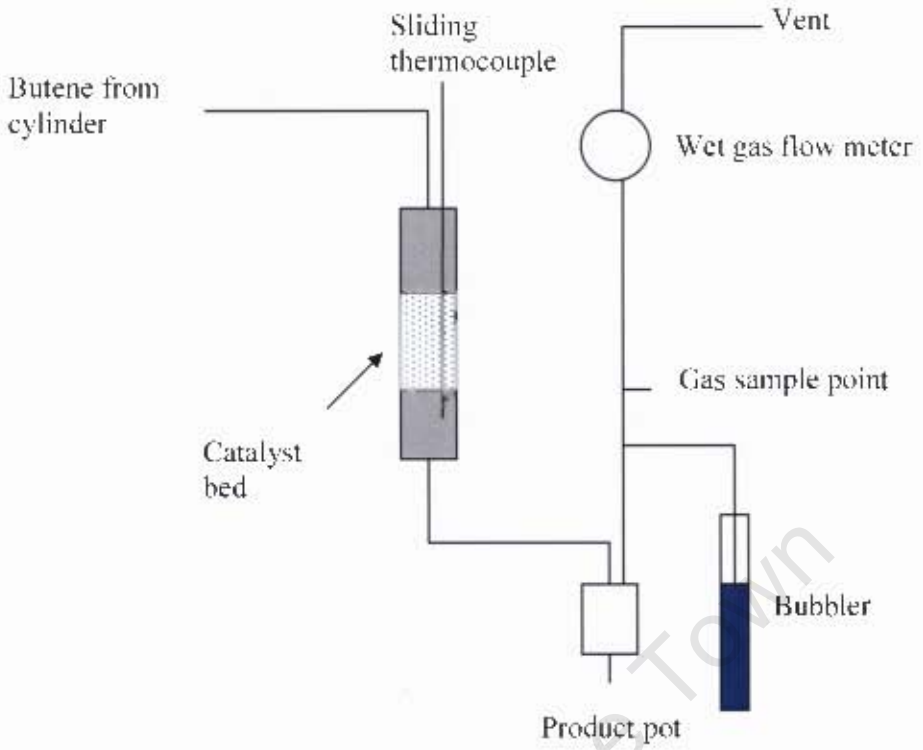

Figure 2.3: Schematic illustration of the reactor set-up

2.3.1.1 Reagents

The feed that was used for all the reactions was 99.38 % pure 1-butene from Air Liquide (see Table 2.2). The majority of the impurities were other C_4-compounds, such as butane and 2-butenes. A filter, containing aluminium oxide was placed in the gas line to remove water from the feed[62].

Table 2.2: The composition (Mass %) of the feed used for the metathesis reactions

Methane	0.018
ethane + ethene	0.001
propane + propene	0.004
C_4 paraffins	0.230
1-butene	99.378
2-butenes	0.365
C_5	0.004
C_6	0.000

2.3.2 Isomerisation Reaction Studies

Isomerisation reactions with a number of support materials were performed using a tubular fixed bed reactor equipped with a sliding thermocouple (see Figure 2.3). The experiments were carried out in the gas phase at atmospheric pressure (0.85 bar). A 10 mm inner reactor diameter was used for all the reactions. A carborandum (24 grit) preheating zone was placed in front of the catalyst bed. The supports were activated *in situ* at 500 °C for 16 hours under a constant nitrogen flow of 25.3 ml (0.85 bar, RT)/minute. After activation, the catalysts were cooled to the desired reaction temperature. The 1-Butene isomerisation was carried out at:

$v_{catalyst}$, ml	2.0
$T_{reaction}$, °C	100
p, bar	0.85 (atmospheric pressure)
GHSV, ml(0.85 bar, RT) /h/$ml_{catalyst}$*	1000
Flow rate, ml(0.85 bar, RT)/minute	33.33

*Reactions were carried out at constant GHSV, thus the volume of catalyst was kept constant, measured with a measuring cylinder.

The feed was 100 % pure 1-butene from Air Liquide. Liquid product was not formed at these reaction conditions. The gaseous product was collected at the gas sample point after the reactor. The off-gas was measured using a wet gas flow meter. Short runs of 6 hours were performed and samples were taken every hour.

2.3.3 Metathesis Reaction Studies

Metathesis reactions with a number of tungsten catalysts supported on different acidic/basic support materials were performed in a tubular fixed bed reactor equipped with a sliding thermocouple (see Figure 2.3). All reactions were done at atmospheric pressure (0.85 bar) and for this purpose a 15 mm inner diameter reactor was used. A carborandum (24 grit) preheating zone was placed in front of the catalyst bed. The experiments were carried out in the gas phase. The catalysts were activated *in situ* at 500 °C for 16 hours under a constant nitrogen flow of 25.3 ml (0.85 bar, RT)/minute. After activation, they were cooled down to the desired reaction

temperature. The liquid product was collected in a product pot and the gaseous product at the gas sample point after the reactor. The off-gas was measured using a wet gas flow meter. Short runs of 6 hours were performed and samples were taken every hour.

The experimental conditions for the 8wt. %WO_3/SiO_2 during metathesis of 1-Butene focussed on maximum propene yield, chemical grade purity for propene (larger than 95%), and minimum coke formation[63]. All metathesis reactions were carried out at the optimised reaction conditions:

$M_{catalyst}$, g	4
$v_{catalyst}$, ml	10.5
$T_{reaction}$, °C	450
p, bar	0.85 (atmospheric pressure)
GHSV, ml(0.85 bar, RT) /h/$ml_{catalyst}$*	500
Flow rate, ml(0.85 bar, RT) /minute	87.5

*Reactions were carried out at constant GHSV, thus the volume of catalyst was kept constant, measured with a measuring cylinder.

2.3.4 Product Analysis

2.3.4.1 Analysis of gas product samples

GC-FID analysis of the gaseous fraction of the product was performed using a HP gas chromatograph equipped with a PLOT fused silica CP-Al_2O_3/KCl column (50 m x 530 μm x 10 μm). Hydrogen was used as the carrier gas. The oven temperature program started at an initial temperature of 70 °C for 3 minute, whereafter it was ramped at a rate of 6 °C/minute to 190 °C, and kept at this temperature for 10 minute. An injection volume of 1 ml and a split ratio of 180:1 were used. A typical gas chromatogram of the gaseous products of 1-Butene metathesis is shown in Figure 2.4.

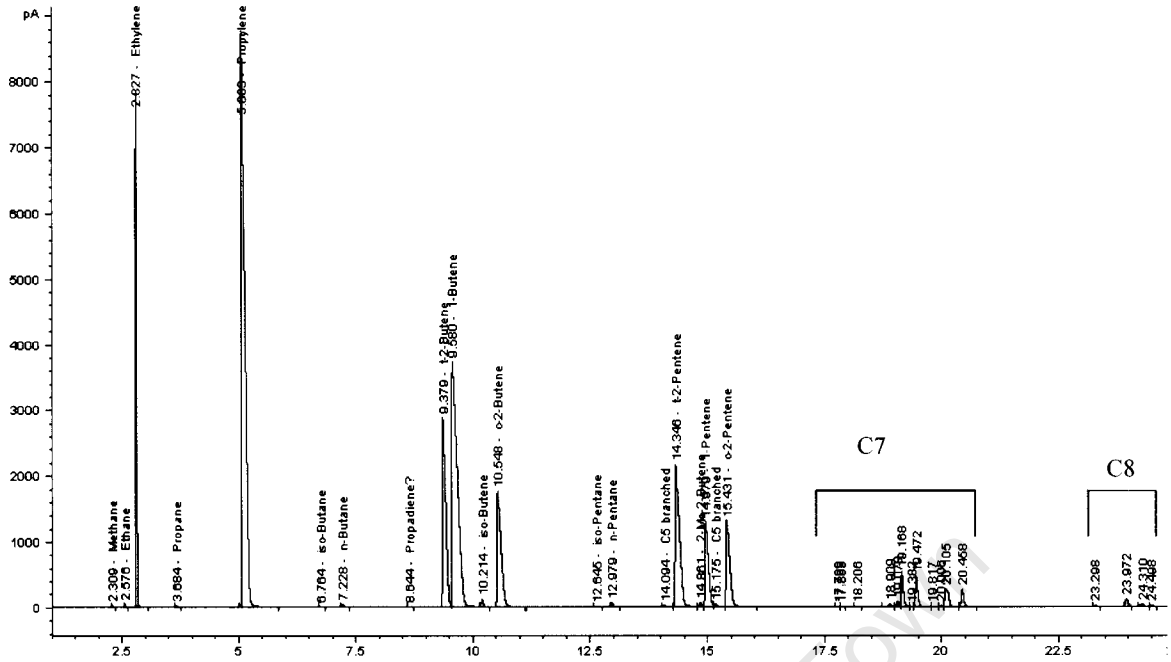

Figure 2.4: Typical gas chromatogram of the gaseous products of 1-Butene metathesis over an 8wt. %WO_3/SiO_2 catalyst

2.3.4.2 Analysis of liquid product samples

GC-FID analysis of the liquid product was performed using a gas chromatograph equipped with a CP Sil PONA column (100 m x 250 μm x 0.50 μm). The oven temperature program started at an initial temperature of 50 °C for 2 minutes, whereafter it was ramped at a rate of 12 °C/minute to 260 °C, and kept at this temperature for 10 minutes. An injection volume of 1 μl and a split ratio of 100:1 were used. Figure 2.5 shows a typical gas chromatogram of the liquid product of 1-Butene metathesis over an 8wt. %WO_3/SiO_2 catalyst.

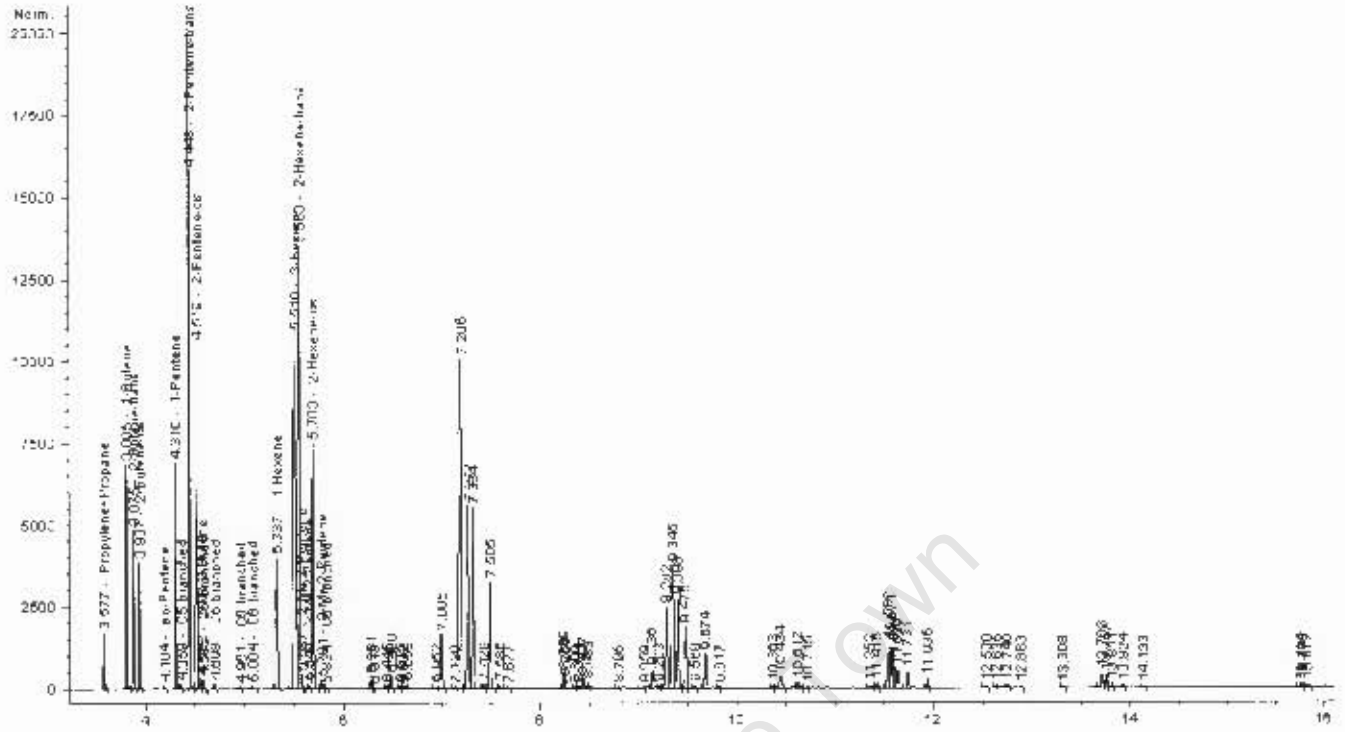

Figure 2.5a: Typical gas chromatogram of the liquid products of 1-Butene metathesis over an 8wt. %WO_3/SiO_2 catalyst, showing the whole chromatogram.

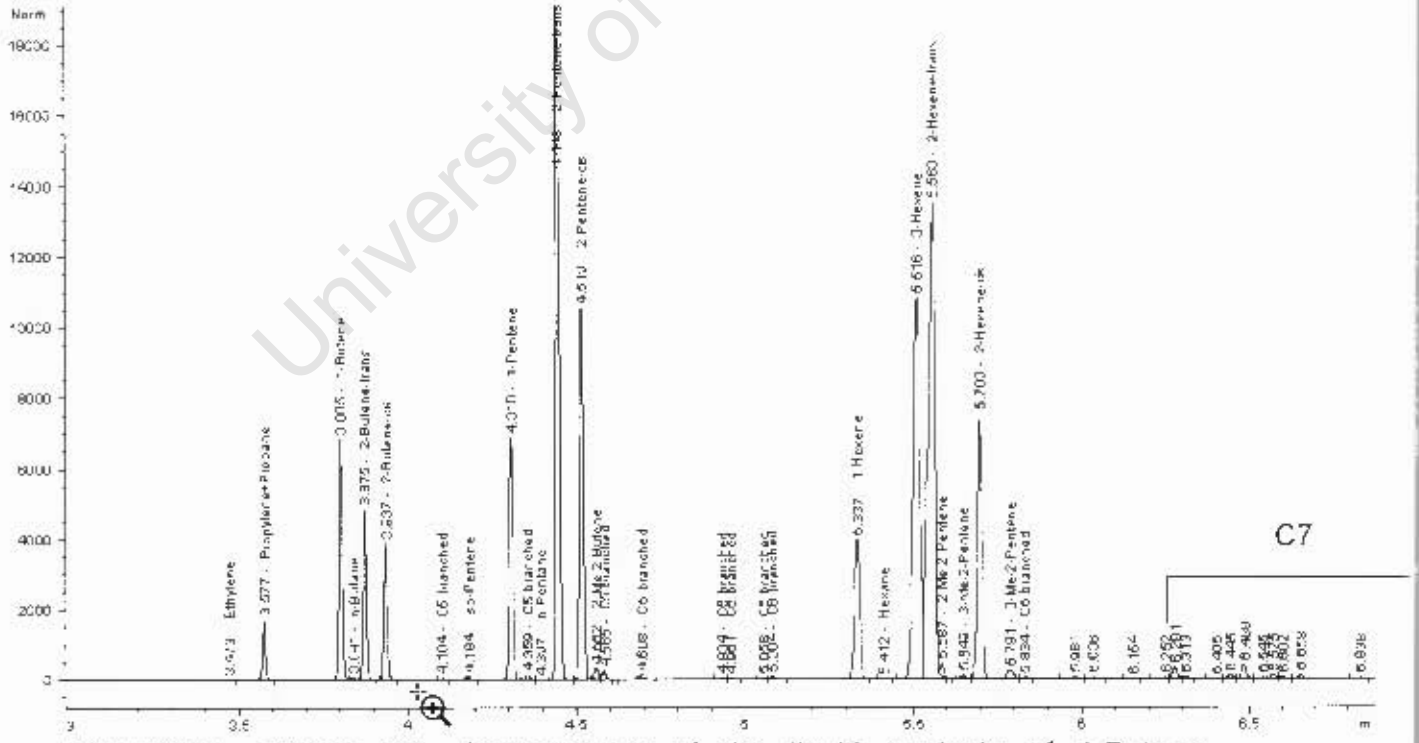

Figure 2.5b: Typical gas chromatogram of the liquid products of 1-Butene metathesis over an 8%WO_3/SiO_2 catalyst, showing the enlarged region (up to C7)

Data Evaluation

The gas flow rate of the off-gas was measured using a wet gas flow meter. Thus, the total number of moles of gaseous products could be determined from the measured volumetric flow rate of the off-gas using the ideal gas law.

$$\dot{n}_{gas,total} = \dot{V}_{gas,measured} \cdot \frac{p_{atmosphere}}{R \cdot T_{ambient}} \quad (2.1)$$

The GC-analysis of the gaseous products yielded the composition of the gas mixture. It was assumed here that the C-based response factor for each of the components was approximately 1[64], since they are hydrocarbons. Thus, the peak area percentage for a certain compound i ($A_{i,gas}$) corresponds to the mass-% of the compound i ($m_{i,gas}$) present in the gas mixture. The molar equivalent of a compound i in the gas phase ($n_{eq,i,gas}$) can thus be calculated knowing the molecular mass of the compound (M_i)

$$n_{eq,i,gas} = \frac{m_{i,gas}}{M_i} = \frac{A_{i,gas}}{M_i} \quad (2.2)$$

The molar flow rate of a compound i in the gas phase is thus given by:

$$\dot{n}_{gas,i} = \frac{n_{eq,i,gas}}{\sum_i n_{gas,i,eq}} \cdot \dot{n}_{gas,total} = \frac{\frac{A_{i,gas}}{M_{i,gas}}}{\sum_i \frac{A_{i,gas}}{M_{i,gas}}} \cdot \dot{n}_{gas,total} \quad (2.3)$$

The mass flow rate of a compound i in the gas phase is thus given by:

$$\dot{m}_{gas,i} = \dot{n}_{gas,i} \cdot M_i = \frac{A_i}{\sum_i \frac{A_i}{M_i}} \cdot \dot{n}_{gas,total} \quad (2.4)$$

The liquid product was collected over a period of time and was weighed and recalculated in a mass flow rate. The GC-analysis of the liquid product was used to calculate the mass flow rate of each compound i in the liquid phase. It was again assumed here that the C-based response factor for each of the components was approximately 1[64], since they are hydrocarbons. Thus, the peak area percentage for a certain compound i ($A_{i,liquid}$) corresponds to the mass-% of the compound i ($m_{i,liquid}$) present in the liquid mixture.

$$\dot{m}_{liquid,i} = A_{i,liquid} \cdot \dot{m}_{liquid,total} \quad (2.5)$$

The total amount of each component was thus calculated using the amounts of the component in g/h in the gaseous product as well as the liquid product.

$$\dot{m}_{total,i} = \dot{m}_{gas,i} + \dot{m}_{liquid,i} \quad (2.6)$$

2.3.5.1 Conversion, yield, selectivity and purity

The conversion of 1-butene ($X_{1\text{-butene}}$) was calculated knowing the mass flow rate of 1-butene fed (known from the total mass flow rate and the feed purity) and the mass flow rate of the unreacted 1-butene, i.e. 1-butene in the product stream:

$$X_{1-butene} = \frac{\dot{m}_{feed,1-butene} - \dot{m}_{total,1-butene}}{\dot{m}_{feed,1-butene}} = \frac{\dot{m}_{feed} \cdot x_{1-butene,feed} - \dot{m}_{total,1-butene}}{\dot{m}_{feed} \cdot x_{1-butene,feed}} \quad (2.8)$$

The yield of a product i (Y_i) was calculated on a mass basis:

$$Y_i = \frac{\dot{m}_{total,i}}{\dot{m}_{feed,1-butene}} = \frac{\dot{m}_{total,i}}{\dot{m}_{feed} \cdot x_{1-butene,feed}} \quad (2.9)$$

The selectivity for a product compound i (S_i) was calculated from:

$$S_i = \frac{Y_{,i}}{X_{1-butene}} \quad (2.10)$$

In the metathesis reaction, the purity of a product class is of interest as well. The purity of ethene (C_2) was defined as:

$$P_{C_2} = \frac{\dot{m}_{total,ethylene}}{\dot{m}_{total,ethylene} + \dot{m}_{total,ethane} + \dot{m}_{total,methane}} \cdot 100\% \quad (2.11)$$

and the purity of propene (C_3) was defined as:

$$P_{C_3} = \frac{\dot{m}_{total,propylene}}{\dot{m}_{total,propylene} + \dot{m}_{total,propane}} \cdot 100\% \quad (2.12)$$

3. Results

3.1 Introduction

The purpose of the investigation was to study the effect of the acidity of the supported tungsten oxide (8 wt.-% WO_3) catalyst on various support materials on the 1-Butene metathesis with particular emphasis on activity, selectivity and coke formation. The acidity of the support materials and the supported catalysts activity of an 8% WO_3/SiO_2 catalyst was probed using NH_3-TPD, pyridine adsorption and 1-butene isomerisation.

3.2 Characterisation of starting materials

3.2.1 BET-surface area, pore volume and average pore diameter

Table 3.1 shows the BET-surface area, pore volume and average pore diameter for the supported catalysts. Loading tungsten oxide on the surface of the supports leads to a reduction in the BET-surface area and the pore volume (compare with Table 2.1).

Table 3.1: BET-surface area, pore volume and average pore diameter of supported tungsten oxide catalysts

Catalyst	SiO_2 (wt.-%)	Al_2O_3 (wt.-%)	S_{BET} (m^2/g)	V_{Pore} (cm^3/g)	d_{Pore} (Å)
8% WO_3/Al_2O_3	0	100	237	0.70	119
8% WO_3/Siralox 20	20	80	311	0.63	81
8% WO_3/Siralox 40	40	60	328	0.75	92
8% WO_3/Siralox 75	75	25	246	0.25	41
8% WO_3/SiO_2	100	0	260	1.02	156

Figure 3.1 shows the relative reduction in the BET-surface area, pore volume and average pore diameter as a function of the silica content in the carrier. The relative decrease in the surface area is the highest for the support containing 75 wt.-% silica. The less strong decline in the pore volume in comparison to the decline in the BET-surface area leads to an increase in the average pore diameter. The average pore diameter for alumina increases, since the decline in the pore volume is larger than the decline in the BET-surface area. It is expected that with the loading of the metal

onto the supports, the BET-surface area and pore volume would decrease, because metal is deposited. This trend was indeed observed. The likely cause for the loss of pore volume and BET-surface area is probably the formation of a multilayer of crystalline material, which could lead to the restriction of the smallest micro pores[65].

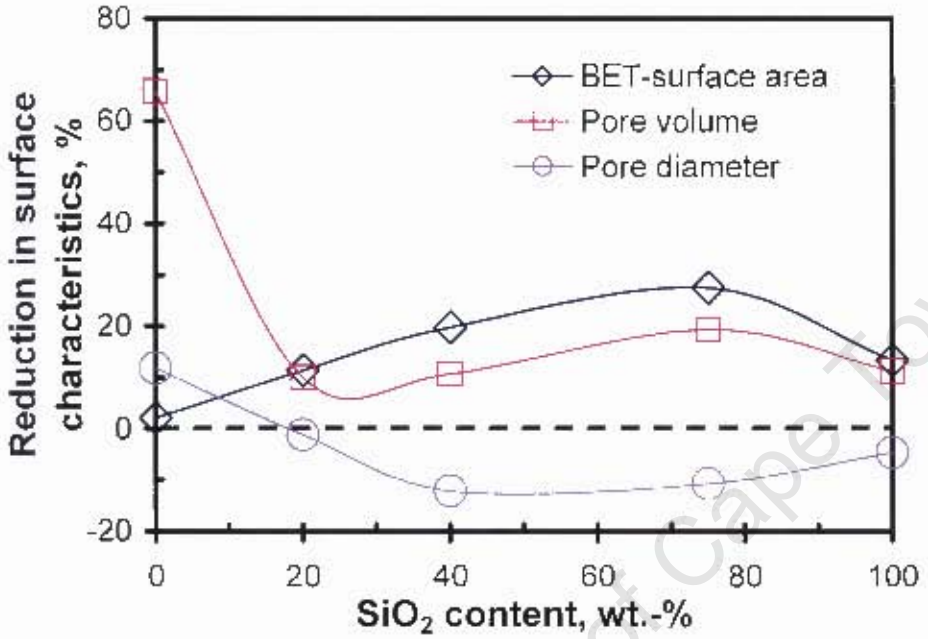

Figure 3.1: Relative reduction in BET-surface area, pore volume and average pore diameter in the calcined 8 wt.-% WO_3 catalysts as a function of the silica content of the support material

3.2.2 Crystallinity of supported WO_3-catalysts

XRD analysis was performed on the fresh catalysts to determine the crystallinity of the tungsten oxides (see Figure 3.21 A.1 – 3.21 A.4 on p66-p68). The scans of the spent residues have been overlaid with the respective scans of the fresh preparations. Scans in blue are of the fresh preparations while the ones in pink (on the same set of axis) are of the spent residues. WO_3 on alumina support shows only broad reflections attributable to γ-Al_2O_3 (See Figure 3.21 A.1 p66). WO_3 on alumina is thus XRD-amorphous.

Tungsten oxide is not visible in the XRD patterns of WO_3/Siralox 20 in both fresh and spent preparations (See Figure 3.21 A.2 p67). Graphitic carbon is identified in the spent WO_3/Siralox 20 sample.

The unidentified crystalline phase in the Siralox 40 support material disappears upon the introduction of WO_3 on to the support. Reflections attributable to tungsten oxide cannot be observed with Siralox 40 as a support, and thus tungsten oxide on Siralox 40 is XRD-amorphous (See Figure 3.21 A.2 p67).

Tungsten oxide is not visible in the XRD patterns of WO_3/Siralox 75 in both fresh and spent preparations (See Figure 321 A.3 p68).

On the contrary, XRD patterns for WO_3 on silica support exhibit crystalline tungsten oxide phases. For fresh catalyst the orthorhombic WO_3 phase could be identified (See Figure 3.21 A.3 and A.4 p68). The observed crystalline tungsten phase was identified as stoichiometric WO_3 orthorhombic (oxidation state +6) in the fresh catalyst preparation, but the spent catalyst transforms into the lower symmetry monoclinic sub-stoichiometric $WO_{2.9}$ phase with possible reduction of tungsten oxidation state.

The average crystallite size (CSP) was determined using the Debye-Scherrer equation:

$$CSP = k\lambda / (B \cdot \cos\Theta)$$

where:

k = a constant (0.9 when FWHM is used)

λ = wavelength of the radiation

B = peak width in radians

Θ = diffraction angle

The observed average crystallite size is affected by both the size of the crystals and the disorder within the crystals. The average crystallite size is given in Table 3.2 for the samples with definite crystalline phases. Some crystal growth of the alumina phase may have happened during the impregnation of the support material with tungsten. Only with silica as a support, diffraction lines attributable to tungsten oxides were observed. The silica-supported catalyst large tungsten oxide crystals are observed.

Table 3.2: Average Crystallite sizes using the Debye-Scherrer equation[66]

Support		$d_{\gamma\text{-}Al_2O_3}$, Å	d_{WO_x}, Å
Alumina	Fresh catalyst	47	
	Spent catalyst	46	
Siralox 20	Fresh catalyst	41	
	Spent catalyst	42	
Siralox 40	Fresh catalyst		
	Spent catalyst		
Siralox 75	Fresh catalyst		
	Spent catalyst		
Silica	Fresh catalyst		>500 (WO_3)
	Spent catalyst		>500 ($WO_{2.9}$)

XRD analysis gives information on how the crystal structure changes in going from the fresh to the spent catalyst. It can also used to determine the oxidation state of tungsten before and after the reactions in order to see how much of the tungsten was reduced to the active oxidation state and whether any of the tungsten was over-reduced. This information can be used to explain the activity of tungsten on different acidic supports. In the metathesis of butene to propene under the specified reaction conditions, it is believed that the active form of the tungsten oxide catalysts is in the reduced form ($WO_{2.95}$) in the +5 oxidation state. The amount of tungsten in the +5 oxidation state should be related to the metathesis activity of the different catalysts. The amount of tungsten in the +5 oxidation state will indicate how easily the tungsten was reduced to the active oxidation state. The XRD analysis revealed tungsten in the form of WO_3 and $WO_{2.95}$ which corresponds to W^{6+} and W^{5+} on the spent catalysts which corresponds to the literature[67]. It was found that this slightly reduced blue oxide was more active than the WO_3. Active species can thus be concluded to be W^{5+} species. It was found that the rate of catalytic reactions on tungsten oxide

catalysts increases with a slight reduction of the W^{6+} centres, which often occurs during catalytic reactions in reducing hydrocarbon environments[100]. It was first reported by Sabatier that yellow WO_3 crystallites were readily reduced to a stoichiometry corresponding to $WO_{2.95}$[34].

3.2.3 SEM Analysis

SEM analysis was done on the catalysts to obtain visual results of the dispersion of tungsten on the support materials. SEM images of tungsten oxide on the various support materials are shown in Figure 3.3.

The γ-alumina supported catalysts shows clearly the support particles consisting of smaller grains. The Siralox support materials show much clearer both the particles and the grains on this scale. It is noteworthy that the particles of Siralox are less smooth than the particles of γ-alumina. Silica has a different, but also smooth morphology. Only with the WO_3/SiO_2 catalysts could WO_3 crystallites be seen. These results confirm the XRD-analysis, showing high dispersion (XRD-amorphous) for the Siraloxes and Alumina, and low dispersion (large crystallites) for silica. The WO_3 crystallites are thus well dispersed over the silica support.

Fresh WO_3/Al_2O_3

Fresh WO_3/Siralox 20

Fresh WO_3/Siralox 40

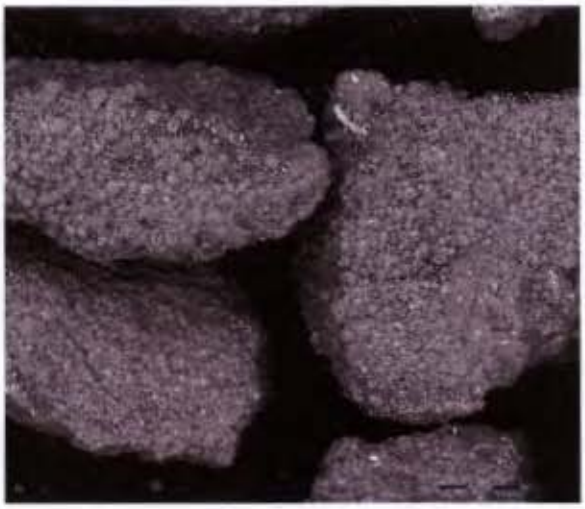

Fresh WO_3/Siralox 75

Fresh WO_3/SiO_2

Figure 3.3: SEM-images of WO_3 on various support materials (bar indicates 200 µm)

3.2.4 Reducibility of supported WO_3-catalysts

The effect of silica content on the reducibility of the tungsten impregnated support materials was investigated by means of temperature programmed reduction (TPR) with hydrogen. Figure 3.4 shows the TPR-profiles of the 8 wt.-% WO_3-catalysts. The first peak at 720 °C represents the reduction of tungsten from the +6 oxidation state to the +5 oxidation state[65, 67, 21, 34]. The second peak at 820 °C in the TPR profile of the WO_3/SiO_2 catalyst represents further reduction from +5 to a lower oxidation state, tungsten in the +4 oxidation state[65, 67, 21, 34]. The catalyst containing no alumina, WO_3/SiO_2, showed the lowest reduction temperature. The reduction of tungsten impregnated on pure silica support was more facile than the reduction of tungsten on

Shown below are the TPR Profiles of the WO_3 supported catalysts

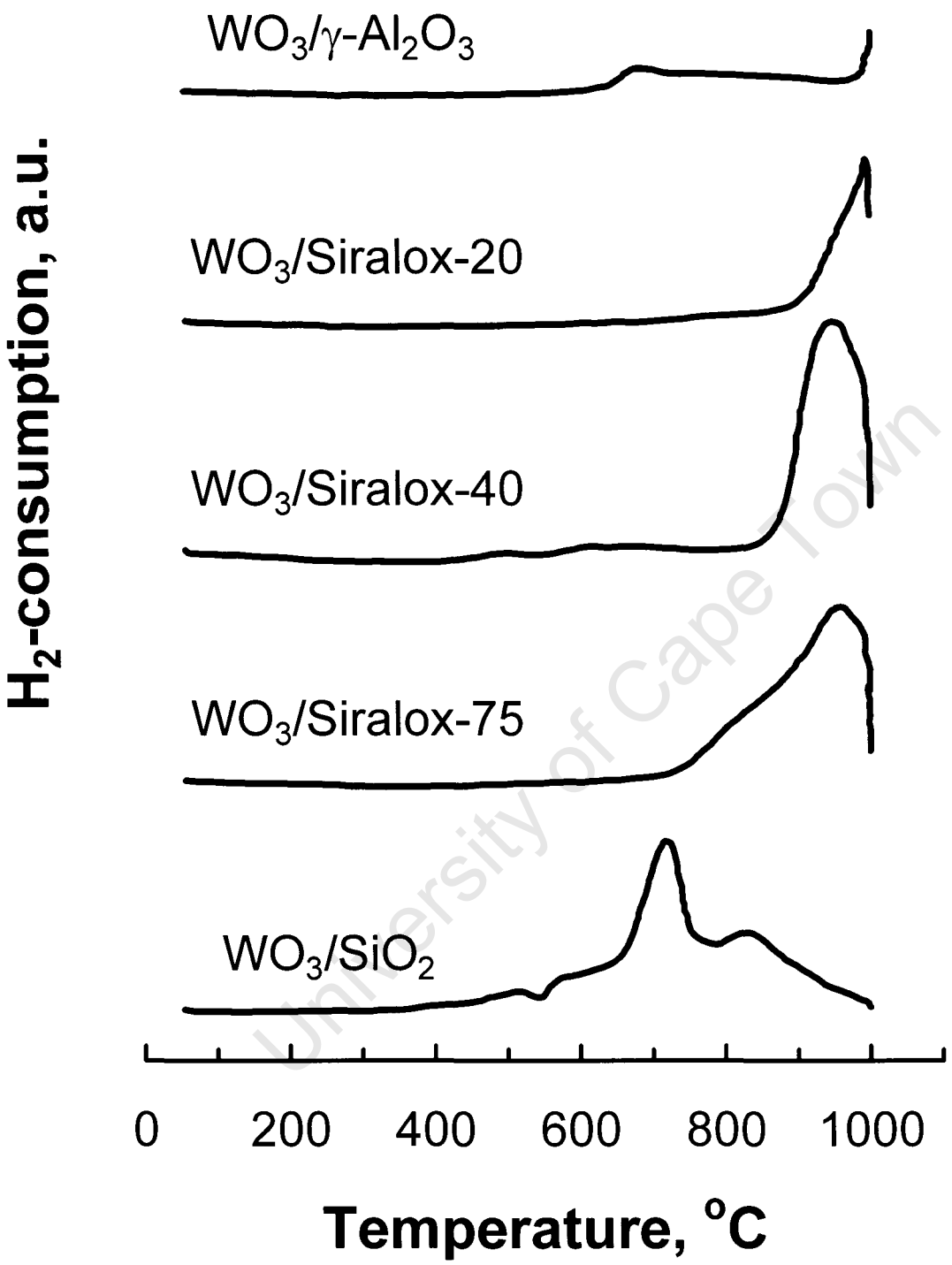

Figure 3.4: TPR-profiles of tungsten supported on various support materials

3.2.5 Characterisation of acidity using NH_3-TPD

The total acidity of the support materials and of the 8 wt.-% WO_3 on the various support materials was determined by means of NH_3–TPD. Figure 3.5 shows the TPD-profiles of the support materials and the corresponding supported catalysts.

From the TPD profiles, it is evident that more than one peak is present, which is attributed to NH_3 desorption from different Brønsted and Lewis acid sites. However, these peaks are overlapping and can not be deconvoluted. The overlapping peaks would represent the amount of strong and weak acid sites. The NH_3-TPD method could only be used to obtain the total acidity which includes the amount of Brønsted and Lewis acid sites.

The total acidity as measured using NH_3-TPD is given in Table 3.4. The total acidity increases with increasing silica content for the alumina containing support materials up to Siralox 40 after which it decreases again. The presence of tungsten oxide in the catalyst increases the total acidity implying that tungsten oxide itself is acidic or induces acid sites. For alumina and Siralox 20 (80 wt.-% Al_2O_3) an increase of 0.07 mmol/g was obtained, whereas for Siralox 40 an increase of 0.06 mmol/g was observed and Siralox 75 an increase in total acidity of 0.12 mmol/g was obtained. The silica supported tungsten catalyst showed the lowest increase of ca. 0.04mmol/g. This represents an acidity, which might be attributable to tungsten, of 0.5 mmol of acid sites per gram of WO_3 for silica supported tungsten and between 0.9 and 1.0 mmol of acid sites per gram of WO_3 for alumina and Siralox supported tungsten. The higher acidity per gram of WO_3 for alumina and Siralox supported tungsten might be related to the higher dispersion of tungsten on these materials.

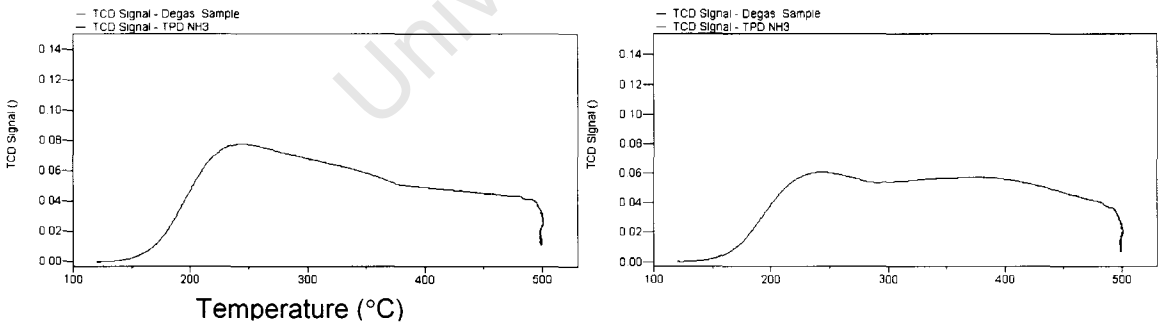

NH_3-TPD profile of the Al_2O_3 support (left) and 8 wt.-% WO_3/Al_2O_3 (right)

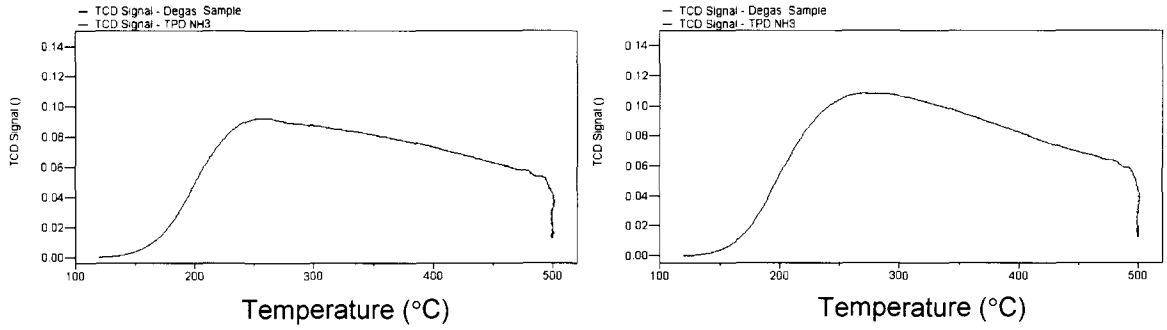

NH_3-TPD profile of the Siralox 20 support (left) and 8 wt.-% WO_3/Siralox 20 (right

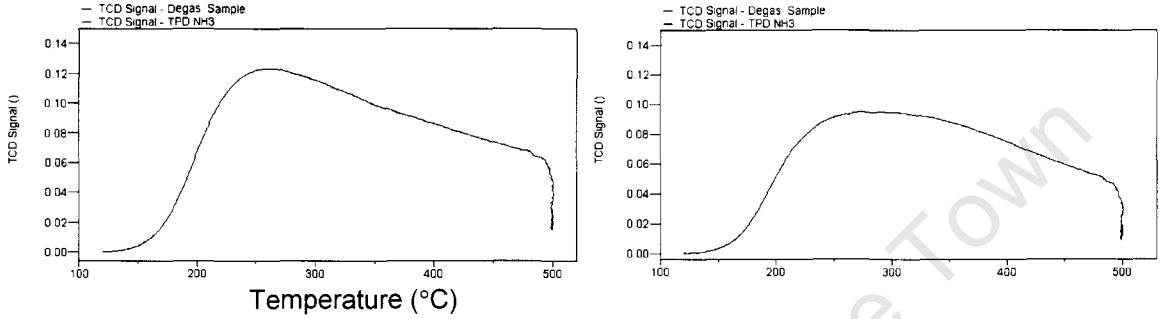

NH_3-TPD profile of the Siralox 40 support (left) and 8 wt.-% WO_3/Siralox 40 (right)

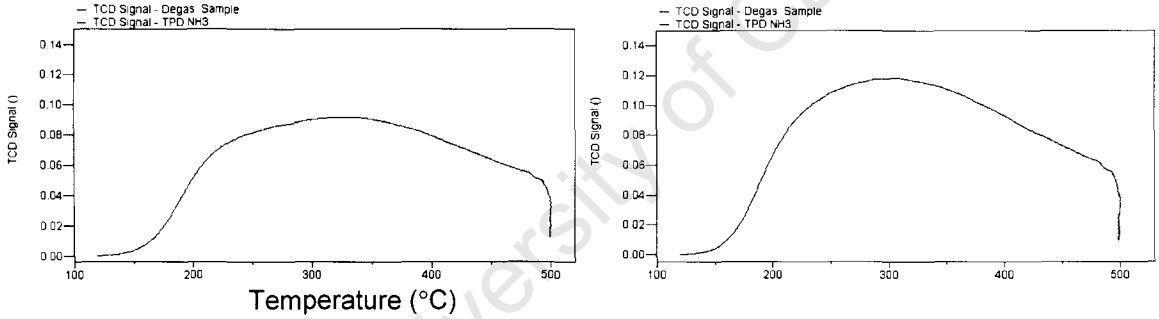

NH_3-TPD profile of the Siralox 75 support (left) and 8 wt.-% WO_3/Siralox 75 (right)

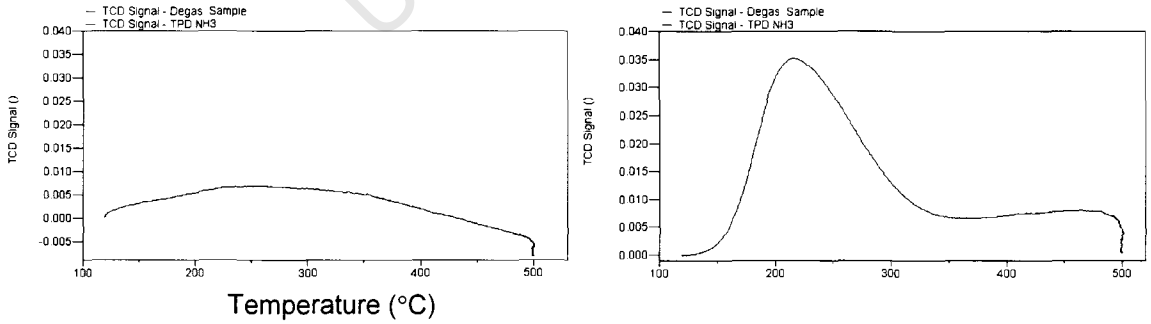

NH_3-TPD profile of the SiO_2 support (left) and 8 wt.-% WO_3/SiO_2 (right)

Figure 3.5: NH_3-TPD-profiles of support materials and tungsten supported on various support materials

Table 3.4: Total acidity of support materials and tungsten supported on the various carriers as determined by NH_3-TPD

Support Material	SiO_2 (wt.-%)	Al_2O_3 (wt.-%)	Total acidity of support (mmol/g)	Total acidity of 8 wt.-% WO_3 on support (mmol/g)
Al_2O_3	0	100	0.16	0.23
Siralox 20	20	80	0.22	0.29
Siralox 40	40	60	0.27	0.37
Siralox 75	75	25	0.25	0.33
SiO_2	100	0	0.01	0.05

The acidity results were used to investigate the effect of silica content on the total acidity of the acidic support materials and catalysts. Results revealed an increase in acidity with increasing silica content for the support materials. The total acidity reached a maximum with 40% silica content for the support materials and supported catalysts, whereafter it starts to decrease again up to 100 % silica content. From the TPD spectra, it is evident that more than one peak is present, which is attributed to NH_3 desorption from different Brønsted and Lewis acid sites. The presence of tungsten oxide in the catalyst increases the total acidity implying that tungsten oxide itself is acidic or induces acid sites. The higher acidity per gram of WO_3 for alumina and Siralox supported tungsten might be related to the higher dispersion of tungsten on these materials.

3.2.6 Characterisation of acidity using pyridine adsorption

FTIR of adsorbed pyridine was used to study the Brønsted and Lewis acidity of the range of supports and the corresponding supported tungsten catalysts. Pyridine FTIR is a technique which has the ability to differentiate between different types of acidity, i.e. Brønsted and Lewis acid sites[75]. According to the literature[75], the characteristic bands of pyridine protonated by Brønsted acid sites (pyridinium ions), appear at ~1543 cm^{-1} and 1640 cm^{-1} while the bands from pyridine coordinated to Lewis acid sites appear at ~1453 cm^{-1} and 1621cm^{-1}. The peak appearing at 1621cm^{-1} is thus associated with Aluminium in the tetrahedral coordination[76], while the small peak at 1612 cm^{-1} is due to Aluminium in the octahedral environment[76]. The peak appearing at 1453 cm^{-1} represents the total amount of Lewis acid sites in the

tetrahedral and octahedral environment. The peak associated with the band appearing at 1543cm^{-1}, is accompanied by the vibration of the pyridinium ion resulting from the protonation of pyridine by Brønsted acid sites.

Previous studies revealed Silica-Alumina to have well-known Brønsted and Lewis acidity that increases with increasing Silica content[76]. The modification of Al_2O_3 with silica led to the creation of both highly acidic Lewis and Brønsted acid sites, the former through isomorphous substitution of Si^{4+} by Al^{3+} ions at tetrahedral lattice sites and the latter through formation of bridged hydroxyl groups.

Data resulting from FTIR of adsorbed pyridine revealed the presence of IR peaks characteristic to Lewis and Brønsted acid sites for the range of commercial Siralox support materials and the corresponding supported tungsten catalysts (Figures 3.6 and 3.7). The observed IR peaks for Lewis and Brønsted acid sites is in good agreement with those presented in literature[75]. Results from this study revealed that the catalyst composition i.e. silica and alumina content definitely has an effect on the acidity of the Siralox support materials. Differences in the Brønsted and Lewis acidic character was observed with varying amounts of silica and alumina.

Figure 3.6 shows FTIR spectra of the support materials used as. All supports except pure silica contain Lewis acid sites (1453 cm^{-1}). Brønsted acid sites (1543 cm^{-1}) are only present in the samples that contain silica as well as alumina. No Brønsted acidity was observed for γ-Al_2O_3 and SiO_2.

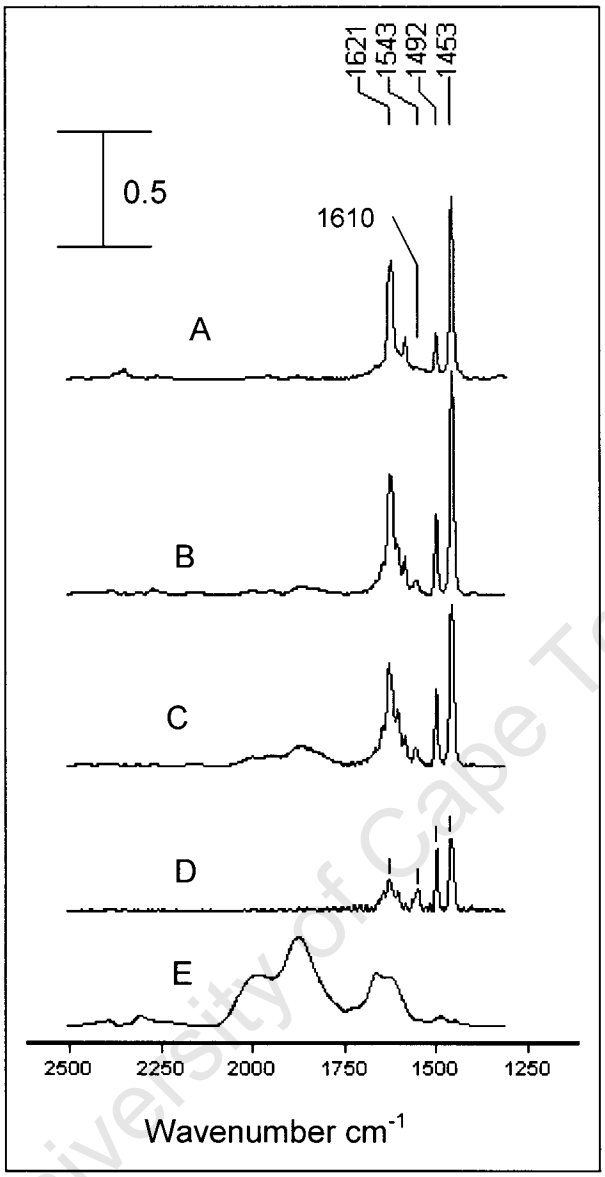

Figure 3.6: FTIR spectra of support materials (A) Al_2O_3 (B) Siralox 20 (C) Siralox 40 (D) Siralox 75 (E) SiO_2

Figure 3.7 shows FTIR spectra of the tungsten-impregnated supports. The FTIR spectra possess bands at 1451 cm^{-1} which corresponds to pyridine coordinated to Lewis acid sites. This peak represents the total amount of Lewis acid sites. The peaks appearing at 1548cm^{-1} indicate the presence of pyridinium ions which originates from pyridine protonated by Brønsted acid sites. This behaviour was observed only for the catalysts containing 20, 40, 75 % silica. For the pure alumina supported tungsten, no such peak was observed. The peak at 1491 cm^{-1}, is accompanied by the vibration of the pyridinium ion.

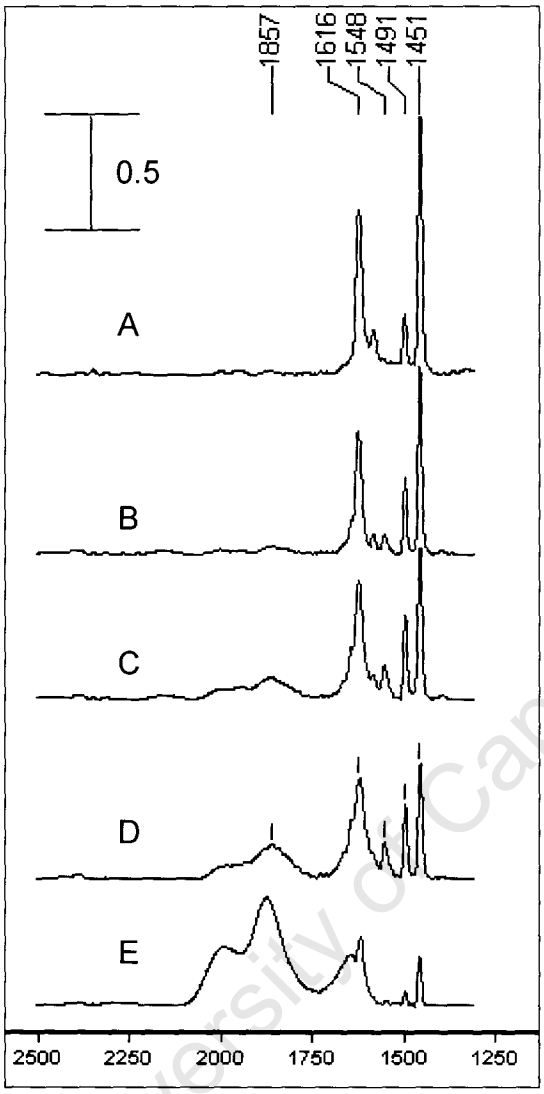

Figure 3.7: FTIR spectra of catalysts containing 8 wt.-% WO_3 supported on (A) Al_2O_3 (B) Siralox 20 (C) Siralox 40 (D) Siralox 75 (E) SiO_2

It was shown that pure silica does not contain any Lewis or Brønsted acid sites. However, when tungsten is loaded onto the support, the presence of Lewis sites is observed. The peak at 1451 cm^{-1} representing the Lewis acidity of WO_3/SiO_2 is thus due to the Lewis acidity of the tungsten impregnated onto the support. The pyridine is thus coordinated to the Lewis acid sites of the tungsten. For all the supports, the peaks appearing at 1451cm^{-1} due to pyridine coordinated to Lewis acid sites, is thus the total Lewis acidity of pyridine coordinated to Lewis acid sites on the tungsten as well as pyridine coordinated to Lewis acid sites on the supports, except for the pure silica support. The strength of the Lewis acid sites depicted by a shift in peak has not

been affected by the metal loading. Metal loading onto the support only resulted in an increase in the total acidity of the catalyst.

Brønsted Acidity

The Brønsted acid sites in Silica-Alumina type of materials are generated as a result of charge imbalance in the structure. The charge difference is a result of the difference in the valence state of aluminium and silicon when Si-O-Al type of bonds is formed. If a silicon atom is replaced by a tetrahedral Al atom, the AlO_4 part is unsaturated by a whole valence unit, which can be compensated by protonation[112] and these protons are responsible for the Brønsted character of the Silica-Alumina type of materials.

The characteristic Brønsted peaks found in Siralox 20, Siralox 40 and Siralox 75 (Figure 3.6) is thus due to the silica-alumina structure. SiO_2 support is acidic, but too weak to chemisorbed pyridine[75] and no Brønsted or Lewis acidity was observed for the pure SiO_2 support. The acidity of alumina sample is that of a classical alumina, which shows that this material contains only Lewis acid sites under FTIR of adsorbed pyridine. The hydroxyl groups present in alumina are of such a nature that they cannot protonate pyridine to form pyridinium ion therefore they cannot be classified as being Brønsted acid sites.

It was concluded from molecular orbital calculation studies on Silica-Alumina clusters, that the H in the hydroxyl group becomes protonic by coordination of Al to an oxygen atom bridging a Si atom[77, 78]. The coordination of Al to an oxygen atom bridging the Si atom corresponds to a Lewis acid base interaction, and the stronger the interaction, the stronger the Brønsted acid strength of the bridging oxygen associated H.

Calculations showed that the Brønsted acid sites of Silica-Alumina oxides are bridged hydroxyl groups and water molecules coordinated on a trigonal aluminium atom[79].

Lewis Acidity

Lewis acidity was observed for all the support materials except for pure silica support. The Al_2O_3 support contained only Lewis acidity. This observation is in good agreement with what was indicated in previous studies that the surface of γ-alumina contains only Lewis acid sites, as measured by adsorption of pyridine. Although some evidence of Brønsted acidity has been observed, these acid sites are not strong enough to protonate pyridine and are not expected to be catalytically active in most industrial reactions[80, 81]. Results from FTIR of adsorbed pyridine in this study (Figure 3.6) revealed no Brønsted acidity for pure alumina support. The observation that pyridine adsorbed on tetrahedral Al gave a band at 1620 cm^{-1} whereas those on octahedral Al absorb at 1612 cm^{-1} proves that pyridine chemisorbs more strongly on tetrahedral Al than on octahedral Al.

The Lewis acid sites resulting from alumina in the tetrahedral coordination will thus be the strongest Lewis acid sites, therefore the suggestion that alumina in the tetrahedral coordination should be maximized. The observation that Lewis acidity increases with increasing silica content is thus due to the increasing ratio of tetrahedral/octahedral Al with increasing silica content in Silica-Aluminas[75].

Influence of metal-impregnation on total acidity of support material

From the above FTIR results, it can be concluede that all the metal supported catalysts contain Lewis acidity and that the strength of Lewis acid sites depicted by the shift in the peak has not been affected by the metal loading. It was noted that all the metal supported catalysts contain Brønsted acid sites except for tungsten supported on alumina. The results show that the total acidity of the catalysts has been enhanced by the addition of the metal. The observation that the deposited tungsten has generated additional acidity can be related to the synergistic effect of the support and the metal.

It was observed by Rajagopal[110] that the generated acidity upon deposition of Mo oxide on SiO_2 is of Lewis type. This observation can also be made with deposition of tungsten on silica. Results in this study showed no presence of Lewis acidity on SiO_2 support. However with impregnation of tungsten oxide, Lewis acid sites emerged

alumina-containing support materials. Results revealed an extreme difficulty to reduce tungsten impregnated on alumina support as well as on the Siralox support materials. Reduction temperatures of a 1000°C were observed for WO_3/Al_2O_3 and WO_3/Siralox 20. However, as the silica content is increased, the reduction temperatures decreases, thus, reduction of tungsten became easier with decreasing amount of alumina (See Table 3.3). It is generally known that the active sites for Mo and W based heterogeneous metathesis catalysts are obtained when the metal is in an oxidation state lower than +6[68, 69, 70] . It is also known that alumina-supported MoO_3 and WO_3 catalysts are highly resistant to reduction[71]. MoO_3 and WO_3 are reduced at temperatures considerably above the usual reaction temperatures and their reducibility decreases with decreasing metal oxide content[72, 73, 74]. It is thus easy to account for the small activities observed for Al_2O_3 supported on MoO_3 and WO_3 catalysts with low metal oxide content[32]. Hydrogen TPR studies revealed the interaction of tungsten with the different acidic support materials. Tungsten supported on alumina was found to be extremely difficult to reduce and very high reduction temperatures were observed. As the silica content increases, it became easier to reduce the tungsten. With increasing silica content, lower reduction temperatures were observed. Tungsten supported on silica seemed to be the most reducible catalysts. It can thus be concluded that tungsten supported on alumina will have the least amount of active sites for metathesis, while tungsten supported on silica would have the largest amount of active sites for metathesis. This is because the interaction between tungsten and silica is of such a type that it allows the reduction of tungsten in the +6 state to tungsten in the +5 state which is the most active state towards metathesis.

Table 3.3 Effect of silica content on reducibility of tungsten

Catalyst	**$T_{reduction}$, °C**	
	+6→+5	**+5→+4**
WO_3/Al_2O_3	1000	
WO_3/Siralox 20	995	
WO_3/Siralox 40	950	
WO_3/Siralox 75	940	
WO_3/SiO_2	710	820

(Figure 3.7). These acid sites can be attributed to the coordinatively unsaturated tungsten atoms on the catalyst.

The conclusion can therefore be drawn that additional Lewis acid sites are created with deposition of tungsten on various support materials, therefore the increase in acidity.

3.2.7 Probing acidity using 1-butene isomerisation

Reaction studies with different support materials were carried out and related to the total acidity of each support. The isomerisation of 1-butene was carried out at 100°C, GSHV = 1000 ml (0.85 bar, RT) / (ml/h) and atmospheric pressure (0.85 bar).

Figures 3.10 shows the time on-line behaviour of the different supports materials in terms of 1-butene conversion

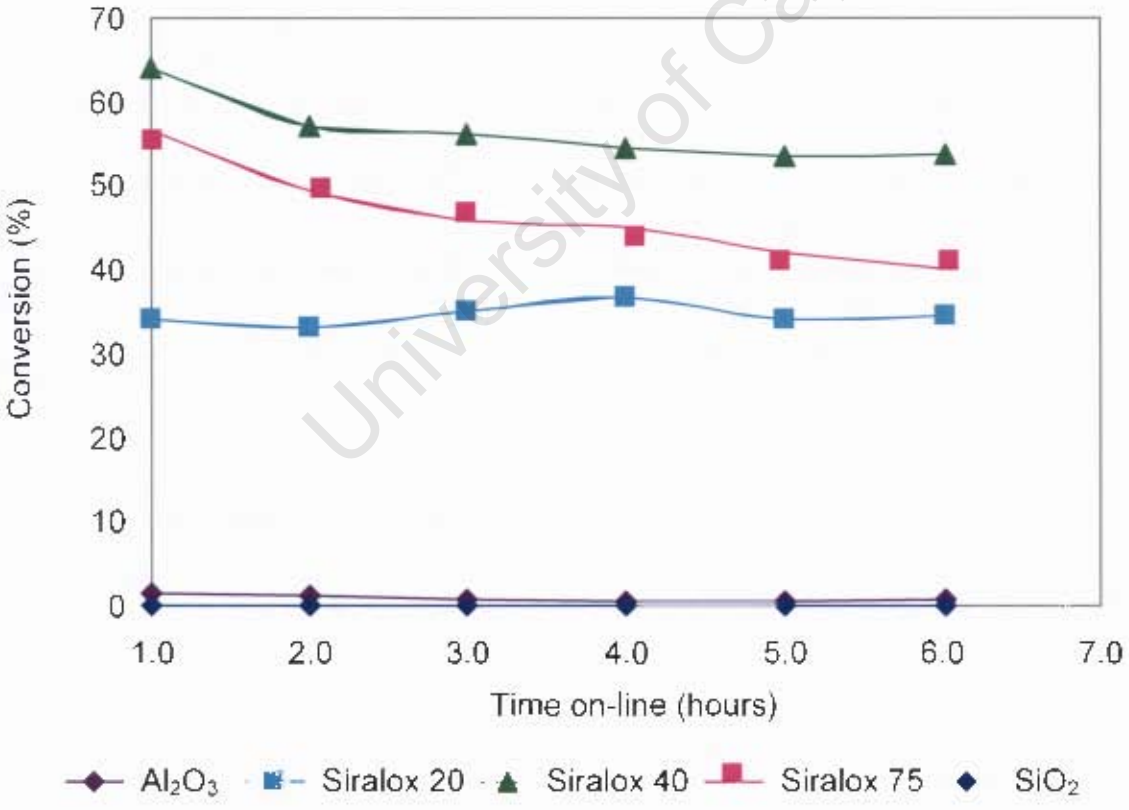

Figure 3.10: Conversion as a function of Time on-line in 1-butene isomerisation over various support materials

The conversion as a function of silica content was carried out in order to investigate the effect of silica content on the 1-butene double bond isomerisation activity, using different supports (see Figure 3.11). The 1-butene isomerisation passes a maximum at 40 wt.-% silica after which a decrease in activity was observed.

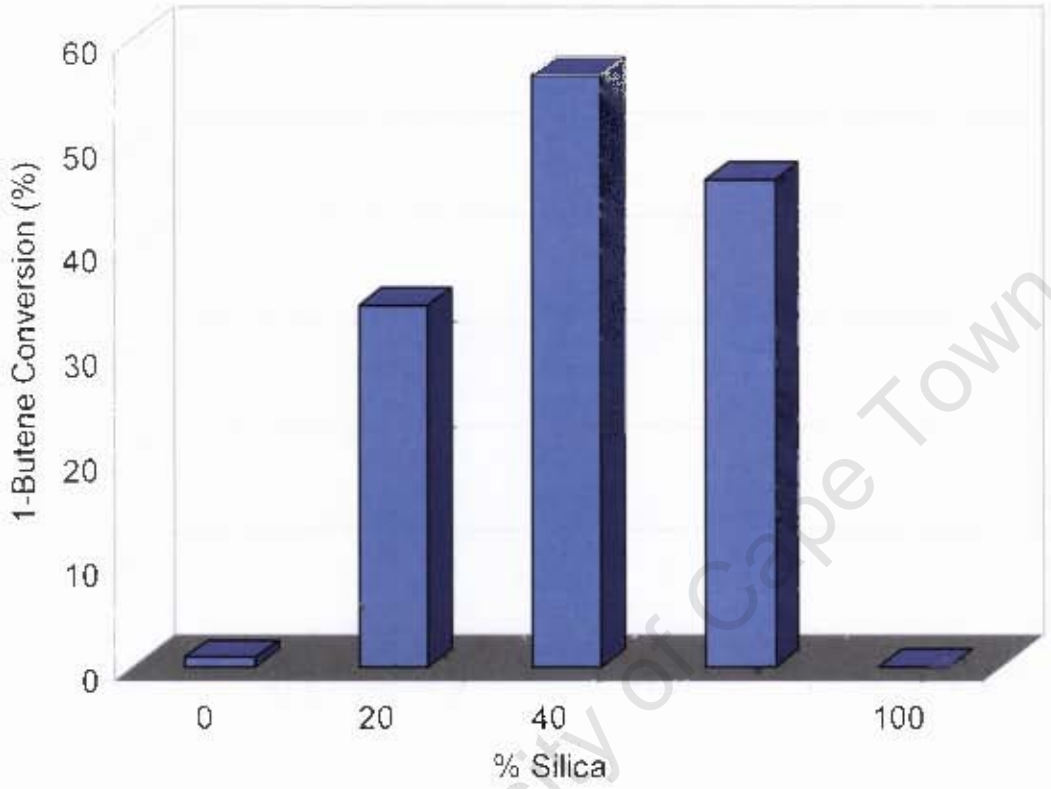

Figure 3.11: Effect of silica content on double bond isomerisation activity at 100°C, 1000 h^{-1} and atmospheric pressure (0.85 bar), time on-line = 6 hours

High double bond isomerisation activity was observed with the acidic support materials. An increase in catalytic activity with an increase in silica content was observed. The catalytic activity reached a maximum at 40 wt% silica. This observation can be explained in terms of the maximum total acidity at a silica content of 40 wt% obtained from the NH_3 TPD studies. The Siralox 40 support material would thus have the total acidity, which would be responsible for the high isomerisation activity of the Siralox 40 support.

3.3 Metathesis studies

Figures 3.12-3.17 show the time on-line behaviour of the different supported tungsten catalysts in terms of 1-butene conversion, ethene and propene purities, ethene and propene selectivity's and the mass balance obtained during the duration of the

reaction studies. Metathesis of 1-butene was carried out at 450°C, atmospheric pressure and GHSV = 500ml/ (ml/h). Metathesis activity reached a maximum with the 8wt% WO_3/SiO_2 and a maximum activity was not obtained with the 8wt% WO_3/Siralox 40 as was the case with the support materials only (see Table 3.5).

Table 3.5: Effect of total acidity on the metathesis activity of 1-butene

Support Material	Total Acidity (mmol/g)	1-butene conversion (%)
WO_3/Al_2O_3	0.23	12.70
WO_3/Siralox 20	0.29	38.51
WO_3/Siralox 40	0.37	52.64
WO_3/Siralox 75	0.33	54.55
WO_3/SiO_2	0.05	67.58

The mass balance obtained for each reaction was typically better than 95% (see Figure 3.12). Hence, the results obtained can be taken with reasonable accuracy.

The Mass Balance of the reaction was calculated as follows:

Mass balance = (Mass gas (g/h) out) + Mass liquid (g/h) out / Mass feed (g/h) in)x100

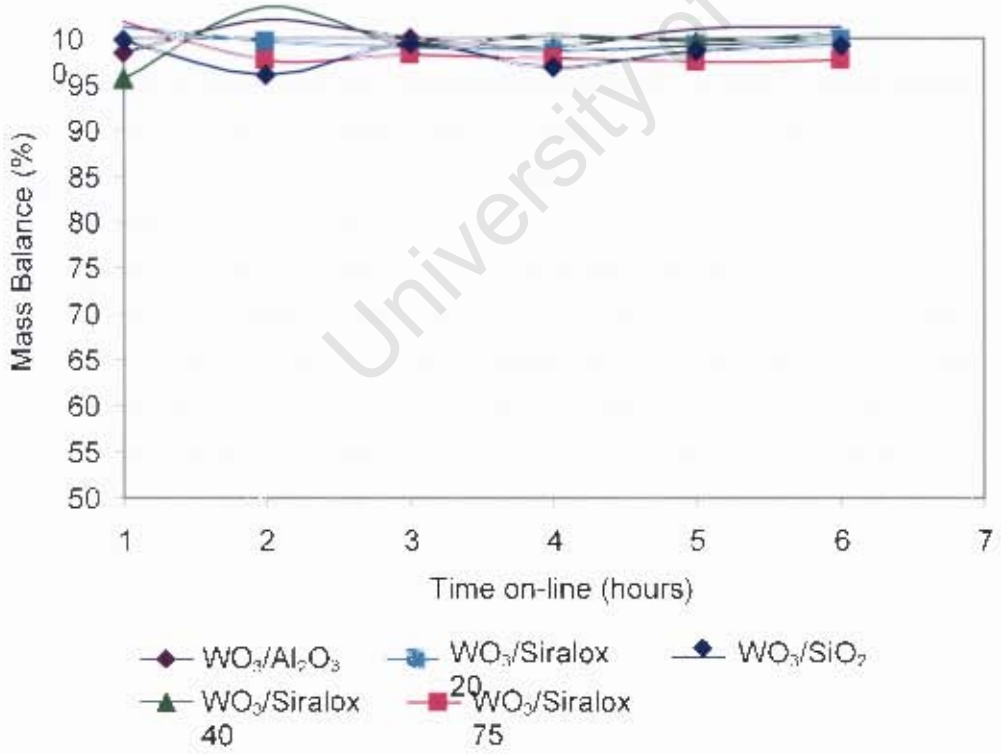

Figure 3.12: Mass balances during 1-butene metathesis over several of supported tungsten catalysts (T =450°C, atmospheric pressure (0.85 bar), GHSV = 500 h^{-1})

Figure 3.13 shows the conversion of 1-butene in 1-butene metathesis as a function of time-on-line. Tungsten supported on alumina showed the lowest activity. The conversion after 4 hours on line increases with increasing silica content in the support. The conversion obtained with the silica supported catalyst is close to the thermodynamically controlled conversion. It can be further noted that the catalyst containing alumina show some degree of deactivation, as evidenced by the decline in activity. The degree of deactivation seems to increase with increasing alumina content in the catalyst.

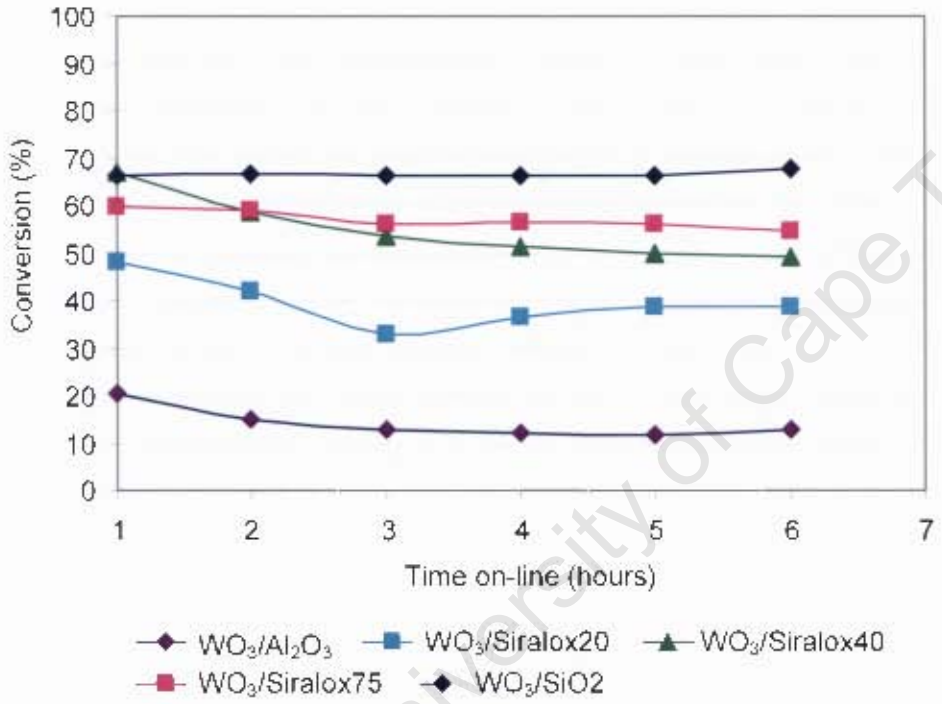

Figure 3.13: Conversion of 1-butene in 1-butene metathesis over supported tungsten catalysts (T =450 °C, atmospheric pressure (0.85 bar), GHSV = 500 h^{-1})

Figure 3.14 shows the selectivity of propene in the 1-butene metathesis as a function of time on line. The selectivity of propene is close to 40%, as was expected based on the (limited) thermodynamic evaluation of 1-Butene metathesis (see Chapter 1).

Figure 3.15 shows the propene purity obtained during 1-butene metathesis over supported tungsten catalysts as a function of time on-line. Propene purity is defined as the fraction of propene in the fraction of propene and propane. All catalysts show close to 100% propene purity implying that hydrogenation of the product propene by hydrogen transfer does not take place to a significant extent.

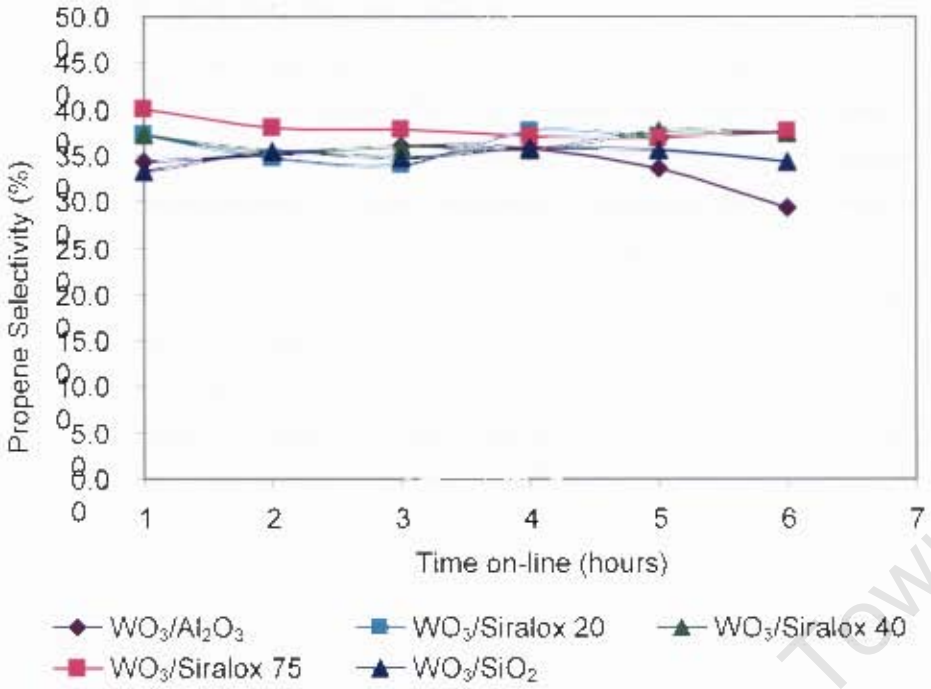

Figure 3.14: Propene selectivity in 1-butene Metathesis over supported tungsten catalysts (T =450°C, atmospheric pressure (0.85 bar), GHSV = 500 h^{-1})

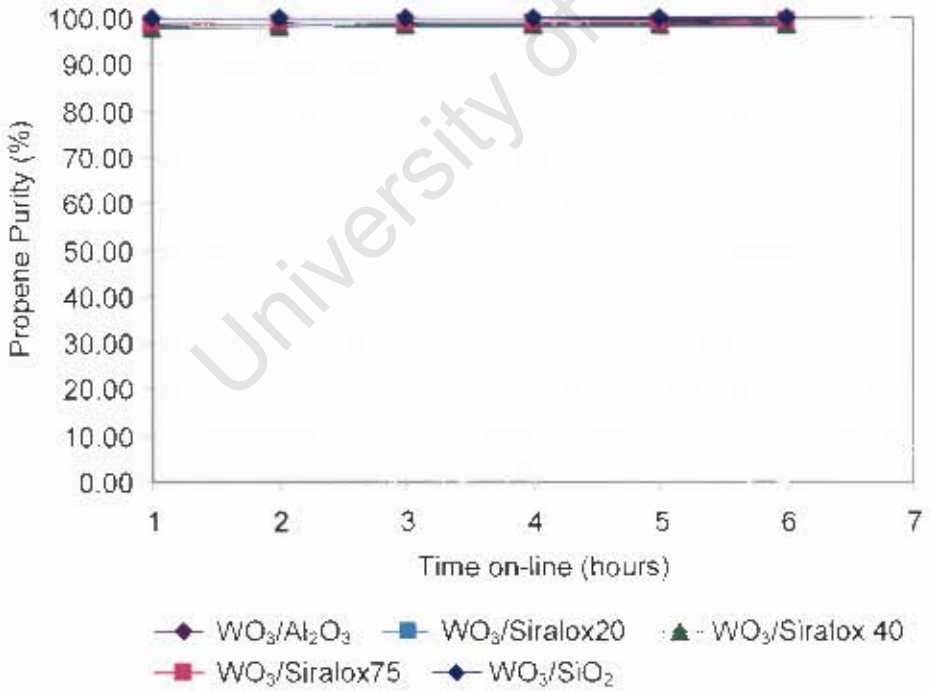

Figure 3.15: Propene purity obtained from 1-butene metathesis over supported tungsten catalysts (T =450°C, atmospheric pressure (0.85 bar), GHSV = 500 h^{-1})

Figure 3.16 shows the ethene selectivity obtained in the 1-butene metathesis for the various supported tungsten catalysts as a function of time on line. From the graph it can be seen that the catalysts with the highest silica content yields the highest selectivity towards ethene.

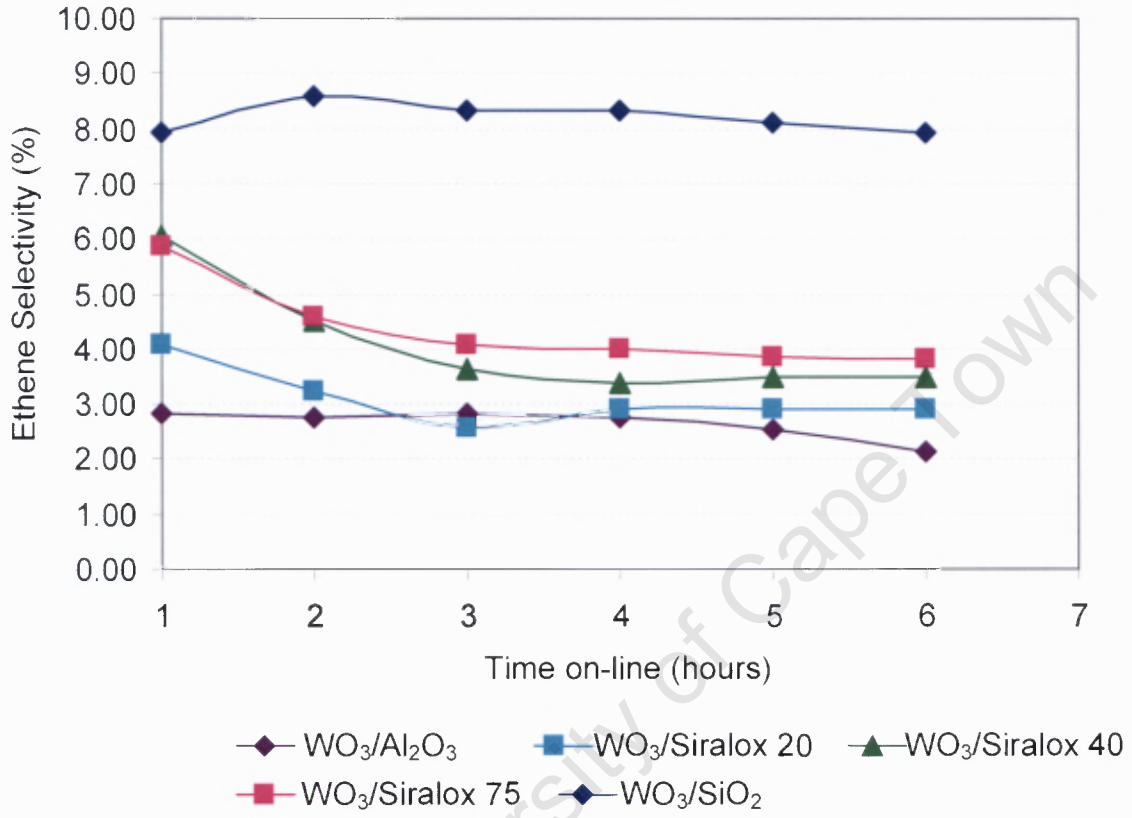

Figure 3.16: Ethene selectivity obtained in 1-butene metathesis over supported tungsten catalysts as a function of time-on-line. (T =450°C, atmospheric pressure (0.85 bar), GHSV = 500 h^{-1})

Figure 3.17 shows the ethene purity obtained in the 1-butene metathesis for the various supported tungsten catalysts as a function of time on line. The ethene purity is defined as the mass fraction of ethene in the C_1-C_2-fraction containing methane, ethane and ethene. Low ethene purity can thus be caused by extensive cracking (and thus yielding more methane) or by some hydrogenation yielding ethane (and as a co-product a dehydrogenated product, which may act as a coke precursor). The ethene purity obtained with tungsten on silica is close to 100%. Catalyst with higher alumina content shows lower ethene purity and thus more methane/ethane.

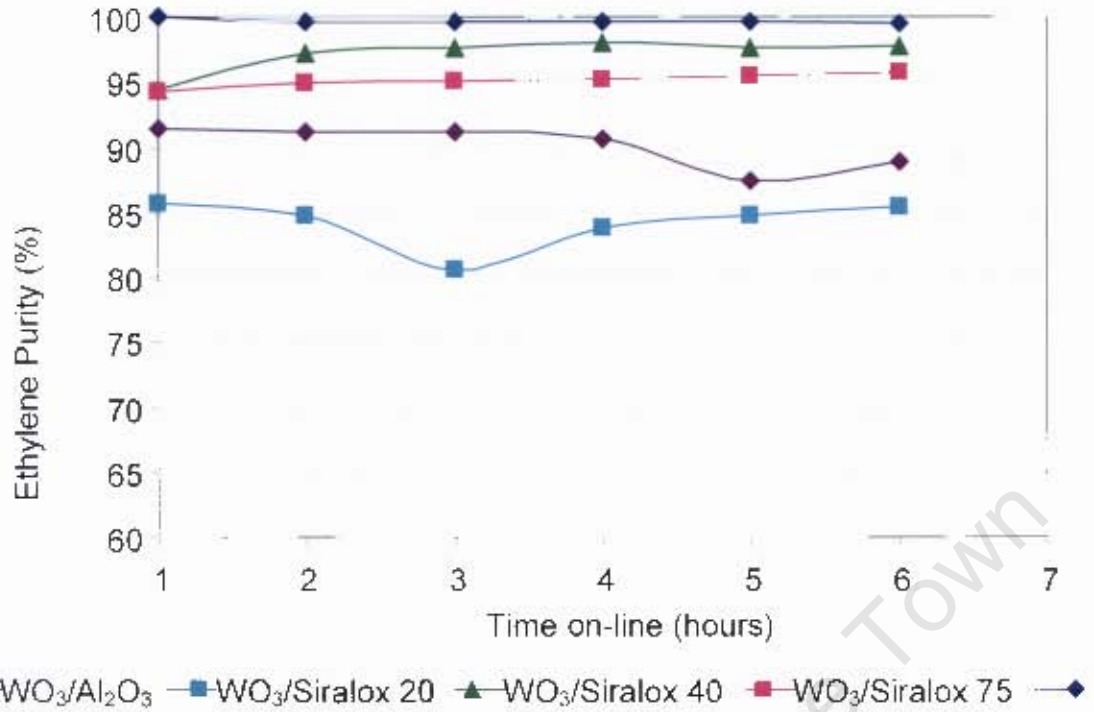

Figure 3.17: Ethene purity obtained from 1-butene metathesis over supported tungsten catalysts (T = 450 °C, atmospheric pressure (0.85 bar), GHSV = 500 h^{-1})

Figure 3.18 shows the yield for the formation of methane and ethane for the various tungsten-based catalysts. A similar trend as obtained for the ethene purity is obtained, since both terms are linked. The WO_3/SiO_2 catalyst has the lowest yield for the formation of methane and ethane.

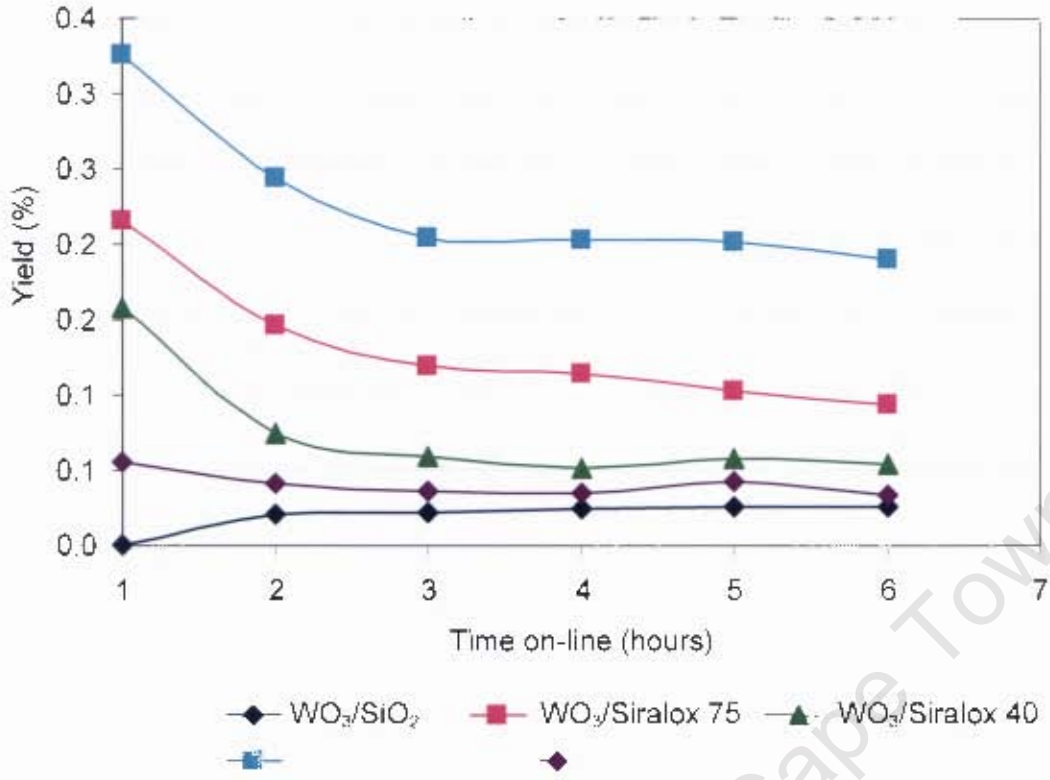

Figure 3.18: Formation of Methane and Ethane during 1-Butene metathesis over various supported tungsten catalysts (T = 450 °C, atmospheric pressure (0.85 bar), GHSV = 500 h^{-1})

3.4 Characterisation of spent catalyst

The spent catalyst was first cooled down under nitrogen and then removed from the reactor in an air atmosphere. Characterisation studies, e.g. TGA, etc., includes a drying step where H_2O and O_2 that condensates on the surface under ambient conditions are removed before the catalyst is characterized.

3.4.1 Crystallinity of tungsten supported catalysts

XRD analysis was performed on the fresh and spent catalysts to determine the crystallinity of the tungsten. XRD was also used to determine the oxidation state of tungsten before and after the reactions to see how much of the tungsten was reduced to the active oxidation state and whether any of the tungsten was over- or under-reduced. The information could be used to explain the activity of tungsten of different acidic supports. In the metathesis of butene to propene and under the specified reaction conditions, it is believed that the active form of the tungsten oxide

catalyst is in the reduced form ($WO_{2.95}$) in the +5 oxidation state. XRD experiments were carried out to track the form of tungsten oxide before and after the metathesis reaction. The amount of tungsten in the +5 oxidation state could be related to the metathesis activity of the different catalysts. The amount of tungsten in the +5 oxidation state will also indicate how easily the tungsten was reduced to the active oxidation state.

As shown in Figure 3.19, no crystalline phases were detected either for samples of WO_3 on Siralox 40 support, for both fresh (Figure 3.19, Spectrum **3**) and spent catalysts (Figure 3.19, Spectrum **4**).

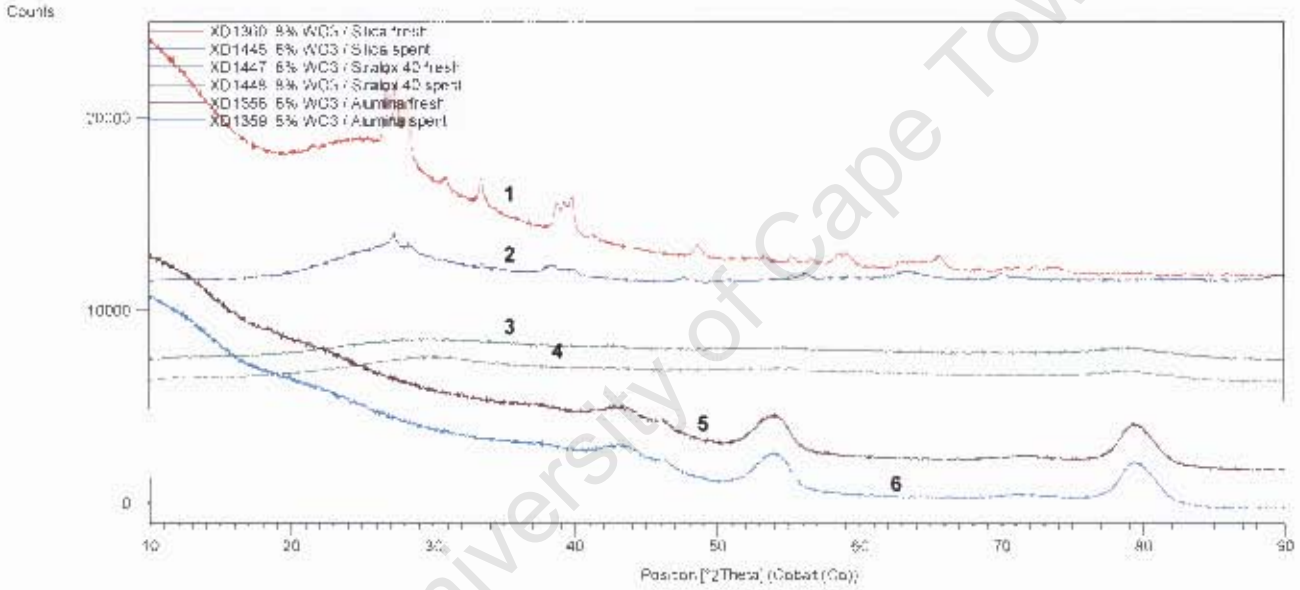

Figure 3.19 X-ray powder diffraction patterns of all eight samples overlaid on one set of axis. Spectrum: **1** = WO_3/SiO_2 fresh, **2** = WO_3/SiO_2 spent, **3** = WO_3/Siralox 40 fresh, **4** = WO_3/Siralox 40 spent, **5** = WO_3/Al_2O_3 fresh, **6** = WO_3/Al_2O_3 spent.

It should be noted that the intensity counts on the y-axis scale should only be used relatively, as graphs were simply staggered on top of each other by translations along the y-axis.

No crystalline phases were detected, except for the broad reflections belonging to

gamma alumina (Figure 3.19, Spectra **5** and **6** and Figure 3.20).

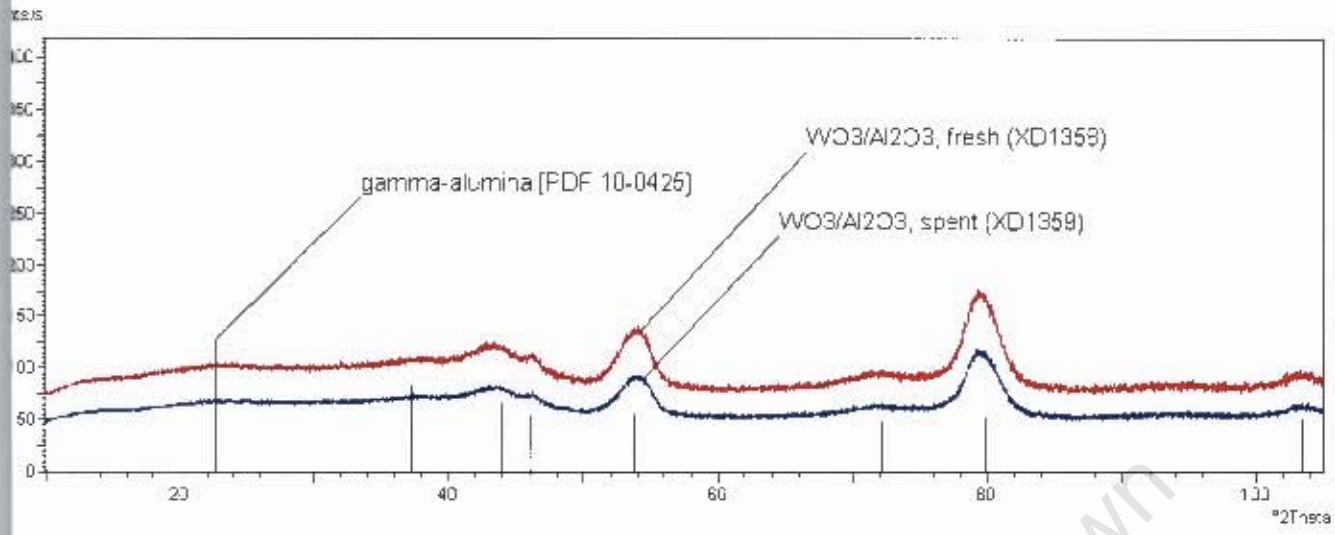

Figure 3.20: Diffraction spectra of WO_3 on Al_2O_3 support staggered on one set of axis. Shown in stick mode is the reference powder pattern fitting the observed reflections in these two catalysts

To the contrary, XRD spectra for WO_3 on silica support exhibit crystalline tungsten oxide phases, for both fresh and spent material (see Figure 3.21). The observed crystalline tungsten phase was identified as stoichiometric WO_3 orthorhombic (oxidation state +6) in the fresh catalyst preparation, but the spent catalyst transformations into lower symmetry monoclinic sub-stoichiometric $WO_{2.9}$ phase with possible reduction of tungsten oxidation state. The average crystallite size was determined using the Debye-Scherrer equation[66] and are quoted in Table 3.2

It seems that tungsten supported on high silica content samples are reduced with much more ease. The samples with the highest amount of silica contained the highest amount of tungsten in the +5 oxidation state, which is active for metathesis.

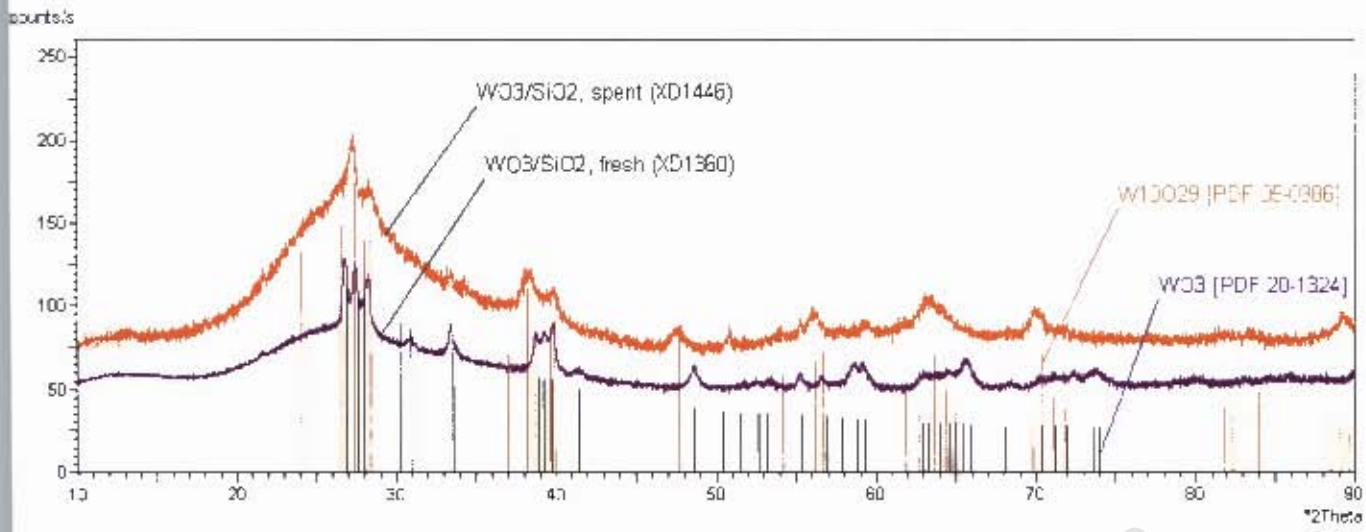

Figure 3.21 Overlay presentations of diffraction patterns of WO_3 on SiO_2 support of both the spent catalyst and the fresh preparation. Shown in stick mode are the reference powder patterns fitting observed XRD traces for each catalyst sample.

The XRD patterns of all the catalysts respectively Figure 3.21 A.1 – 3.21 A.4) are shown below. Scans in blue are of the fresh preparations while the ones in pink (on the same set of axis) are of the spent residues.

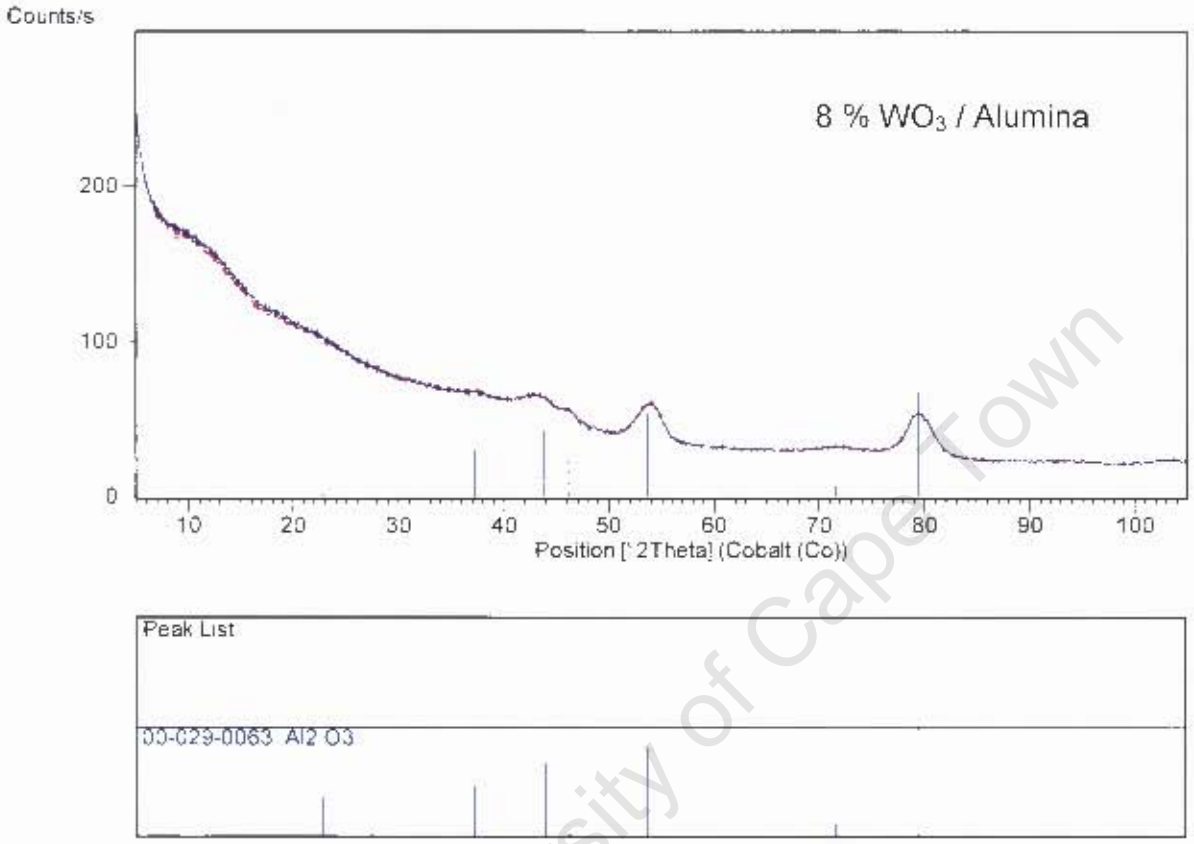

Figure 3.21 A.1: X-ray powder diffraction patterns of the fresh and spent 8 % WO_3 / Alumina

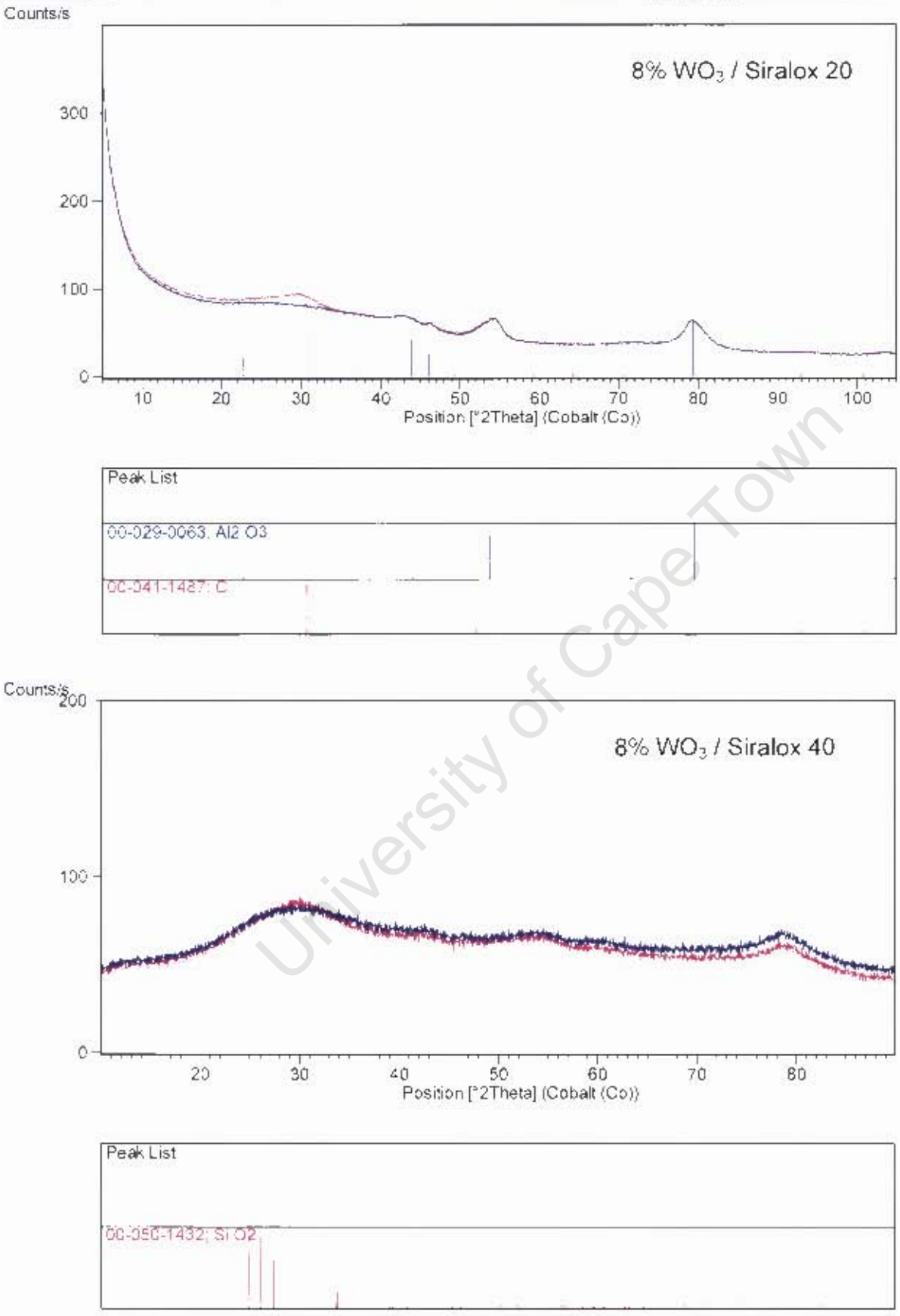

Figure 3.21 A.2: X-ray powder diffraction patterns of the fresh and spent 8 % WO_3/ Siralox 20 and 8 % WO_3/ Siralox 40

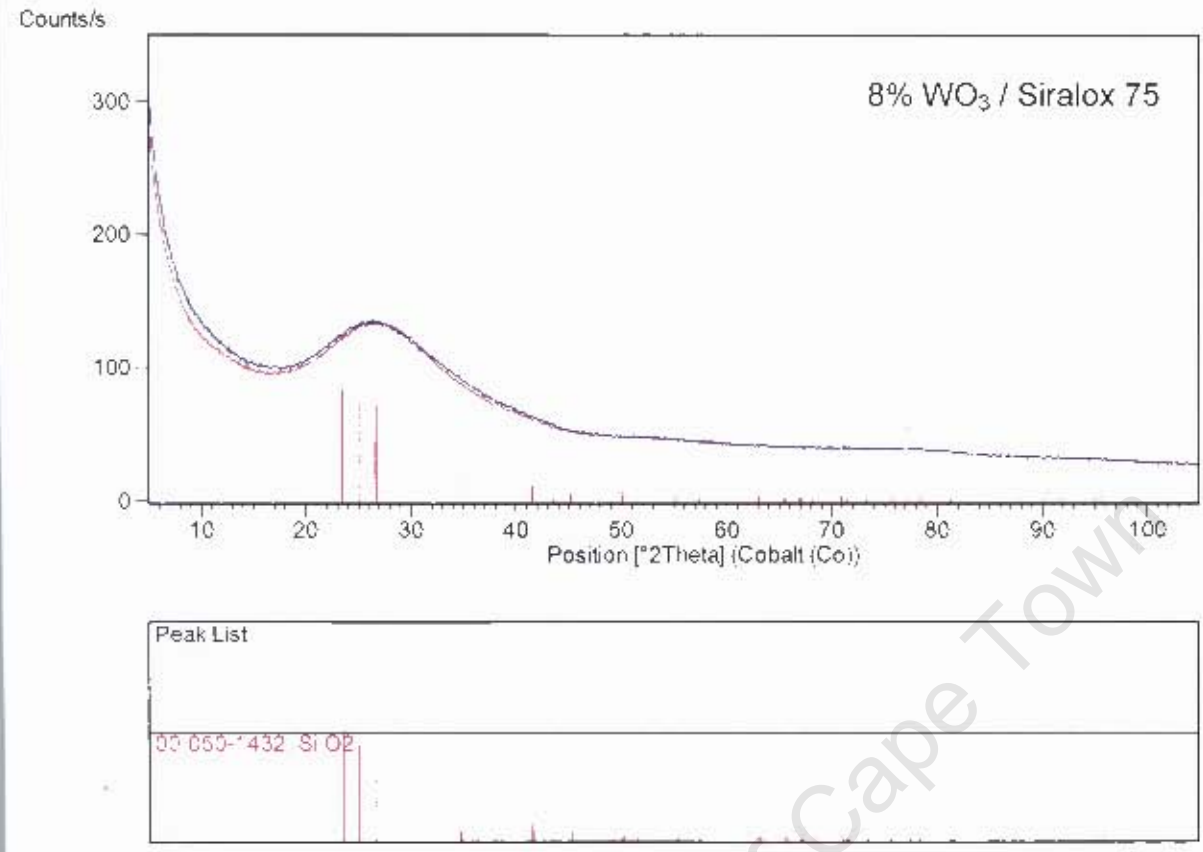

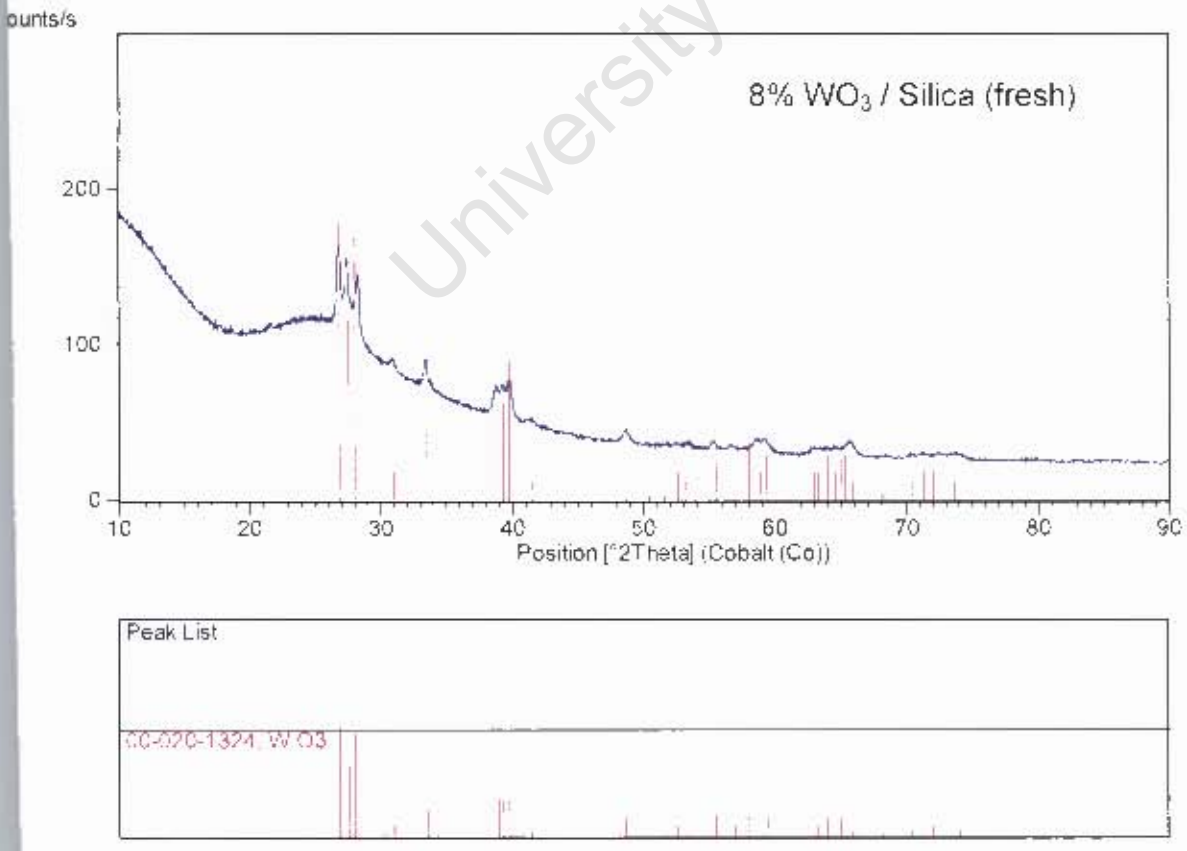

Figure 3.21 A.3: X-ray powder diffraction patterns of the fresh and spent catalysts.

8% WO_3 / Siralox 75 and 8% WO_3 / Silica (fresh).

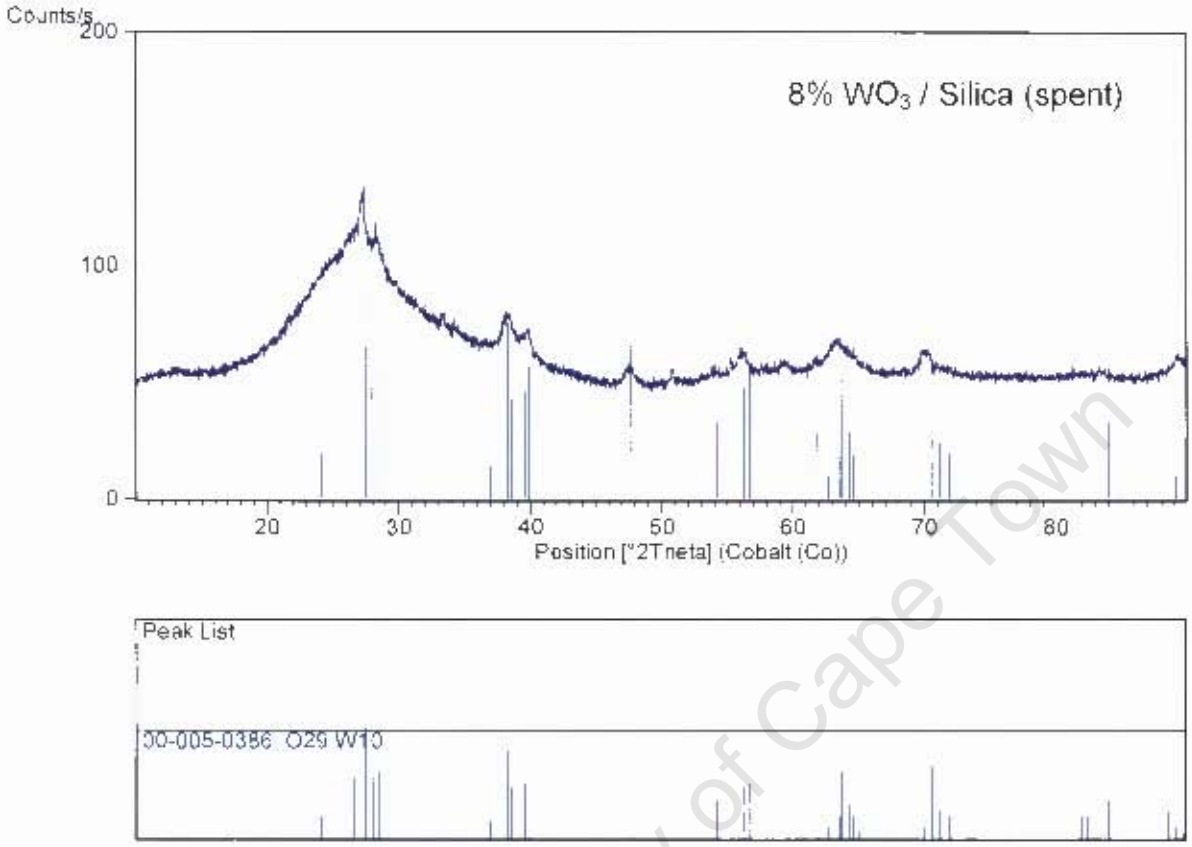

Figure 3.21 A.4: X-ray powder diffraction patterns of 8% WO_3 / Silica (spent)

3.4.2 SEM analysis on spent catalyst

SEM analysis was done on the fresh and spent catalysts in order to obtain visual effects of the dispersion of tungsten on the different supports. SEM images of different tungsten impregnated support materials are illustrated in Figures 3.22-3.31. No sintering or break-up of the catalysts was observed in going from the fresh to the spent catalyst. Clear evidence of carbon deposits can not be seen from these images. The WO_3/SiO_2 catalyst showed a very good distribution of the active metal on support. This is not the case with the tungsten supported on the Siralox materials. Several articles stated the importance of optimum dispersion for maximum metathesis actvity[81, 23]. It seems that the catalysts with high amounts of silica exhibited better dispersion of tungsten on the support material. According the visual observation, the tungsten dispersion increased with increasing amount of silica.

Figure 3.22 SEM image of fresh WO_3/Al_2O_3

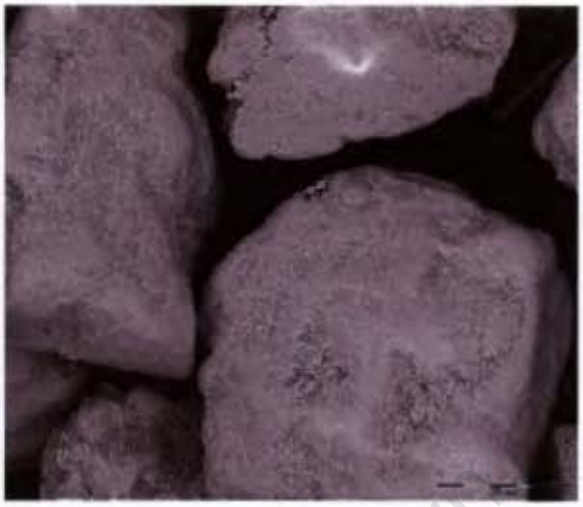

Figure 3.23 SEM image of fresh WO_3/Al_2O_3

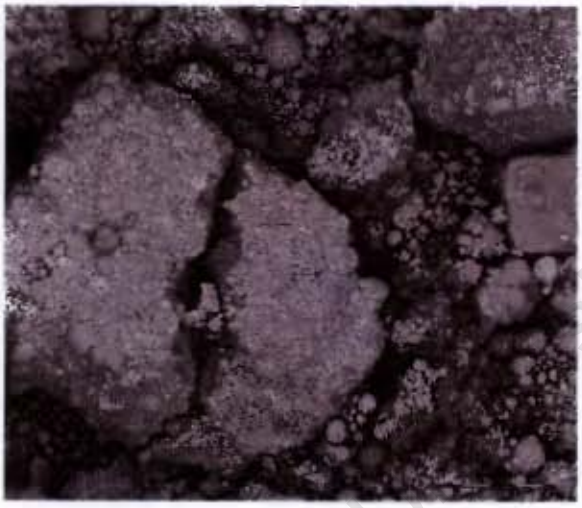

Figure 3.24 SEM image of fresh WO_3/Siralox 20

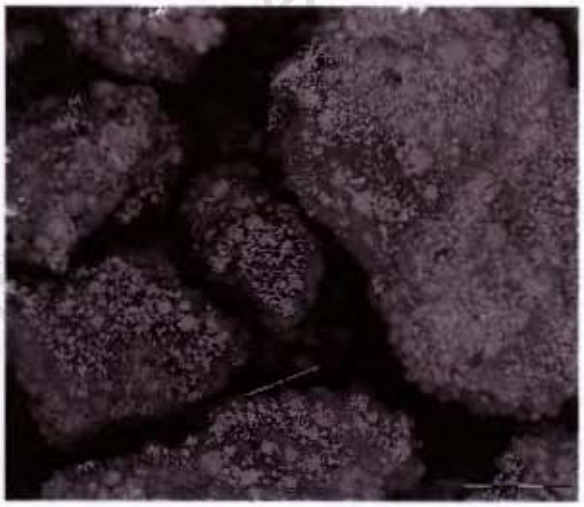

Figure 3.25 SEM image of spent WO_3/Siralox 20

Figure 3.26 SEM image of fresh WO_3/Siralox 40

Figure 3.27 SEM image of spent WO_3/Siralox 40

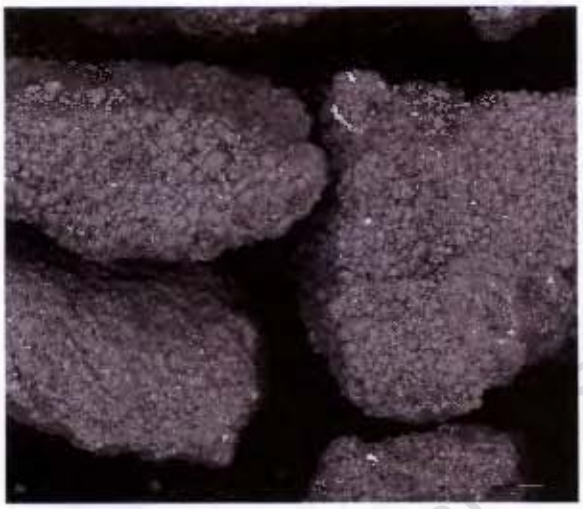

Figure 3.28 SEM image of fresh WO_3/Siralox 75

Figure 3.29 SEM image of spent WO_3/Siralox 75

Figure 3.30 SEM image of fresh WO_3/SiO_2

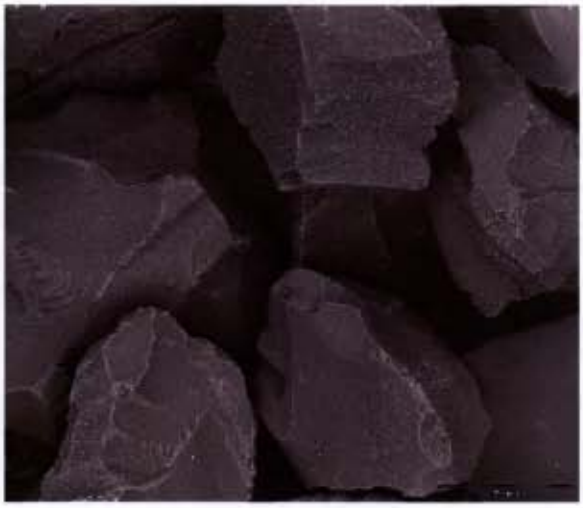

Figure 3.31 SEM image of spent WO_3/SiO_2

3.4.3 Coke formation on the catalysts

The coke content in the catalysts were characterised after the metathesis reaction by TGA. Figure 3.32 shows a typical TGA curve (obtained with the spent 8wt.% WO_3/Siralox 75 catalyst tested for the metathesis activity of 1-butene at 450 °C, 500 h^{-1} and atmospheric pressure). Weight loss was observed at various stages, viz. 25-100 °C, between 100-190 °C, 280-550 °C and finally during the isothermal phase at 550 °C. The first three stages of weight loss are also observed for the fresh 8wt.% WO_3/Siralox 75 (see Figure 3.33). Hence, the last stage of weight loss was taken as weight loss due to coke combustion.

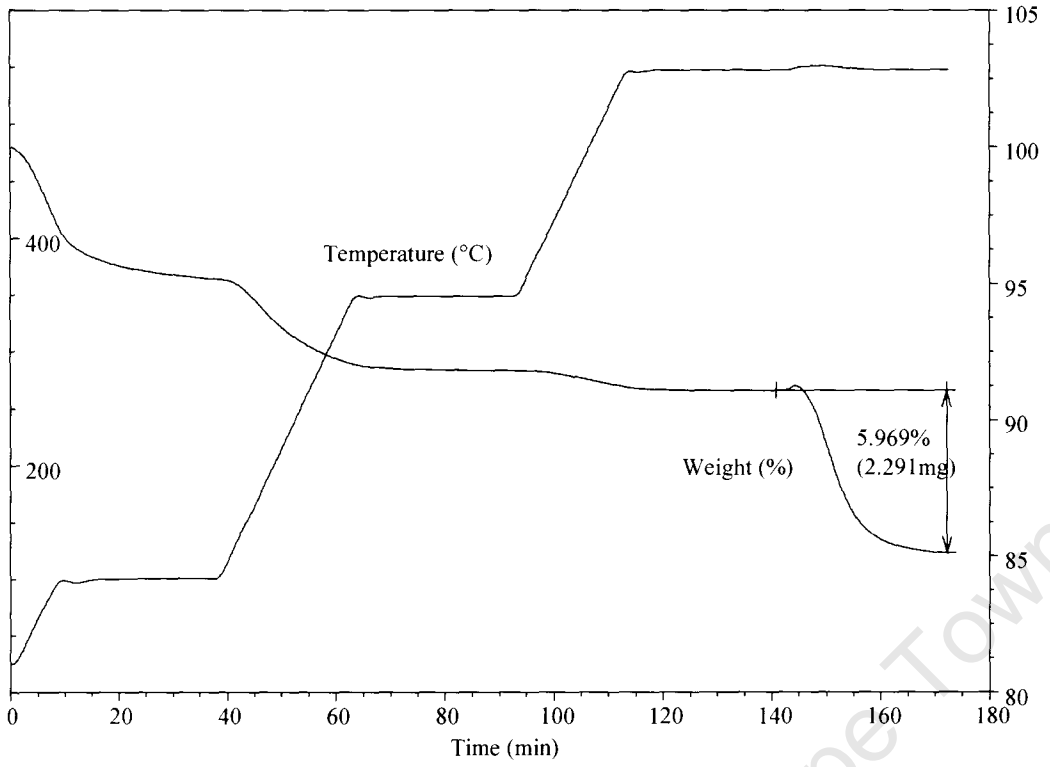

Figure 3.32: A typical TGA curve for a spent 8%WO_3/Siralox 75 catalyst sample

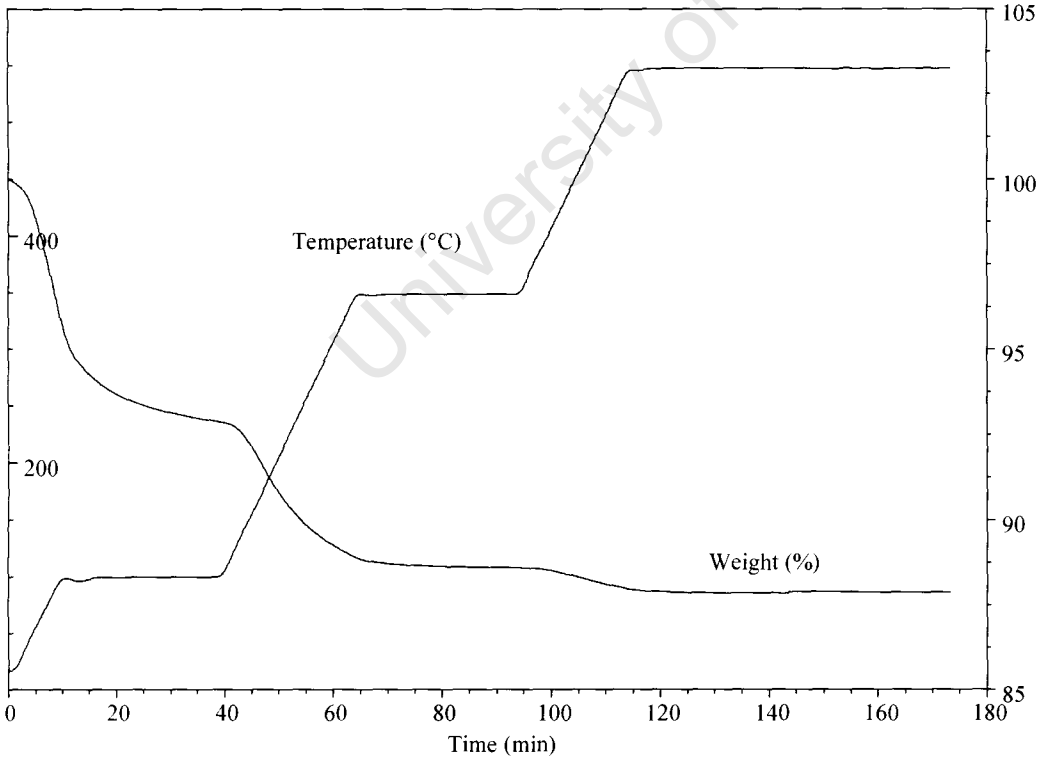

Figure 3.33: A typical TGA curve for a fresh 8%WO_3/Siralox 75 catalyst sample

3.4.3.1 Influence of Silica Content on Coke Formation during isomerisation of 1-butene with acidic support materials

During the following reactions, the coke formation on different acidic support materials were investigated after being exposed to the isomerisation of 1-butene at 100 °C, 1000 h^{-1} and atmospheric pressure. TGA experiments were performed on spent supports after isomerisation reaction studies with 1-butene to determine the effect of silica content on the coke formation. Results revealed an increase in coke formation with an increase in silica content up to 40% silica content. Thereafter a decrease in coke formation was observed approaching pure silica support (see Figure 3.34).

The formation of coke on oxide catalysts is mainly due to cracking reactions involving coke precursors like olefins or aromatics which are catalyzed by Brønsted acid sites on the catalysts surface[82]. Coke deposition on oxide catalysts mainly occur on strong acid sites[83] and it was found that coke formation on acidic supports such as silica-aluminas etc. is in line with its large total acidity[84]. It has also been establish that coke formation increases with increasing acidity and that both Lewis and Brønsted acid sites take part during coke formation[82].

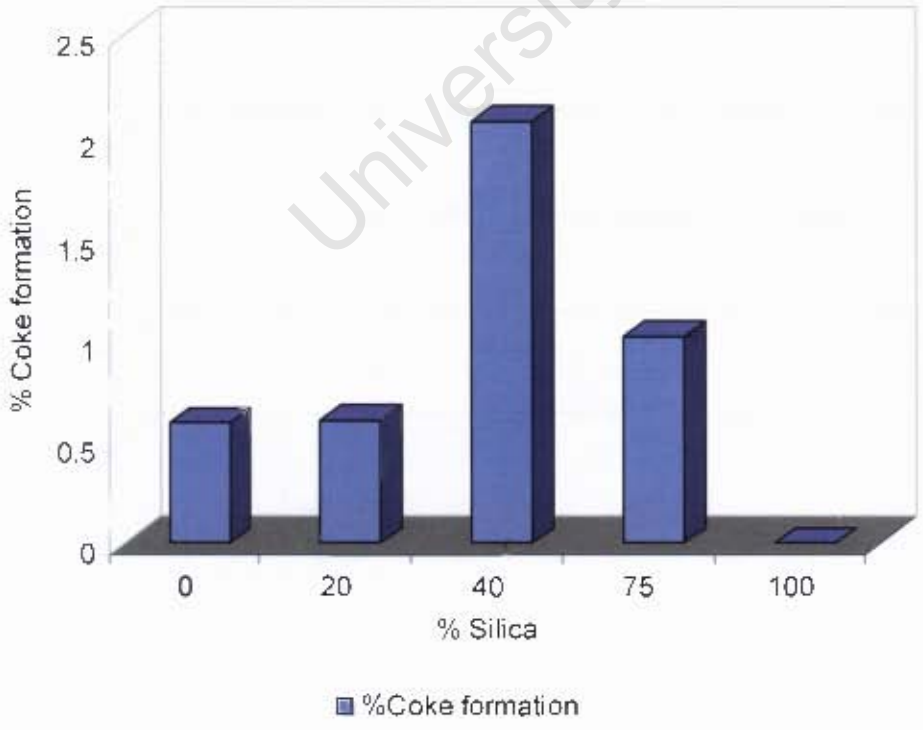

Figure 3.34: Effect of silica content on coke formation of acidic supports at 100°C, 1000h^{-1}, atmospheric pressure and time on-line = 6 hours.

3.4.3.2 Influence of Silica Content on Coke Formation during Metathesis of 1-butene with metal supported catalysts

TGA experiments were performed on spent tungsten impregnated supports after metathesis reaction studies at 450 °C, 500 h^{-1} and atmospheric pressure (0.85 bar) with 1-Butene to determine the effect of silica content on the coke formation. Reactions were run for 6 hours. Results revealed an increase in coke formation approaching WO_3/Siralox 40, after which a decrease in coke formation was observed approaching WO_3/SiO_2 (see Figure 3.35).

As discussed above, coke formation is due to the existence of side reactions like cracking, dehydrogenation, aromatization and polymerisation[85]. Cracking occurs especially in the case with high acidity tungsten based catalysts. High coke formation was observed with tungsten supported on the different Siralox support materials. This can be explained by means of the high total acidity of the tungsten based catalysts. By reducing the acidity on the catalyst, cracking reactions can be limited. It was previously observed that dehydrogenation does occur with tungsten-based catalysts, resulting in the formation of dienes, trienes, and aromatics[80]. The active species of the WO_3/SiO_2 catalyst is the W^{5+} species. A slight reduction of W^{6+} thus takes place to obtain the active metathesis species. Over-reduction of the active species can very easily occur resulting in a system that is active for dehydrogenation and aromatization.

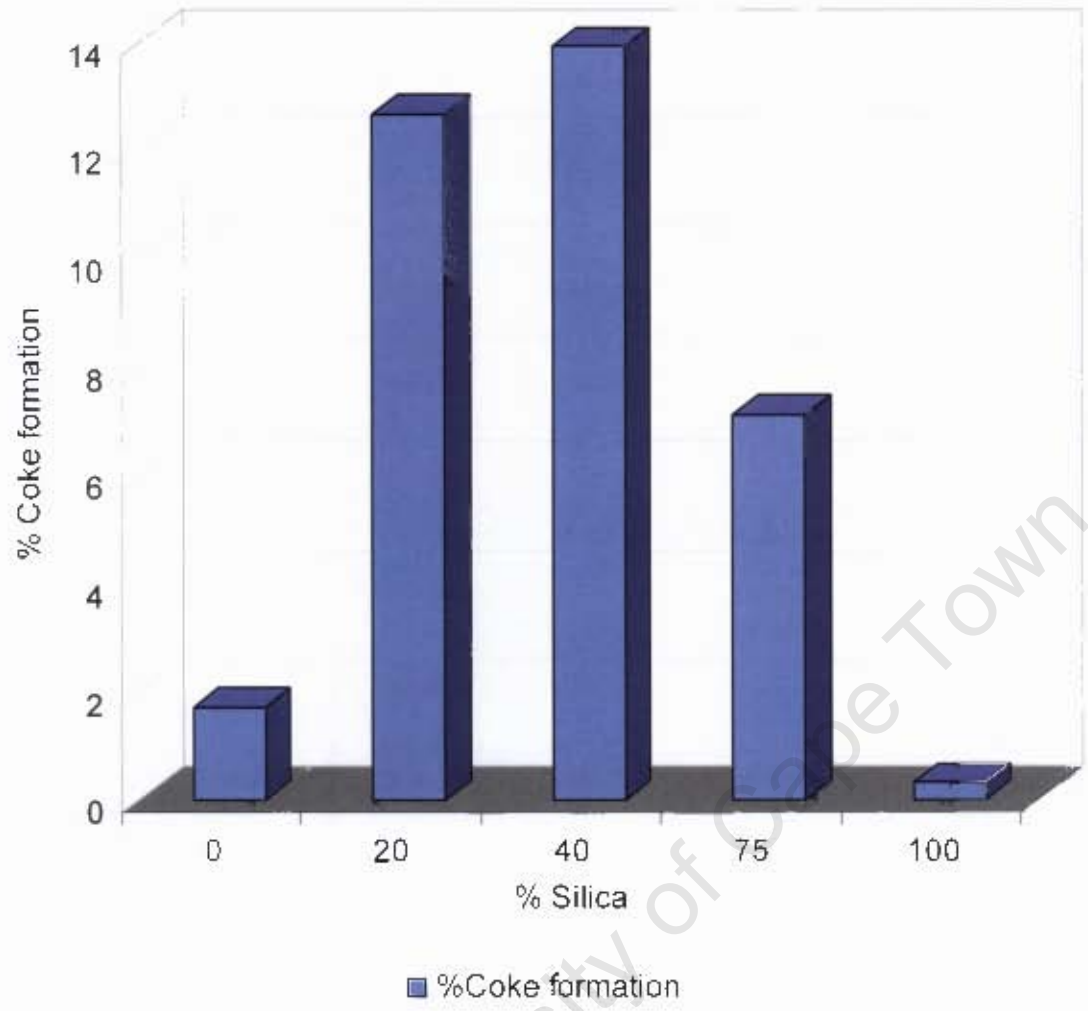

Figure 3.35: Effect of silica content on coke formation of metal impregnated supports at 450°C, 500h^{-1} and atmospheric pressure.

Previous results from BET studies indicated that most of the coke deposits occur inside the pores of the WO_3/SiO_2 catalyst[48]. This was observed in a decrease in surface area in going from the fresh to the spent catalyst. The same observation was made in this study (Table 3.6). Results show the comparison of the BET-surface area of the spent and fresh catalyst after the metathesis reaction at 450°C. BET results of different tungsten impregnated catalysts revealed a decrease in surface area in going from the fresh to the spent catalysts. A drastic reduction in the BET-surface area is obtained for the Siralox support materials, whereas the reduction in the BET-surface area for the alumina and silica supported materials are much less. Coking may lead to blocking of the pores. The blockage of relatively small pores would lead to a

drastic surface area reduction. Siralox have smaller average pore sizes that either silica or alumina.

Table 3.6: BET surface area (SA) of spent and fresh catalysts and supports

Catalyst	**Fresh catalyst (m^2/g)**	**Spent catalyst (m^2/g)**
WO_3/Al_2O_3	237	220
WO_3/Siralox 20	311	235
WO_3/Siralox 40	328	193
WO_3/Siralox 75	246	136
WO_3/SiO_2	260	233

4. Discussion

The main focus of this project was to improve the propene yield and minimize the formation of carbonaceous deposits due to side-reactions during the metathesis reaction.

Thus, the major important factors are:

- To increase metathesis activity by increasing the propene yield and improve the isomerisation activity.
- To increase the lifetime of the catalyst by minimizing the coke formation

4.1 Acidity vs Activity in the Catalyst

Total acidity was determined by means of NH_3-TPD for the support materials and the tungsten supported catalysts (Table 4.1). This was then compared with the activity of 1-butene to find a correlation between the acidity and activity of the catalysts.

Table 4.1 Total acidity of support materials and tungsten supported on the various carriers as determined by NH_3-TPD

Support Material	**SiO_2 (wt.-%)**	**Al_2O_3 (wt.-%)**	**Total acidity of support (mmol/g)**	**Total acidity of 8 wt.-% WO_3 on support (mmol/g)**
Al_2O_3	0	100	0.16	0.23
Siralox 20	20	80	0.22	0.29
Siralox 40	60	60	0.27	0.37
Siralox 75	75	25	0.25	0.33
SiO_2	100	0	0.01	0.05

The total acidity for the support materials as well as for the tungsten supported catalysts reached a maximum at Siralox 40. The presence of tungsten oxide in the catalysts increases the total acidity, implying that tungsten oxide itself is acidic or induces acid sites.

Reaction studies with different support materials were carried out in order to investigate the effect of silica content on the double bond isomerisation activity. These results revealed an increase in isomerisation activity with increasing alumina

content up to Siralox 40 after which it decreases again approaching the activity of pure silica (Figure 4.1). This can be explained in terms of an increase in the total acidity with an increase in silica content, up until a silica content of 40 wt%.

An increase in total acidity for each support was observed with the deposition of tungsten onto the support materials. The total acidity of the catalysts followed the same trend as was observed with the support materials. Increasing acidity was observed with increasing silica content, reaching a maximum at silica content of 40 wt %.

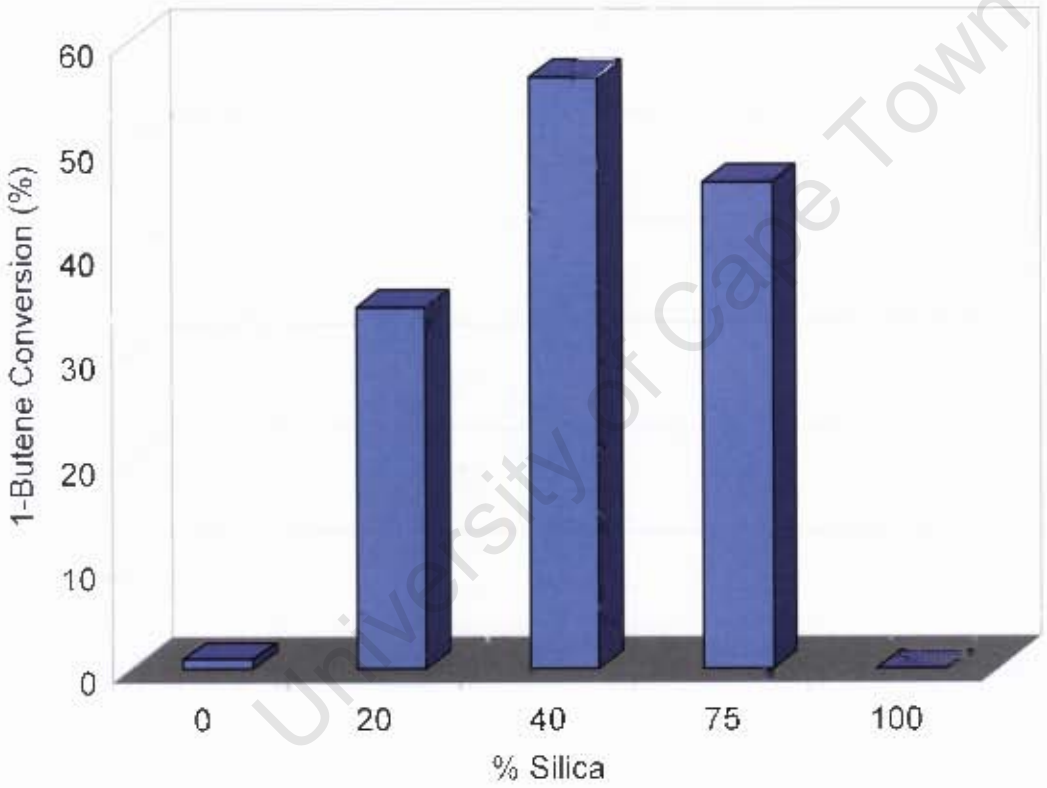

Figure 4.1: Effect of silica content on double bond isomerisation activity at 100°C, 1000h^{-1} and atmospheric pressure (0.85 bar).

These results were combined to find a correlation between the acidity of a support material and its activity towards 1-butene double bond isomerisation. By looking at the obtained results it seems that with increasing silica content up to Siralox 40, an increase in both activity and acidity is observed. These two factors follow the same trend. The conclusion can thus be drawn that the extra incorporated acidity by

combining silica alumina did help to increase the isomerisation activity, which on its turn might help to increase metathesis activity.

Double bond isomerisation is not necessarily associated directly with the active sites for metathesis. The acidic support material on its own can be active for isomerisation[86]. Double bond isomerisation occurs as a side reaction during olefin metathesis over the WO_3/SiO_2 catalyst. If an alkene molecule adsorbs molecularly, it forms a π-complex on the surface, with the C=C bond co-ordinated to the supported cation (Lewis acid site). If Brønsted acid sites are present, protonation of the alkene can occur, resulting in an carbocation where the C=C character has been lost. Subsequent loss of a proton from a different carbon atom results in isomerisation (Figure 4.2)[87].

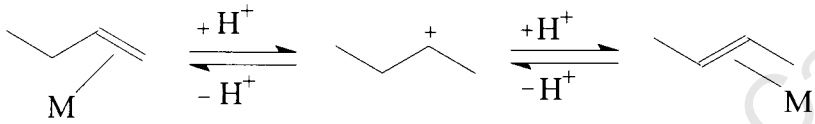

Figure 4.2: Isomerisation via an carbocation – Brønsted-type mechanism[87]

Double bond isomerisation of an olefin could also occur through an allylic intermediate. If the first step involves C-H cleavage, an allylic intermediate is formed. Subsequent hydrogenation at a different carbon atom results in isomerisation (Figure 4.3)[136].

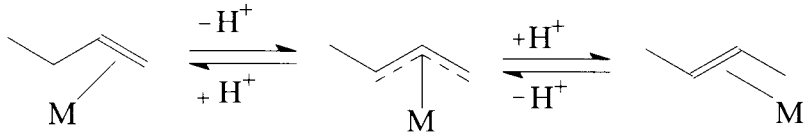

Figure 4.3: Isomerisation via an allylic intermediate (Lewis-type mechanism) [87]

Double bond isomerisation on WO_3/SiO_2 catalysts can thus occur through both the alkoxide and allylic intermediate, and have been observed[36]. It can thus be concluded that isomerisation can occur on both Brønsted and Lewis acid sites and thus both of these types of acid sites will contribute to the total isomerisation activity.

Early work on metathesis and isomerisation activity of WO_3/SiO_2 revealed isomerisation to occur through a carbocation intermediate[88].

Reaction studies with different support materials to investigate double bond isomerisation activity revealed a correlation between total acidity and activity. With increasing acidity, and increase in double bond isomerisation was observed. This is explained in terms of the maximum amount of tetrahedrally coordinated alumina at a silica content of 40 wt% silica. Siralox 40 would thus have the maximum amount of strong acid sites, which would be responsible for the high isomerisation activity with the Siralox 40 support material.

4.2 Acidity vs Reducibility of the Catalyst

The effect of silica content on the reducibility of the tungsten impregnated catalysts was investigated by means of temperature programmed reduction (TPR) with hydrogen. This was compared to the total acidity of each catalyst in order to try and find a correlation between acidity and reducibility (Table 4.2).

Table 4.2 Relation between Total acidity and reducibility

Catalyst		Total acidity (mmol/g)	$T_{reduction}$ (°C)
WO_3/Al_2O_3	(0% Si)	0.23	1000
WO_3/Siralox 20	(20% Si)	0.29	995
WO_3/Siralox 40	(40% Si)	0.37	950
WO_3/Siralox 75	(75% Si)	0.33	940
WO_3/SiO_2	(100% Si)	0.05	710

The results from TPR showed a decrease in reduction temperature with an increase in silica content. Thus, as the acidity increases with increasing silica content, peaking at WO_3/Siralox 40, the reduction temperature decrease with an increase in silica content all the way to silica content of 100%. It can thus be seen that there is no correlation between acidity and reducibility of the tungsten catalysts, but rather an increase in reduction temperature with an increase in alumina content.

4.3 Activity in 1-butene metathesis

4.3.1 The effect of reducibility on metathesis activity

The effect of reduction temperature on the activity of the catalysts was investigated by carrying out reaction studies with the metal impregnated support materials at 450 °C, 500 h^{-1} and atmospheric pressure. The activity of a specific catalyst was then related to the degree of ease it is being reduced. Results from reaction studies revealed very low conversions with high reduction temperatures as is the case with the tungsten supported on alumina and tungsten supported on Siralox 20. These two catalysts have extremely high reduction temperatures, which are being reflected in their activity. As the degree of ease of reduction is increased, higher activities become evident. This can be seen with an increase in activity until the highest activity is reached with the tungsten on silica catalyst (See Figure 4.4). This corresponds well with the low temperature at which it is being reduced to the active oxidation state.

Figure 4.4: 1-Butene Conversion (■) at 450 °C, 500 h^{-1} and atmospheric pressure (0.85 bar) of tungsten catalysts versus Reduction temperature (◆) at time on-stream = 6 hours.

It was found that the density and strength of acid sites and the rate of catalytic reactions on tungsten oxide catalysts increase with a slight reduction of the W^{6+} centres, which often occurs during catalytic reactions in reducing hydrocarbon

environments[21]. It was first reported by Sabatier that WO_3 crystallites were readily reduced to a stoichiometry corresponding to $WO_{2.95}$[34]. It was found that this slightly reduced oxide was more active than the WO_3.

Reduction of the metal sites to an active species take place during initial contact with an olefin, and "break-in" time is observed. Reduction of the catalysts to a lower oxidation state which is active towards metathesis thus takes place to obtain reduced break-in time. From the proposed mechanism of metathesis, it is clear that a metal carbene is required as an active catalyst for the metathesis reaction. Active species can be concluded to be W^{5+} species. Previous XRD studies of the fresh catalyst, showed the presence of only WO_3 i.e. W in the +6 oxidation state. Reduction of the catalyst took place as was observed from XRD studies of the spent catalyst. Tungsten in the form of WO_3 and $WO_{2.95}$ which corresponds to W^{6+} and W^{5+} were observed on the spent catalyst[67]. In the metathesis of propene with MoO_3/Al_2O_3 and WO_3/Al_2O_3, it was observed by Thomas and Mouljin that there exists a positive correlation between reducibility of the catalysts and catalytic activity for metathesis of propene which confirms that reduction is the fundamental step in the generation of active sites[32]. It was observed in this study that the catalytic activity increase with an increase in reducibility of the catalysts. Tungsten supported on alumina which is the most difficult to reduce, has been observed to have the lowest catalytic activity. An increase in catalytic activity was observed with an increase in silica content and the maximum catalytic activity was observed with the tungsten supported on silica catalysts was observed. This catalyst is thought to have the largest amount of reduced tungsten and thus the largest amount of sites active for metathesis. It can thus be concluded that the reducibility of the catalysts has a larger effect on the catalytic activity than the acidity of the catalysts. It is thus very important to have a good interaction between metal and support in order to have maximum catalytic activity.

4.4 Effect of silica content on Metathesis activity

Reaction studies with different metal impregnated supports were carried out in order to investigate the metathesis activity of 1-butene in the presence of different supported tungsten catalysts (Figure 4.5). Metathesis of 1-butene was carried out at 450°C, atmospheric and GHSV=500 ml/(ml.h). With increasing content of silica, an

increase in metathesis activity was observed. However, no maximum in activity was obtained at silica content of 40% as was the case with the support materials. The activity increased constantly with an increase in silica content. A maximum activity was obtained with the WO_3/SiO_2, although this catalyst has the lowest acidity (Table 4.3).

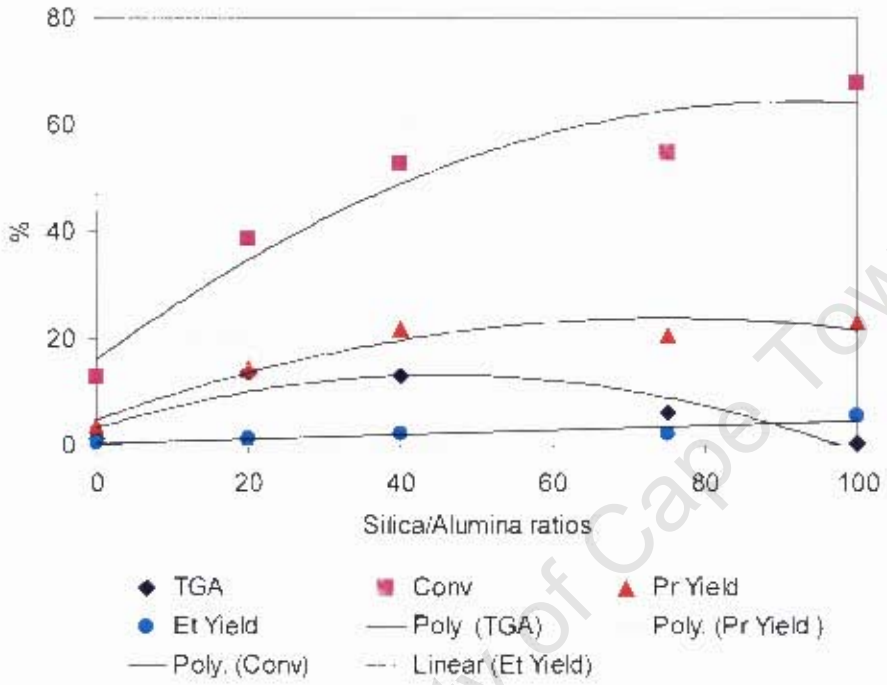

Figure 4.5 Effect of silica content on metathesis activity with metal impregnated support materials at 450°C, 500h ^{1} and atmospheric pressure.

When taking into consideration the thermodynamic calculations done in Chapter 1, it can be seen that the maximum conversion that can be obtained in the primary metathesis reaction, is ca 70%. Thus, the metathesis reactions reported here are at close to equilibrium conversion. Furthermore, the thermodynamically determined selectivity for propene is ca. 40%, which was also obtained in the experimental studies. Hence, the propene yield is close to its maximum value (Figure 4.5).

It seems though as if the ethene yield (Figure 4.6) is lagging behind the propene yield (Figure 4.7) implying that the reaction of 2-butene with 1-butene is somewhat faster on the catalysts than the reaction of 1-butene with 1-butene. This would be expected if a fast double bond isomerisation exists, the concentration of 2-butene would be ca. 3 times higher than that of 1-butene.

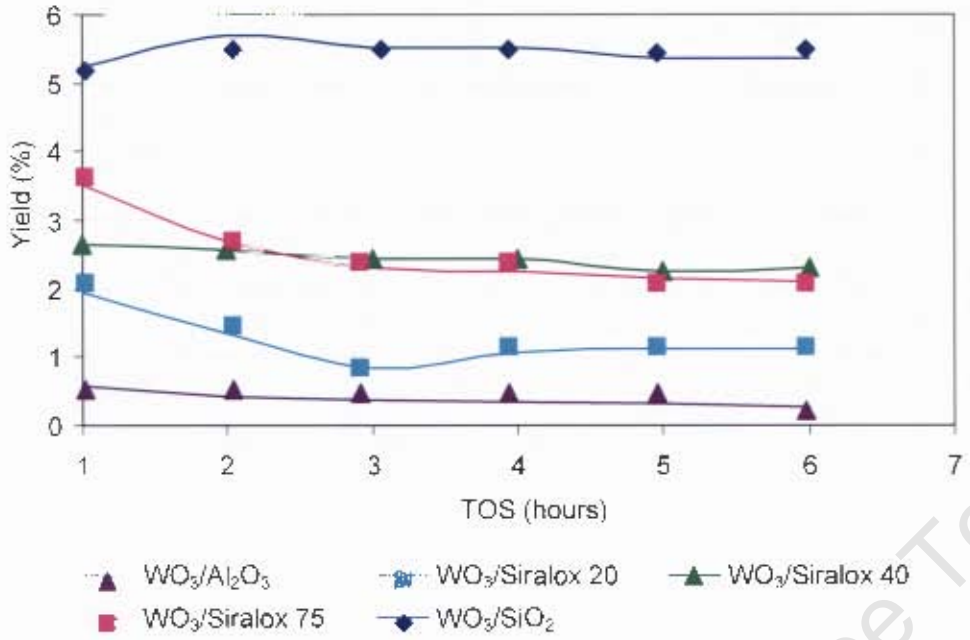

Figure 4.6 Ethene yield vs Time-on-stream for the different Tungsten supported Catalysts

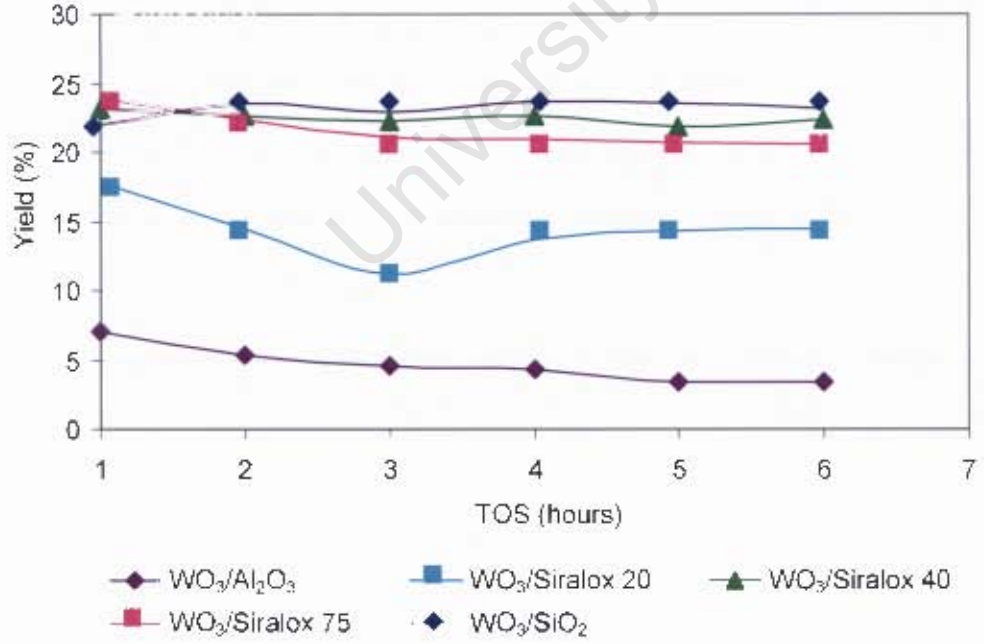

Figure 4.7 Propene yield vs Time on-stream for the different Tungsten supported catalysts

4.5 Effect of total acidity of support material on metathesis activity

As previously discussed, an increase in acidity of the support material, may help to obtain optimum isomerisation between 1-butene and 2-butene, which will increase the propene yield. The total acidity of the support materials were thus determined by means of NH_3 – TPD and correlated to the conversion of 1-butene in the metathesis reaction (Table 4.3).

Table 4.3: Effect of total acidity on the metathesis activity of 1-butene

Support Material	Total Acidity (mmol/g)	1-butene conversion (%)
WO_3/Al_2O_3	0.23	12.70
WO_3/Siralox 20	0.29	38.51
WO_3/Siralox 40	0.37	52.64
WO_3/Siralox 75	0.33	54.55
WO_3/SiO_2	0.05	67.58

As previously discussed, double bond isomerisation is not necessarily associated directly with the active sites for metathesis. It was found by Andreini et al. that the Brønsted acidity does not seem to play a role in the metathesis reaction by evaluating several acidic supports for metathesis activity at different activation temperatures[38]. They observed that the Brønsted acidity decreased with increasing activation temperature while metathesis activity increased.

It was suggested that the acidity needed for the formation of the initial metal carbene intermediate in the metathesis reaction) to be available from a Lewis site-alkene complex located on the transitional metal ion[35]. The generation of active centres for metathesis activity was explained by van Roosmalen and co-workers as proton donation by the Lewis acid site-alkene complexes to tetravalent tungsten[75]. They concluded that activated WO_3/SiO_2 contains silanol groups with Lewis acidity. The Si-O bridges to the silica lattice are electron-attracting groups, due to the p_π-d_π back bonding between oxygen and silicon resulting in the Lewis acidity. In the presence of an olefin, the olefin can chemisorb onto the tungsten surface compound (Figure 4.8) to form a Lewis acid-alkene complex (Figure 4.9).

acidity of all the catalysts, it showed the highest activity in the metathesis of 1-butene.

Low propene yields were thus observed with tungsten supported on the Siralox support materials. An increase in propene yield was observed with increasing silica content of the support, probably because of a better metal-support interaction.
The conclusion can be made that the metathesis reaction needed a certain amount of acidity for the reaction to proceed, where after other factors, like reducibility and metal-support interaction plays a more important role in the reaction.

4.6 Deactivation in 1-butene metathesis

Deactivation for the tungsten supported catalysts can be defined as the decrease in activity after 6 hours on-line vs. the activity after 1 hour on-line. It can also be defined in terms of the amount of carbonaceous deposits formed on the catalyst.

Main causes of deactivation in the catalyst system:

- Deactivation due to the **formation of coke**, blocking the active sites of the catalyst and coke formation due to **side-reactions** and **high acidity.**
- Deactivation due to poor activity which is caused by tungsten not being in the **active oxidation state for metathesis.**

From reaction studies, all catalysts show close to 100% propene purity implying that hydrogenation of the product, propene by hydrogen transfer does not take place to a significant extent.

Catalysts containing higher amounts of alumina show somewhat lower ethene purity (Figure 4.12), which could be caused by extensive cracking (and thus yielding more methane) or by some hydrogenation yielding ethane (and as a co-product a hydrogenated product, which may act as a coke precursor). The ethene purity obtained with tungsten on silica is close to 100%. Catalysts with higher alumina content show lower ethene purity and thus more methane/ethane.

It can be noted that the catalyst containing alumina show some degree of deactivation, as evidenced by the decline in the activity (Figure 4.10). The degree of deactivation seems to increase with increasing alumina content in the catalyst. It should thus be noted that the catalysts with the highest amount of methane, ethane and propane should show the highest deactivation. From Figure 4.11, it can be seen that the catalysts on the mixed silica-alumina catalysts has got higher yields of methane/ethane than the tungsten/silica catalyst, thus causing the deactivation of these catalysts.

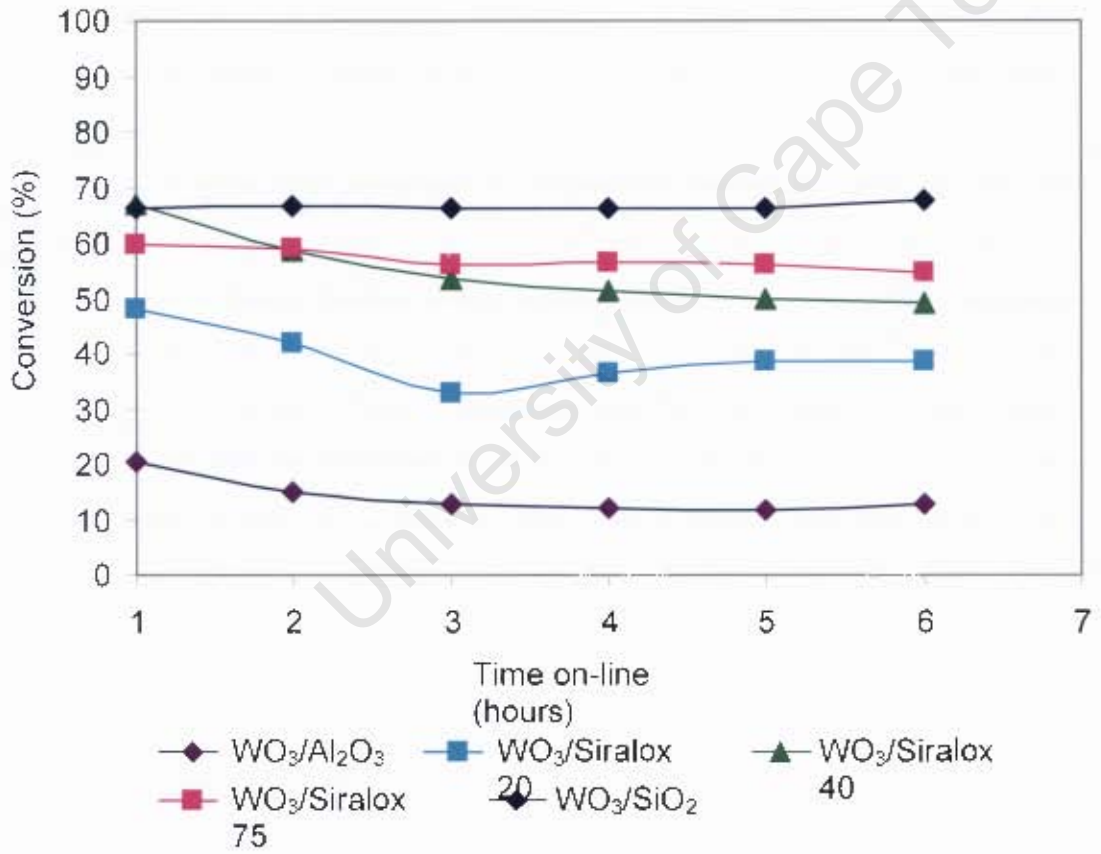

Figure 4.10: Conversion of 1-Butene in 1-Butene metathesis over supported tungsten catalysts (T =450 °C, atmospheric pressure (0.85 bar), GHSV = 500 h^{-1})

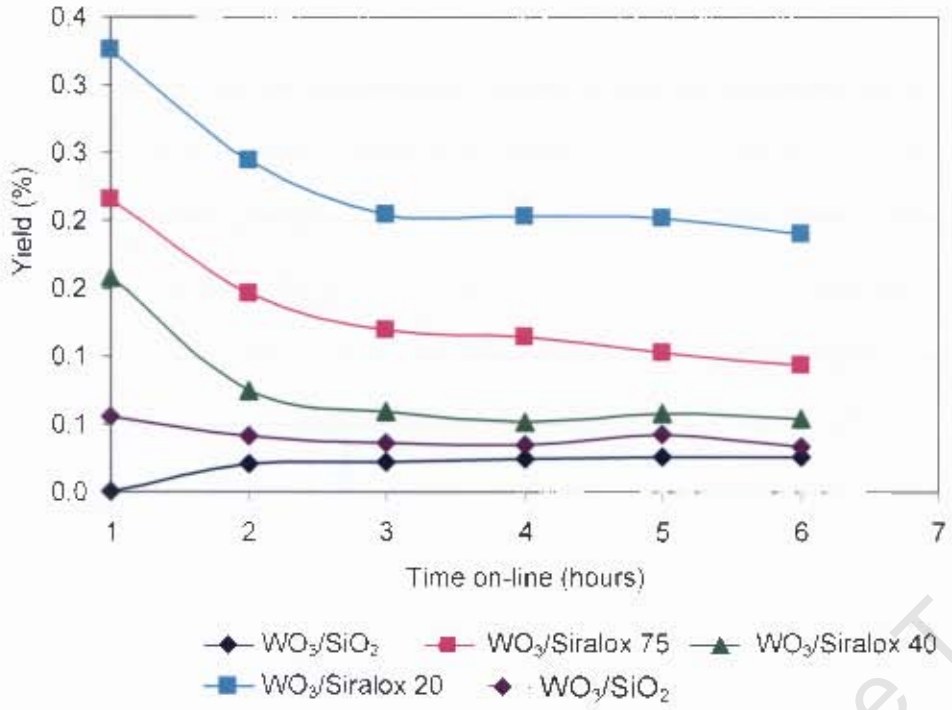

Figure 4.11: Formation of Methane and Ethane in 1-Butene metathesis over various supported tungsten catalysts (T =450 °C, atmospheric pressure (0.85 bar), GHSV = 500 h^{-1})

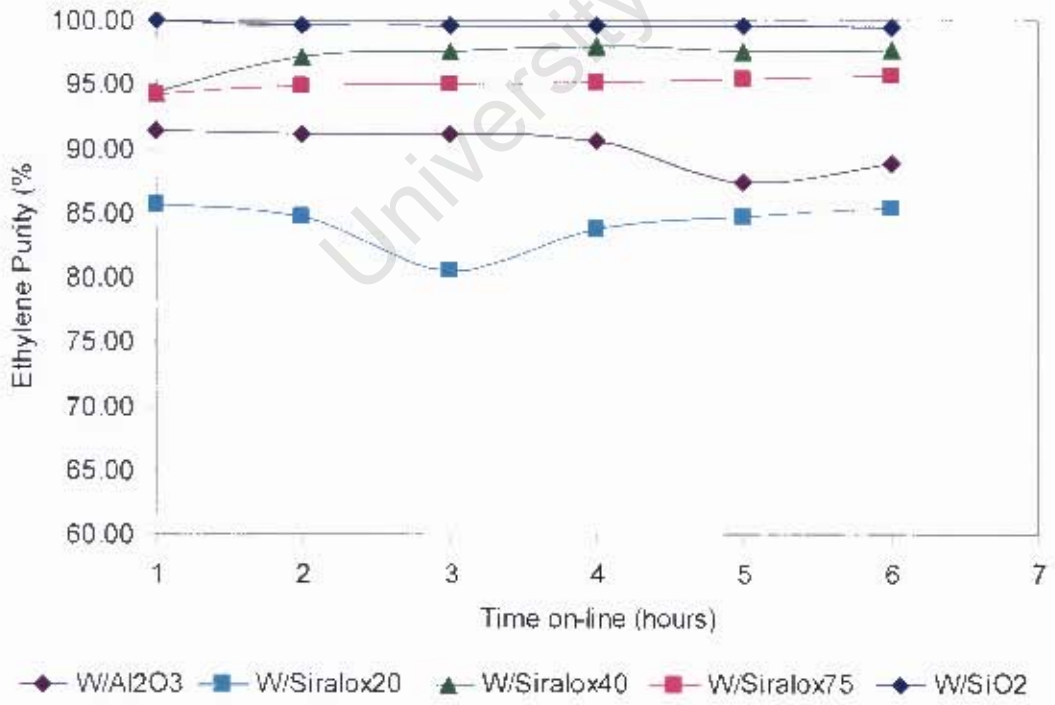

Figure 4.12: Ethene purity obtained from 1-butene metathesis over supported tungsten catalysts (T =450°C, atmospheric pressure (0.85 bar), GHSV = 500 h^{-1})

4.7 Correlation between deactivation and total acidity of the tungsten supported catalysts

The formation of coke on oxide catalysts is mainly due to cracking reactions involving coke precursors like olefins or aromatics which are catalyzed by acidic sites on the catalyst surface[46]. It is suspected to see an increase in coke formation with an increase in acidity. With increasing acidity, an increase in cracking will be observed, which is responsible for the formation of products like methane and ethane, which when formed will also form hydrogenated products which will act as coke precursors. One of the factors that can be responsible for deactivation of the catalyst is the amount of carbonaceous deposits formed on the catalyst, which will block the active sites on the catalyst.

Table 4.4 Relation between Total acidity and Coke formation

Catalyst	Total Acidity (mmol/g)	Coke formation (%)
WO_3/Al_2O_3	0.23	1.714
WO_3/Siralox 20	0.29	12.66
WO_3/Siralox 40	0.37	13.92
WO_3/Siralox 75	0.33	7.112
WO_3/SiO_2	0.05	0.3118

Deactivation can be linked to total acidity of the catalysts which in turn catalyzes the formation of carbonaceous deposits on the catalyst. From Table 4.4 it can be seen that there definitely exists a relation between the formation of coke and the total acidity of the catalysts. The total acidity increases with increasing silica content, reaching a maximum at 40 wt% silica, after which it decreases again approaching 100 wt% silica. The formation of coke on the catalysts follows exactly the same trend. Thus it can be concluded that with increasing acidity, increasing amounts of coke is formed, which in turn can explain the deactivation of the catalysts supported on the mixed silica/alumina.

The initial focus of this project was to improve the propene yield in 1-butene metathesis over a supported tungsten catalyst. Propene is formed by metathesis of 1-butene and 2-butene. Hence, propene yield should be increased by favouring double bond isomerisation. It was initially believed that this could be achieved by using alternative support material with higher acidity for the existing tungsten on silica catalyst. It was observed that the propene yield under the chosen reaction conditions for 1-butene metathesis over WO_3/SiO_2 is close to equilibrium (a conversion of 70% and selectivity of 40% was obtained). Hence, catalytic performance cannot be further improved.

A series of tungsten supported on silica-alumina catalysts were synthesized, characterized and tested for their activity in 1-butene metathesis. It was believed as stated above that with increasing acidity, the activity should increase, because increased isomerisation activity will have been achieved. From reaction studies though, it has been revealed that that metathesis activity does not increase with increasing acidity (silica/alumina ratio). The activity actually goes down in going from tungsten on pure silica to increasing ratios of silica/alumina. Thus, the activity actually goes down with increasing acidity. This was described in terms of the strong interaction between tungsten and alumina. This interaction gets stronger with increasing amounts of alumina, thus preventing the reduction of tungsten to the active oxidation state for metathesis, and hence resulting in a decreased activity for metathesis over the silica/alumina support materials.

A further objective of the study was to improve the catalyst lifetime by minimizing coke formation. The rate of coke formation is also a function of acidity and pore structure of the catalyst[44]. It has been established that coking increases with increasing acidity of the surface. It is believed that both Lewis and Brønsted acid sites may take part during coking, the former by strongly interacting with basic species in the feed, and the latter by supplying protons to form carbocation cations, which are also responsible for the formation of coke[50]. The amount of coke formed after 1-butene metathesis on each catalyst was determined by means of TGA. This was related to the acidity of each catalyst. Coke formation increases with increasing acidity, meaning the

acidic support materials adds to the formation of coke on the catalyst, and thus decreasing the lifetime of the catalyst.

It is thus suggested to use a more basic catalyst to minimize the coke formation in 1-butene metathesis. Base-catalyzed reactions proceed via carbanion intermediates, whereas coking proceeds via carbocation intermediates[27]. Hence, minimizing acidity in the catalyst may enhance the lifetime of the 1-butene metathesis catalyst.

6. References

1. Propylene Prospectus 2003, "Technology Development in Propylene and Propylene derivatives", Nexant Chem Systems, www.nexant.com.
2. J.G. Lacson, "Propylene, CEH Marketing Research Report 436.0000A", (2004).
3. J.C. Mol, *J. Mol. Catal. A: Chemical* **213** (2004) 39–45.
4. E.P. Moore, W. Spaleck, "Propylene Handbook. Polymerization, Characterization, Properties, Processing, Applications", Vol. 7 (1996).
5. Chemical and Engineering News, March 24 (1997).
6. J.M. Botha, M.M. Mbatha, B. Nkosi, A. Spamer, J. Swart, International Patent WO 001/14038 (2000).
7. R.A. Grey, "The 2000 Benjamin Franklin Medal in Chemistry presented to Robert H. Grubbs", *J. Franklin Inst.* **337** (2000) 793-805.
8. H.S. Eleuterio, *J. Mol. Catal.* **65** (1991) 55-61
9. H.S. Eleuterio, *German Patent 1 ,072, 811* (1961) 16005.
10. H.S. Eleuterio, *US Patent 3 ,074 ,918* (1963).
11. A.W. Anderson, N.G. Meckling, *US Patent 2, 721, 189*, (1955).
12. E.F. Peters, B.L. Lansing, *US Patent 2, 963, 447* (1960).
13. a. R.L. Banks, CHEMTECH, **16**, (1986) 112.
    b. R. L Banks, *US Pat. 4,605, 810*, (1986) 155076
14. K. Weissermel, H.J. Arpe, "Industrial Organic Chemistry", (1993), 85-88.
15. N. Calderon, "Olefin metathesis reaction", *Acc of Chem. Res.* **5** (1972) 127-132.
16. P.J.L. Herisson, Y. Chauvin, *Makromo. Chem.* **141** (1970) 161-176.
17. R. H. Grubbs, P. L. Burke, D. D. Carr, J. Am. Chem. Soc. **97**. (1975), 3265-3267
18. M.F. Farona, R.I. Tucker, *J. Mol. Cat.* **8** (1980) 85-90.
19. Y. Iwasawa, H. Kubo, H. Hamamura, *J. Mol. Catal.* **28** (1985) 191-208.
20. D.J. Moodley, "The metathesis activity and deactivation of heterogeneous metal oxide catalytic systems", MSc Thesis, Potchefstroomse Universiteit vir Christerlike Hoër Onderwys, (2003) 19-25.

21. D.G. Barton, S.L. Soled, E. Iglesia, "Solid acid catalysts based on supported tungsten oxides", *Topics in Catalysis* **6** (1998) 87-99.
22. D.R. Stull, E.F. Westrum, G.C. Sinke, "The chemical thermodynamics of organic compounds", John Wiley & Sons, New York (1969).
23. K.J. Ivin, J.C. Mol, "Olefin Metathesis and Metathesis Polymerization", Vol. 2 (1997) 25.
24. C. Pariya, K.N. Jayaprakash, A. Sarkar, "Alkene metathesis: New developments in catalyst design and application", *Coord. Chem. Rev.* **168** (1998) 4.
25. P.B. Venuto, L.A. Hamilton, P.S. Landis, J. J. Wise, *J. Catal.* **5** (1966) 81-98.
26. D.M. Bouwer, *J. Catal.* **1** (1962) 22-31.
27. H. Hattori, "Heterogeneous basic catalysts", *Chem. Rev.* **95** (1995) 537-558.
28. X. Xu, C. Boelhouwer, D. Vonk, J.I. Benecke, J.C. Mol, *J. Mol. Catal.* **36** (1986) 47-66.
29. X. Xu, J.C. Mol, C. Boelhouwer, J. Chem. Soc., Far. Trans.1, **82** (1986) 2707.
30. R. Spronk, "Alkene Metathesis over Supported Rhenium Catalysts", Ph.D. Thesis, University of Amsterdam (1991) 5.
31. J. Engelhardt, J. Goldwasser, W.K. Hall, *J. Mol. Catal.* **15** (1982) 173-185.
32. R. Thomas, J.A. Moulijn, *J. Mol. Catal.* **15** (1982) 157-172.
33. C.H. Kline, V. Kollonitsch, "The catalytic activity of tungsten–I", *Ind. Eng. Chem.* **57** (1965) 53-63.
34. P. Sabatier, *J. Am. Chem. Soc.*, **45** (1923) 1854–1862
35. A.J. van Roosmalen, J.C. Mol, *J. Catal.* **78** (1982) 17-23.
36. A. Corma, "Inorganic solid acids and their use in acid-catalyzed hydrocarbon reactions", *Chem. Rev.* **95** (1995) 559-614.
37. H.G. Karge, V. Dondur, *J. Phys. Chem.* **94** (1990) 765-772.
38. A. Andreini, J.C. Mol, *J.Chem. Soc., Far.Trans. 1* **81** (1985) 1705.

39. A.J. van Roosmalen, D. Koster, J.C Mol, *J. Phys. Chem.* **84** (1980) 3075-3079.
40. A.J. van Roosmalen, J.C. Mol, *J. Chem. Soc., Chem. Commun. (*1980a) 704.
41. A. Spamer, T.I. Dube, D.J. Moodley, C. van Schalkwyk, J.M. Botha, *Appl. Catal. A: Gen.,* **255** (2003) 153-167.
42. W. Grunert, R. Feldhaus, K. Anders, "Thermal activation of Al_2O_3 supported MoO_3 and WO_3 metathesis catalysts", *Reac. Kin. and Catal. Lett.* **36** (1988) 195-200.
43. J.G. Santiesteban, J.C. Vartuli, S. Han, R.D. Bastian, C.D. Chang, *J. Catal.* **168** (1997) 431-441.
44. C.H. Bartholomew, A*ppl. Catal. A: Gen.* **212** (2001) 17-60.
45. J. Oudar, H. Wise, "Deactivation and Poisoning of Catalysts", Marcel Dekker, New York (1985).
46. J.R. Rostrup-Nielsen, *Catal. Today* **37** (1997) 225-232.
47. B.C. Gates, J.R. Katzer, G.C.A. Schuit, Chemistry of Catalytic Processes, McGraw-Hill, New York (1979).
48. C. van Schalkwyk, A. Spamer, D.J. Moodley, T. Dube, J. Reynhard, J.M. Botha, *Appl. Catal. A: General* **255** (2003) 121-131.
49. A. Spamer, T.I. Dube, D.J. Moodley, C. van Schalkwyk, J.M. Botha, *Appl. Catal. A: General* **255** (2003) 133-142.
50. R.J. Farrauto, C.H. Bartholomew, "Fundamental of Industrial Catalytic Processes", (2002).
51. D.L. Trimm, *Appl. Catal. A: General* **212** (2001) 153-160.
52. S. D. Robertson, B. D. McNicol, J. M. De Baas, S. C. Kloet, J. W. Jenkins, *J. Catal.*, **37** (1975) 424.
53. H. G. Karge, J. Schweckendied, "In Proceedings of the 5th International Symposium in Heterogeneous Catalysis", Varna Bulgaria, 1983; Shopov, D., et al., Eds.; Publishing House of the Bulgarian Acad. Sci.: Sofia, (1983) 429.

54. R. A. Serway, J. S. Faughn, C. Vuille, C. A. Bennet, College Physics, 7th ed., Thomson Brooks/Cole, Belmont, CA, (2006) 235.
55. W.N. Delgass, G.L. Haller, R. Kellerman, J.H. Lunsford, "Spectroscopy in Heterogeneous Catalysis", Academic Press, New York, (1979).
56. G.T. Haller, *Catal. Rev. Sci. Eng.*, (1981) 477.
57. J.W. Ward, *J. Catal.*, **17**, (1970) 348.
58. M.W. Anderson, J. Klinowski, "Zeolites", **6** (1986) 455.
59. T.R. Hughes, H.M. White, *J. Phys. Chem.*, **71** (1967) 2192.
60. J. Datka, A.M. Turek, J.M. Jehng, I.E. Wachs, *J. Catal.*, **135** (1992) 186.
61. C.A. Emeis, J. Catal., **141** (1993) 347.
62. P. Johnson, "Proceedings of the 7thWorld Petrochemical Congress", (1967) 247.
63. C. van Schalkwyk, A. Spamer, D.J. Moodley, T. Dube, J. Reynhardt, J.M. Botha, *Appl. Catal.* A: General **255** (2003) 121-131.
64. I.A. Fowlis, "Gas Chromatography", John Wiley & Sons (Chichester), (1995) 141.
65. A. Spamer, T.J. Moodley, C. van Schalkwyk, J.M. Botha, *Appl. Catal.* **255** (2003) 153 – 167.
66. F.H. Chung, D.K. Smith, "Industrial Applications of X-Ray diffraction" **19** (2000), 503.
67. A.G. Bazur, S.R. Patwardhan, S.N. Vyas, *J. Catal.*, **127** (1991) 86-95.
68. A.N. Startsev, B.N. Kuznetsov, Yu.I. Yermakov, *React. Kinet. Catal. Lett.*, **4**, (1976) 321.
69. Y. Iwasawa, H. Kubo, H. Hamamura, *J. Mol. Catal.*, **28** (1985) 191.
70. B.N. Shelimov, I.E. Elev, V.B. Kazansky, *J. Catal.*, **98** (1986) 70.
71. W. GrÜnert, R. Feldhaus, K. Anders, "Thermal Activation of Al_2O_3 Supported MoO_3 and WO_3 Metathesis Catalysts", **36** (1988) 195-200.
72. R. Thomas, E.M. van Oers, V.H. J. de Beer, J. Medema, J.A. Moulijn, *J. Catal.*, **76** (1982) 241.
73. T.A. Patterson, J.C. Carver, D.E. Leyden, D.M. Hercules, *J. Phys. Chem.*, **80** (1976) 1700.

74. S.B. Nikishenko, A.A. Slinkin, E.S. Shpiro, G.V. Antoshin, Kh. M. Minachev, *Kinet. Katal.*, **20** (1979) 524.
75. H.A. Benesi, B.H.C. Winquist, *Adv. Catal.*, **27** (1978) 97.
76. S. Rajagopal, J.A. Marzari, R. Miranda, *J. Catal.*, **151** (1995) 192-203.
77. J.A. Schwarz, B.G. Russel, H.F. Harnsberger, *J. Catal.*, **54** (1978) 303.
78. C.L. Thomas, *Ind. Eng. Chem.*, **41** (1949) 2564.
79. K. Tamele, *Disc. Faraday Soc.*, **8** (1950) 270.
80. J.B. Peri, *J. Phys.* Chem., **69** (1965) 231.
81. H. Dunken, P. Fink, *Z. Chem.*, **5** (1965) 432.
82. B.C. Gates, J.R. Catzer, G.C.A. Schuit, "Chemistry of Catalytic Processes", McGraw-Hill, New York (1979), Ch. 1 & 5.
83. R.J. Farrauto, C.H. Bartholomew "Fundamentals of Industrial Catalytic Processes" (2005) 265.
84. A.M. Venezia, V.La Parola, B. Pawelec and J.L.G. Fierro, Appl. Catal. A: General 264 (2004) 43-51.
85. C. van Schalkwyk, A. Spamer, D.J. Moodley, T. Dube, J. Reynhardt, J.M. Botha and H.C. M. Vosloo, Appl. Catal. A: General **255** (2003) 143–152.
86. A.J. van Roosmalen, J.C. Mol, *J. Mol. Catal.*, **78** (1982) 17
87. N.C. Ramani, D.L. Sullivan, J.G. Ekerdt, *J. Catal.*, **173** (1998) 105
88. A. J. Van Roosmalen, J. C. Mol, *J. Chem. Soc., Chem. Commun.*, **15**, (1980) 704

"I know the meaning of plagiarism and declare that all the work in the document, save for that which is properly acknowledged, is my own".